Title
Monitoring Particulate Matter with Commodity Hardware

Author
Holstius, David

Publication Date
2014

Peer reviewed|Thesis/dissertation

Monitoring Particulate Matter with Commodity Hardware

by

David Holstius

A dissertation submitted in partial satisfaction of the

requirements for the degree of

Doctor of Philosophy

in

Environmental Health Sciences

in the

Graduate Division

of the

University of California, Berkeley

Committee in charge:

Professor Kirk R. Smith, Co-chair
Associate Professor Edmund Seto, Co-chair
Professor Rachel Morello-Frosch
Professor Ronald C. Cohen

Spring 2014

Monitoring Particulate Matter with Commodity Hardware

Abstract

Monitoring Particulate Matter with Commodity Hardware

by

David Holstius

Doctor of Philosophy in Environmental Health Sciences

University of California, Berkeley

Professor Kirk R. Smith, Co-chair

Associate Professor Edmund Seto, Co-chair

Health effects attributed to outdoor fine particulate matter ($PM_{2.5}$) rank it among the risk factors with the highest health burdens in the world, annually accounting for over 3.2 million premature deaths and over 76 million lost disability-adjusted life years. Existing $PM_{2.5}$ monitoring infrastructure cannot, however, be used to resolve variations in ambient $PM_{2.5}$ concentrations with adequate spatial and temporal density, or with adequate coverage of human time-activity patterns, such that the needs of modern exposure science and control can be met. Small, inexpensive, and portable devices, relying on newly available off-the-shelf sensors, may facilitate the creation of $PM_{2.5}$ datasets with improved resolution and coverage, especially if many such devices can be deployed concurrently with low system cost.

Datasets generated with such technology could be used to overcome many important problems associated with exposure misclassification in air pollution epidemiology. Chapter 2 presents an epidemiological study of $PM_{2.5}$ that used data from ambient monitoring stations in the Los Angeles basin to observe a decrease of 6.1 g (95% CI: 3.5, 8.7) in population mean birthweight following *in utero* exposure to the Southern California wildfires of 2003, but was otherwise limited by the sparsity of the empirical basis for exposure assessment. Chapter 3 demonstrates technical potential for remedying $PM_{2.5}$ monitoring deficiencies, beginning with the generation of low-cost yet useful estimates of hourly and daily $PM_{2.5}$ concentrations at a regulatory monitoring site. The context (an urban neighborhood proximate to a major goods-movement corridor) and the method (an off-the-shelf sensor costing approximately USD $10, combined with other low-cost, open-source, readily available hardware) were selected to have special significance among researchers and practitioners affiliated with contemporary communities of practice in public health and citizen science. As operationalized by correlation with 1 h data from a Federal Equivalent Method (FEM) β-attenuation data, prototype instruments performed as well as commercially available equipment costing considerably more, and as well as another reference instrument under similar conditions at the same timescale ($R^2 \approx 0.6$). Correlations were stronger when 24 h integrating times were used instead ($R^2 = 0.72$).

Chapter 4 replicates and extends the results of Chapter 3, showing that similar calibrations may be reasonably exchangeable between near-roadway and background monitoring sites. Chapter 4 also employs triplicate sensors to obtain data consistent with near-field (<50 m) observations of plumes from a major highway (I-880). At 1 minute timescales, maximum $PM_{2.5}$ concentrations on the order of 100 $\mu g\,m^{-3}$ to 200 $\mu g\,m^{-3}$ were observed, commensurate with the magnitude of plumes from wildfires on longer timescales, as well as the magnitude of plumes that might be expected near other major highways on the same timescale. Finally, Chapter 4 quantifies variance among calibration parameters for a large sample of the sensors, as well as the error associated with the remote transfer of calibrations between two sufficiently large sets ($\pm$ 10 % for $n = 12$). These findings suggest that datasets generated with similar sensors could also improve upstream scientific understandings of fluxes resulting from indoor and outdoor emissions, atmospheric transformations, and transport, and may also facilitate timely and empirical verification of interventions to reduce emissions and exposures, in many important contexts (e.g., the provision of improved cookstoves; congestion pricing; mitigation policies attached to infill development; etc.). They also demonstrate that calibrations against continuous reference monitoring equipment could be remotely transferred, within practical tolerances, to reasonably sized and adequately resourced participatory monitoring campaigns, with minimal risk of disruption to existing monitoring infrastructure (i.e., established monitoring sites). Given a collaborator with a short window of access to a reference monitoring site, this would overcome a nominally important barrier associated with non-gravimetric, *in-situ* calibration of continuous $PM_{2.5}$ monitors. Progressive and disruptive prospects linked to a proliferation of comparable sensing technologies based on commodity hardware are discussed in Chapter 5.

To Cristen, my partner in all things,

and to Benjamin, my hope and joy.

Contents

List of Figures

List of Tables

Preface

All of the work presented henceforth was conducted under the supervision of the Graduate Group in Environmental Health Sciences at the University of California, Berkeley.

A version of Chapter 2 has been published in *Environmental Health Perspectives* [Holstius D, Reid C, Jesdale B, Morello-Frosch R. Birth Weight Following Pregnancy During the 2003 Southern California Wildfires. *Environ Health Perspect* 120(9):1340–5, 2012]. I was the lead author, responsible for the literature review, interrupted time-series design, primary analyses, and primary manuscript composition. The original concept and supporting dataset (birth records) are due to R. Morello-Frosch, who was the supervisory author. C. Reid conducted the secondary analysis pertaining to PM_{10}. B. Jesdale curated the original dataset. R. Morello-Frosch, C. Reid, and B. Jesdale discussed the findings and contributed to the editing and revision of the published manuscript.

A version of Chapter 3 has been published in *Atmospheric Measurement Techniques* [Holstius D, Pillarisetti A, Smith KR, Seto E. Field calibrations of a low-cost aerosol sensor at a regulatory monitoring site in California. *Atmos Meas Tech* 7:1121–1131, 2014]. I was the lead investigator, responsible for all major areas of concept formation, instrument design and construction, field deployment, data collection and cleaning, primary and secondary analyses, and manuscript composition. Figure 3.1 was photographed by A. Pillarisetti. Numerous volunteers helped to assemble instruments, and personnel at the local Air District facilitated access to field sites (see Acknowledgments). E. Seto was the supervisory author. A. Pillarisetti, E. Seto, and K. R. Smith contributed to the editing and revision of the published manuscript.

I was the lead investigator for the project described in Chapter 4, and was solely responsible for all major areas of concept formation, instrument design and construction, field deployment, data collection and cleaning, primary and secondary analyses, and manuscript composition. Personnel at the local Air District again facilitated access to field sites (see Acknowledgments). E. Seto and K. R. Smith supervised the project.

Chapters 1 and 5 are original, unpublished, independent work by the author, D. Holstius.

Acknowledgments

I gratefully acknowledge the SF Bay Area AQMD and UC Berkeley CITRIS for their institutional support of this work, especially Chapters 3 and 4. Phil Martien and Virginia Lau guided the District's sponsorship of fieldwork and analyses, while Glen Colwell, Rob Schusteritsch, and David Beyer generously facilitated access to field sites.

From the beginning, Michael Jerrett, Bob Spear, Kathie Hammond, and many other Berkeley faculty graciously made available their insights, connections, facilities, and resources to get the ball rolling. I was privileged to have the freedom afforded by a Berkeley Fellowship, for which I thank my sponsors immensely. In completing the project, it has been a great honor to work alongside the students and in the lab of Ron Cohen. He provided space to work when it was needed most. I don't know a better scientist.

Chapter 2 is indebted to Rachel Morello-Frosch, Bill Jesdale, and Colleen Reid, who proved to be the best colleagues and co-authors anyone could ask for. I thank Rachel, especially, for her on-the-ground leadership, and for her crucial role in shaping and supporting Chapter 2 "on the side". She has been a truly great mentor in all respects.

Chairing a dissertation is hard and under-appreciated work. My co-chair, Edmund Seto, has been my primary advisor since the beginning. He has served with great forbearance as a source of inspiration and support, both moral and material. Moreover, he has gone to profound lengths to create and sustain environments in which his students can excel. When Edmund departed for rainier pastures, Kirk Smith stepped in to chair this thesis and guide it to the finish line. His group's work steered me onto this path long ago. I owe both of them a great debt.

For their companionship, solidarity, and freely volunteered time and energy, I am grateful to many others at Berkeley, including Molly Davies, Ajay Pillarisetti, Drew Hill, Ben Greenfield, Bob Gunier, Ellen Kersten, Lara Cushing, Amanda Northcross, Zoë Chafe, Eunice Lee, Sally Pusede, Katja Weichsel, Andrew Hooker, Ben Weia, Hilary Ong, Aaron Bestick, Dave Bauer, Victor Shia, Posu Yan, Daniel Wu, Cathy Newman, Holly Maness, Ben Nault, Alexis Shusterman, Tamara Sparks, Megan Viera, Paul Romer, Xueling Liu, Anna Mebust, Lance Lee, Josh Laughner, and Paul Wooldridge. I am especially grateful for the generous friendship of Jill Teige, a fellow PhD student, who made room for me under the aegis of the BEACON project.

For the chance to pursue the work that led to Berkeley, I have long been grateful to Illah Nourbakhsh, Carl DiSalvo, Chris Bartley, Josh Schapiro, Gabriel O'Donnell, Emily Hamner, Tom Lauwers, Ayça Akin, Laura Tomokiyo, Mary Jo Knelly, Ian Ingram, Kristen Stubbs, Jeff Baker, Dror Yaron, and Randy Sargent.

My parents, wife, and family made this possible from the very beginning. Their patience and love have been beyond measure.

Thank you to the ever-resourceful Tracy Allen, and to all the makers who made their know-how freely available. I could not have hacked this together without you, and I hope you find something useful here.

To the people who made it possible not only for myself, but for all of us—Norma Firestone, Margaret Nguyen, Justin Girard, Michael Murphy, María Teresa Hernández, Maria Rodriguez, and innumerable other staff at Berkeley—thank you for your tireless work.

Chapter 1

Introduction

1.1 Background

Health effects attributed to outdoor fine particulate matter ($PM_{2.5}$) rank it among the risk factors with the highest health burdens in the world, annually accounting for over 3.2 million premature deaths and over 76 million lost disability-adjusted life years (Brauer et al., 2012; Lim et al., 2012). Existing $PM_{2.5}$ monitoring infrastructure cannot, however, be used to resolve variations in ambient $PM_{2.5}$ concentrations with adequate spatial and temporal density, or with adequate coverage of human time-activity patterns, such that the needs of modern exposure science and control can be met (McKone, Ryan, and Özkaynak, 2009; National Research Council, 2012). In studies of exposures and health effects, the resulting exposure misclassification may attenuate or bias estimates of health effect relationships, and may also mask or prevent the correct identification of non-PM related pathways plausibly backed by other lines of research (Zou et al., 2009; Health Effects Institute, 2010; Baxter et al., 2013; Özkaynak et al., 2013). Coarsely resolved monitoring data also hinders upstream scientific understandings of fluxes resulting from indoor and outdoor emissions, atmospheric transformations, and transport; downstream, it inhibits timely and empirical verification of interventions to reduce emissions and exposures (e.g., the provision of improved cookstoves; congestion pricing; mitigation policies attached to infill development; etc.).

In the absence of adequate empirical measurements, epidemiological studies focusing on urban-scale datasets have relied upon models to downscale or interpolate available data from satellites, regulatory monitors, land use databases, and emissions inventories (Brauer et al., 2012; Jerrett et al., 2005; Özkaynak et al., 2013; Health Effects Institute, 2010). Epidemiologists have argued that, in principle, increased fixed-site monitoring could improve the coverage and quality of ambient $PM_{2.5}$ datasets, but that the expansion of regulatory networks with current technology is hindered by resource constraints, as conventional techniques require costly equipment (for an overview, see Wilson et al., 2002). More targeted exposure assessments relying on labor-intensive or capital-intensive measurement techniques, such as those that might be conducted within the purview of a cohort study, are forced to trade off between

sampling designs that sacrifice precision in different ways (see McCracken et al., 2009). Some community-engaged participatory research projects have attempted to expand local monitoring coverages by deploying their own fixed-site monitors (Brugge et al., 2010; Hedges, 2002; Loh et al., 2002) or surveying intra-urban variations in $PM_{2.5}$ using portable nephelometers (Kinney et al., 2000; Pastor Jr. Morello-Frosch, and Sadd, 2010). Based on these overlapping arguments and activities, it seems reasonable to suppose that small, inexpensive, and portable devices, relying on newly available off-the-shelf sensors, might improve the capacity of these actors to create, and perhaps to publish or share, authoritative $PM_{2.5}$ datasets with improved resolution and coverage—especially if many such devices could be deployed concurrently with low system cost (Snyder et al., 2013).

Thusly motivated, previous studies of lower-cost aerosol measurement techniques have used observational and experimental methods to characterize instruments incorporating repurposed smoke-detector components (Chowdhury et al., 2007; Edwards et al., 2006; Litton et al., 2004) and consumer-oriented, laser-based particle counters (Northcross et al., 2013; Smith, 2011). Previous studies have also characterized short-term responses of relatively inexpensive optical instruments, both custom-built and commercially available, to particle-generating activities in indoor environments (Budde, Busse, and Beigl, 2012; Nafis, 2012; Olivares, Longley, and Coulson, 2012). A larger body of scientific work has compared commercially available nephelometers, particle counters, and other light-scattering instruments to reference methods (Burkart et al., 2010; Watson et al., 1998; Wilson et al., 2002). A peripheral subset has focused on "citizen scientists" constructing and using their own low-cost air pollution instrumentation (Demuth et al., 2013; Smith and Clark, 2013), as well as efforts to support this kind of innovation and to integrate it with established pollutant monitoring infrastructures (CITI-SENSE, 2012; US EPA, 2013). Reciprocal relationships with research-engineers in atmospheric science (Mead et al., 2013; Teige et al., 2011), networked sensor calibration (Hasenfratz, Saukh, and Thiele, 2012; Balzano, 2007; Xiang et al., 2012) and mobile/participatory air quality sensing (Aoki et al., 2009; DiSalvo et al., 2012; Dutta et al., 2009; Honicky et al., 2008; Jiang et al., 2011; Mun et al., 2009; Nikzad et al., 2012; Paulos, Honicky, and Goodman, 2007; Willett et al., 2010) have generally reinforced visions of improved exposure science catalyzed by technological and methodological advances in related fields.

1.2 Key contributions

The inadequacy of existing monitoring infrastructure is motivated and exemplified by Chapter 2, an epidemiological study that investigated a series of wildfires in Southern California. These wildfires exposed large urban populations to elevated levels of PM over a timeframe of several weeks. Although Los Angeles has one of the largest and densest urban air quality monitoring networks in the world, from the available data and methods it was possible only to conclude that pregnancy during the wildfires was associated with slightly reduced average birth weight among infants exposed in utero (Holstius et al., 2012). A sensitivity analysis, in which mothers were assigned by place of residence to the nearest PM monitoring site, did not reveal any

differences between groups of "high" versus "low" PM exposure, given that operationalization of exposure. Finer-grained metrics of exposure, including personal monitoring, were not available; thus, it was not possible to construct quantitative estimates of dose-response, nor to more specifically characterize the potentially conjoint contributions of PM exposure and psychological stress. Although personal mobility can be an important component of exposure variation in pregnant cohorts (Gilliland et al., 2005; Nethery et al., 2008; Woodruff et al., 2009), it seems plausible that a more spatially and temporally dense fixed-site monitoring network could have improved the retrospective assessment of exposure within the context of this natural experiment, leading to more significant findings.

Chapter 3 begins to explore possibilities for the next wildfire, the next industrial release, or the next study of the more mundane, yet much more costly, chronic PM exposures that occur in the world today. It demonstrates the possibility of generating useful and accurate estimates of hourly and daily $PM_{2.5}$ concentrations at a regulatory monitoring site by combining a newly available low-cost sensor with other low-cost, readily available hardware. Guided by the prior work of Watson, Wilson, Chow and colleagues (Watson, 2002; Watson et al., 1998; Wilson et al., 2002; Wilson et al., 2005; Wilson and Suh, 1997), who extensively analyzed and discussed issues in the augmentation of the then-current Federal Reference Method (FRM) $PM_{2.5}$ network with continuous PM monitors, Chapter 3 concentrates first and foremost on demonstrating a *predictive* relationship between (a) the output of the sensor and (b) regulatory monitoring data that is widely relied upon in air quality regulation and epidemiology. (Given a predictive relationship, further work is still required to establish *equivalency* with $PM_{2.5}$ or any other measures of concentrations or properties.) The intent of Chapter 3 is to demonstrate "proof of concept" in a natural environment of interest, so that the findings and methodology can be extended, critiqued, and replicated or refuted by independent researchers working with this class of sensors. It is apparently the first published work to evaluate such a low-cost sensor (approximately USD 10) under ambient conditions at a United States regulatory monitoring site, and the first to calibrate it using 24 h averages of $PM_{2.5}$ from a reference instrument with Federal Equivalent Method (FEM) status. As operationalized by correlation with an FEM instrument, performance at 1 h scale was comparable to commercially available optical instruments costing considerably more (Holstius et al., 2014).

Findings from Chapter 3 warranted further exploration of the circumstances under which this class of aerosol sensors could profitably be deployed to generate improved $PM_{2.5}$ datasets. Chapter 4 demonstrates that, in addition to being viable components of instruments for observing variations in "background" aerosol concentrations at 1 h to 24 h scale at an existing monitoring site, the same sensors can also be used to observe plumes at a near-roadway site, at scales of 1 min to 10 min and 100 $\mu g\,m^{-3}$ to 200 $\mu g\,m^{-3}$. This strengthens the case that they could be used to observe larger gradients in concentrations over longer durations. Still, further work is required to characterize their upper limits of detection, as well as their sensitivity to aerosols generated by other sources, such as biomass combustion. Collaborative possibilities for this work are naturally of interest. Chapter 4 shows that the sensors in question have an amenability to simple and stable cross-calibrations that could facilitate continuous calibration against reference standards without the risk of interfering with regulatory monitoring, support-

ing prospects for broader participation in collaborative calibration and monitoring campaigns.

Independent confirmation or refutation of these findings, and better characterization of the limitations of these sensors, will be required. However, given the accelerating speed of sensor research and development, it is more important to consider the demonstrations supplied in this thesis as contributions toward frameworks for rapid screening and evaluation of the next generation of aerosol sensors, rather than attempts to fully characterize a specific sensor. The development of new sensors is likely to outpace present capacity for resource-intensive, laboratory-based calibration practices. Chapter 5 concludes this thesis with remarks on pertinent trends, and their relevance for exposure science and control in the near term, as well as a more sociotechnically oriented appraisal of relevant conditions and factors.

Chapter 2

Birth weight following pregnancy during the 2003 Southern California wildfires

2.1 Background

In late October 2003, a series of wildfires burned > 750,000 acres of forest in Southern California (Blackwell and Tuttle, 2003). Strong Santa Ana winds carried the resulting plumes of smoke toward Los Angeles and Orange counties, where a large urban population was exposed to elevated concentrations of air pollutants from the fires (Phuleria, Fine, and Zhu, 2005). An in-depth exposure assessment study estimated the population-weighted PM_{10} (PM with aerodynamic diameter $d_p \leq 10\,\mu m$) and $PM_{2.5}$ (PM with $d_p \leq 2.5\,\mu m$) concentrations, respectively, at 190 and 90 $\mu g\,m^{-3}$ under heavy smoke conditions, and 125 and 75 $\mu g\,m^{-3}$ under light smoke conditions, compared with baseline concentrations of 40 and 20 $\mu g\,m^{-3}$ in the same region (Wu, Winer, and Delfino, 2006).

Using that exposure assessment, a study (Delfino et al., 2009) of cardiorespiratory health effects estimated that elevated $PM_{2.5}$ levels led to a 34 % increase in hospital admissions for respiratory conditions 1–2 days later, with the largest associations observed among the very young (0–4 years, 8.3 % per 10 $\mu g\,m^{-3}$ increase in $PM_{2.5}$) and very old (65–99 years, 10.1 % per 10 $\mu g\,m^{-3}$ increase in $PM_{2.5}$); limited evidence supported a small increase in admissions for cardiovascular conditions as well (Delfino et al., 2009). A separate study found that parental recall of the smell of smoke during these fires was associated with increased medication usage, eye and respiratory symptoms, and physician visits among their children (Künzli et al., 2006).

Particulate matter (PM) is possibly the most important health-related component of wildfire events (Naeher et al., 2007). Wildfire-generated PM may be more toxic, on an equal-mass basis, than ambient PM collected in the same region during non-fire periods (Wegesser, Pinkerton, and Last, 2009), potentially due to the role of atmospheric photochemistry resulting in the formation of secondary pollutants (Wegesser et al., 2010). Wildfires have been shown to enhance $PM_{2.5}$ levels in many parts of the western United States (Jaffe et al., 2008), and recent studies have linked smoke exposure from wildfire events with spikes in morbidity in Canada

(Henderson et al., 2011; Moore et al., 2006), Australia (Cameron et al., 2009; Chen, Verrall, and Tong, 2006; Johnston et al., 2002; Johnston et al., 2002; Morgan et al., 2010; Tham et al., 2009), Southeast Asia (Emmanuel, 2000; Mott et al., 2005; Sastry, 2002), Finland (Hänninen et al., 2009) and California (Delfino et al., 2009; Künzli et al., 2006; Viswanathan et al., 2006); for a review, see Dennekamp and Abramson (2011).

Air pollution may not be the sole mechanism through which wildfire events affect health. For instance, wildfires threaten person and property; and news of an inherently unpredictable force of nature in itself may induce psychosocial stress in the population (Kumagai, Carroll, and Cohn, 2004). Although the main effect of wildfire events on birth weight is likely mediated through their air pollution effects, distinguishing between these potential mechanisms is methodologically challenging.

Objectives and study design

The objective of this study[1] was to estimate the birth weight effects associated with in utero exposure to a wildfire event. As of the time of writing, one abstract had been published concerning the effects of wildfire smoke exposure on birth outcomes (Breton, Park, and Wu, 2011). Although little is known regarding the health effects of acute maternal exposures to smoke from wildfires, chronic maternal exposures to related hazards, including ambient particulate matter and indoor biomass smoke, have been linked to adverse birth outcomes, including lower birth weight. Many epidemiological studies have found associations between exposure to ambient PM and preterm birth or birth weight; for reviews, see Bosetti et al. (2010) and Glinianaia et al. (2004).

A recent meta-analysis of studies examining chronic maternal exposures to indoor air pollution in developing countries, such as that generated by cooking or heating with solid fuels, concluded that such exposures increase the risk of adverse pregnancy outcomes, including percent low birth weight, stillbirth, and reduced mean birth weight (Pope et al., 2010).

The study of natural experiments can be a methodologically useful way to advance research on air pollution and perinatal effects (Parker, Mendola, and Woodruff, 2008; Woodruff et al., 2009). Time-series studies can reduce threats to validity posed by exposure misclassification and confounding by variables that are associated with both ambient air pollution and perinatal outcomes, such as social class (Parker, Mendola, and Woodruff, 2008); thus they are a useful complement to observational studies of chronic exposures. Thus, this time-series study was carried out to examine trimester-specific differences in mean birth weight among infants delivered to mothers residing in the South Coast Air Basin (SoCAB) before, during, and after the Southern California wildfires of 2003.

[1] First published as Holstius et al. (2012).

2.2 Methods

Study population

Birth records were obtained for infants delivered in the South Coast Air Basin (SoCAB) from 1 January 2001 through 31 December 2005 from the Non-Confidential Birth Statistical Master File, provided by California's Center for Health Statistics at the California Department of Health Services (California Automated Vital Statistics System 2006, unpublished data). Preterm births (< 37 weeks gestation), post-term births (> 42 weeks gestation), and births with a reported birth weight < 1 kg or > 6 kg were excluded, yielding a total of 886,034 births for this analysis. Gestational ages were based on the number of days since the mother's reported last menstrual period (LMP).

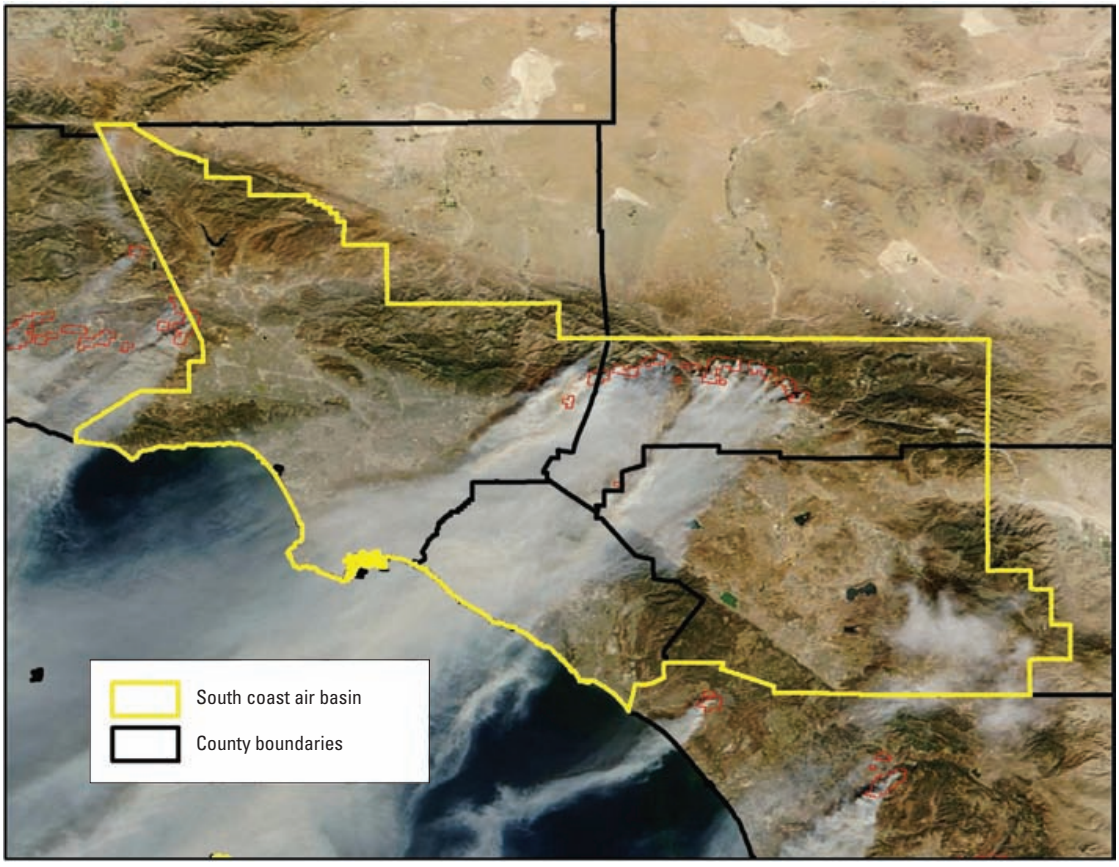

Fig. 2.1: Geographic extent of the SoCAB study area, outlined in yellow, overlaid on MODIS satellite image from 26 October 2003. Active fires were outlined in red by NASA.

The SoCAB, which forms the geographic basis for the study population, includes the entirety of Orange County as well as populous areas within Los Angeles, San Bernardino, and Riverside counties. This air basin was chosen as the boundary for the study on the basis of satellite

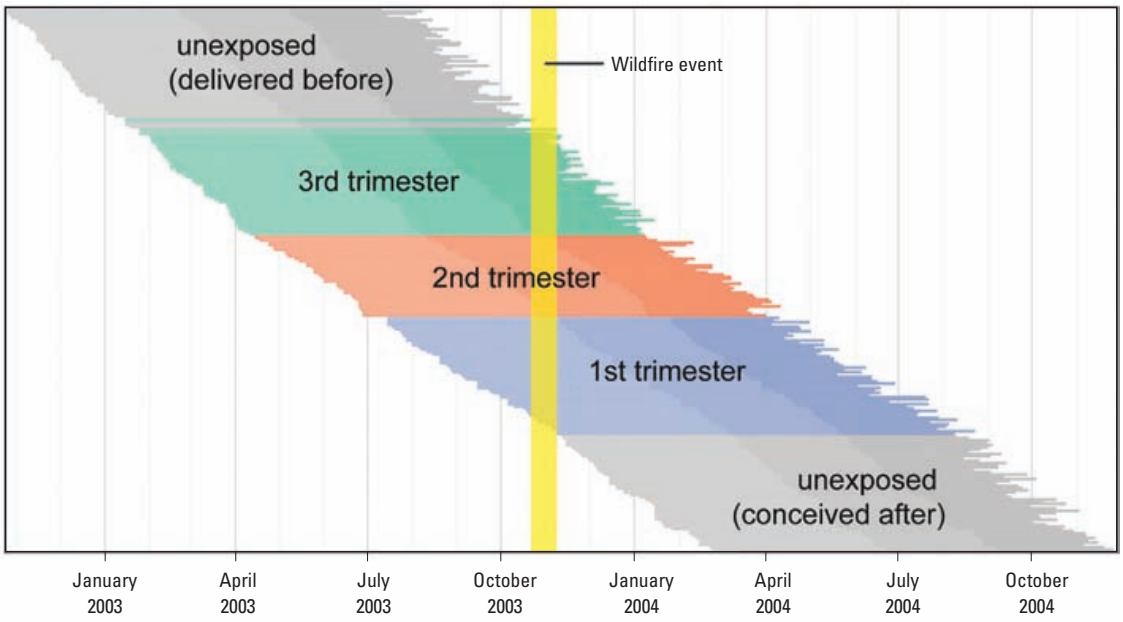

Fig. 2.2: Schematic illustrating exposure assignment. Exposure status was assigned based on the overlap between the wildfire event (yellow) and estimated gestational intervals (horizontal segments). For clarity, gestational intervals are shown ordered from top to bottom by the LMP, and only a 0.1% sample from 2002–2004 is shown. Dates on the x-axis correspond to the beginning of quarters used to adjust for seasonality.

images of the fires; it is partially bounded by mountains that trap air pollution in the absence of wind (Fig 2.1). The SoCAB does not contain Ventura and San Diego counties, which were also exposed to smoke during the 2003 wildfires.

Exposure assessment

On the basis of reports from the California Department of Forestry and Fire Protection (Blackwell and Tuttle 2003) and inspection of Moderate Resolution Imaging Spectroradiometer (MODIS) satellite imagery, the window of potential wildfire exposure was defined as 21 October – 10 November 2003. Most births in the study population ($n = 491,496$) were delivered before 21 October 2003 and could not have been exposed in utero. An additional 256,094 births were assigned a Last Menstrual Period (LMP) later than 10 November 2003, and were also classified as unexposed. All remaining births ($n = 138,444$) were classified as exposed on the basis of temporal overlap between the wildfire exposure window and gestational intervals.

The primary analysis used this temporal contrast as the basis for exposure assessment. However, a sensitivity analysis was also conducted, in which spatial contrasts were examined based on proximity of maternal residence census tracts to air monitors. Tracts closer to monitors with average PM_{10} measures during the fires of $< 40\,\mu g\,m^{-3}$ were classified as low exposure,

and tracts with average daily levels $> 40\,\mu g\,m^{-3}$ were classified as high exposure. This cut point split the PM_{10} monitors in the SoCAB in half, with 36 % of births that gestated during the fires occurring in high exposure census tracts.

Covariates and primary model

Data were fit to a linear fixed-effects model (Equation 1) with birth weight (y_i) as a continuous outcome and x_{ij} as an indicator of exposure for birth i in trimester j. For the primary analysis, x_i was defined as a categorical variable with four levels: exposed in trimester 1; exposed in trimester 2; exposed in trimester 3; or unexposed (Fig 2.2). The first trimester was defined as weeks 1–16 since LMP; the second as weeks 17–28; and the third as week 29 through the end of gestation. When the wildfire event overlapped with two trimesters, exposure was assigned to the trimester with the greater number of days of overlap. Maternal and birth characteristics (z_i) associated with birth weight, and terms based on the date of the LMP (t_i), were included as covariates to control for seasonality and trend.

$$y_i = \beta_0 + \beta_1 x_{i1} + \beta_2 x_{i2} + \beta_3 x_{i3} + \eta' z_i + f(t_i) + \epsilon_i \tag{2.1}$$

Analysis was limited by the availability of information on administrative birth records. From among the variables included on these forms, several were selected to represent maternal characteristics (age, educational attainment, parity, race/ethnicity) and characteristics of the birth itself (infant's sex, gestational age) known to have a substantial influence on birth weight. These variables may have confounding potential, or play a role in explaining variation even in the absence of a confounding effect. Parity of the mother was coded with three levels: first live birth (reference), second live birth, or third or more live births. Gestational age (weeks since LMP) was coded as 37 (reference), 38, 39, 40, 41, or 42 weeks. As a proxy for socioeconomic status, maternal education was coded with four levels: less than a high school education; completed high school or equivalent (reference); 1–3 years of postsecondary education; and $\geq$ 4 years of postsecondary education. Maternal race/ethnicity was coded as non-Hispanic white (reference); Hispanic of any race; non-Hispanic black; non-Hispanic Asian; and unknown/ multiple/other. Fetal sex was coded with male as the referent category.

To account for secular trend and seasonal effects, $f(t_i)$ was parameterized as a combination of a linear secular trend based on the date of the last menstrual period for birth i (t_i) and categorical indicator terms for the season of birth (in quartiles): Q1 (January–March, reference), Q2 (April–June), Q3 (July–September), or Q4 (October–December):

$$f(t_i) = \beta_{trend}(t_i) + \beta_{Q2} I_{Q2} + \beta_{Q3} I_{Q3} + \beta_{Q4} I_{Q4} \tag{2.2}$$

Sensitivity analyses

In addition to the primary analyses, three sensitivity analyses were conducted. In the first, the population was dichotomized according to whether the maternal residence census tract

was closer to a PM_{10} monitor active during the fire period with an average PM_{10} measure $> 40\,\mu g\,m^{-3}$, or closer to a PM_{10} monitor with a lower average PM_{10} during the fire period. In the second, because of the association between season and trimester of exposure (Table 2.1, Figure 2.2), $f(t_i)$ was instead parameterized as a smooth, periodic, sinusoidal function of time known as the cosinor (Barnett and Dobson, 2010) (see Appendix B.1). In the third, because accounts differ concerning the length of the wildfire event, the length of the modeled wildfire event was reduced to peak exposure periods of 2 weeks or 1 week instead of 3 (keeping the starting date unchanged), and exposures were reassigned accordingly.

Statistical software

R version 2.14.0 and the `stats::lm()` function were used for model fitting. To fit the cosinor-based seasonal model, the `season` package, version 0.2–6 (R Project for Statistical Computing, Vienna, Austria) was used.

2.3 Results

Of the 886,034 births in this analysis, 84.4% ($n = 747,590$) were unexposed in utero. Of the 138,444 exposed, 28.0% ($n = 38,739$) were exposed in the third trimester, 28.5% ($n = 39,435$) were exposed in the second trimester, and 43.5% ($n = 60,270$) were exposed in the first trimester (Table 2.1).

Most infants in the study were delivered to Hispanic mothers (60.5%), followed by non-Hispanic white (22.0%), non-Hispanic Asian or Pacific Islander (11.3%), and non-Hispanic black (5.9%) mothers. Most infants were delivered to mothers 18–34 years of age (76.1%), with 20.8% delivered to mothers 35–50 years of age and 3.1% delivered to mothers 15–18 years of age. Approximately one-third of mothers had less than a high school education (32.1%), whereas 28.4% had completed a high school degree or equivalent, 18.1% had 1–3 years of postsecondary education, and 21.4% had ≥ 4 years of post-secondary education.

No substantive differences were observed between the exposed and unexposed with respect to measured covariates, except for season of birth (Table 2.1). Effect estimates for covariates are reported in Table 2.3.

Estimated effects of wildfire exposure

Adjusted models revealed that mean birth weight was 6.1 g lower [95% confidence interval (CI): -8.7, -3.5] among infants exposed in utero during any trimester compared with unexposed infants (Table 2.2). Among those exposed in the third trimester, a reduction of 7.0 g (95% CI: -11.8, -2.2) was observed. The largest estimated effect was observed in the second trimester, with a reduction of 9.7 g (95% CI: -14.5, -4.8). Among infants exposed in the first trimester, a decline in mean birth weight was observed but it was not statistically significant (3.3 g; 95% CI: -7.2, 0.6) (Table 2.2). Both unadjusted and adjusted estimates are reported in Table 2.2;

Table 2.1: Maternal and infant characteristics (%), by wildfire event exposure status and trimester of exposure ($n = 886,034$).

		Trimester exposed		
Variable	**Unexposed** ($n = 747,590$)	**First** ($n = 60,270$)	**Second** ($n = 39,435$)	**Third** ($n = 38,739$)
Fetal sex				
Male	51.0	51.0	50.7	50.9
Female	49.0	49.0	49.3	49.1
Gestational age (weeks)				
37	4.8	4.7	5.0	3.9
38	10.9	10.6	11.1	9.7
39	23.0	22.6	22.9	21.9
40	29.2	29.9	29.5	29.5
41	22.6	22.6	21.9	24.1
42	9.4	9.6	9.6	10.9
Parity				
1	38.1	38.7	38.8	39.5
2	31.8	31.8	31.5	31.3
3 or more	30.1	29.5	29.7	29.1
Maternal age (years)				
Less than 18	3.1	3.0	3.0	3.0
18–34	76.1	75.8	76.0	76.4
35–50	20.8	21.2	21.0	20.5
Maternal education				
Less than high school	32.3	31.0	31.7	31.9
Completed H.S. or equivalent	28.4	27.6	27.8	28.6
1–3 years postsecondary	18.1	18.5	17.8	17.9
$\geq$ 4 years postsecondary	21.2	22.9	22.7	21.5
Maternal race/ethnicity				
Hispanic	60.6	60.0	59.9	60.5
Non-Hispanic White	22.0	22.6	22.3	21.3
Non-Hispanic Asian	11.2	11.4	11.6	11.9
Non-Hispanic Black	5.9	5.7	5.9	6.0
Non-Hispanic other/unknown	0.3	0.3	0.3	0.3
Season				
Q1 (January–March)	24.8	0.0	0.0	87.6
Q2 (April–June)	23.0	0.0	94.8	12.4
Q3 (July–September)	23.0	66.7	5.2	0.0
Q4 (October–December)	29.3	33.3	0.0	0.0

Table 2.2: Estimated effects of wildfire event during gestation on birth weight.

	Unadjusted model		*Adjusted model*	
Trimester of exposure	**Effect (g)**	95 % **CI**	**Effect (g)**	95 % **CI**
Third ($\geq$ 29 weeks)	-7.9	(-12.8, -3.1)	-7.0	(-11.8, -2.2)
Second (17–28 weeks)	-17.1	(-21.9, -12.3)	-9.7	(-14.5, -4.8)
First (1–16 weeks)	-3.9	(-7.8, 0.0)	-3.3	(-7.2, 0.6)
Any trimester	-8.8	(-11.5, -6.1)	-6.1	(-8.7, -3.5)

subsequent discussion is restricted to the adjusted model. Sensitivity to the specification of start and end dates for the wildfire event was assessed by specifying models with the wildfire duration defined as 2 weeks or 1 week of peak intensity instead of 3 weeks to assess sensitivity. Main effects were not substantively altered (data not shown).

Among births in census tracts proximal to monitors with higher average PM_{10} during the wildfire event, the estimated decrement in birth weight associated with pregnancy (any trimester) during the event was 6.6 g (95 % CI: -11.0, -2.2). In tracts more proximal to monitors with average PM_{10} levels $< 40\,\mu g\,m^{-3}$, the estimated decrement in birth weight associated with pregnancy during the event was 5.9 g (95 % CI: -9.2, -2.6). These estimates were not discernibly different from each other (Table 2.5).

Seasonality and trend

Over the entire period, 2001–2005, there was a secular decline in mean birth weight of 6.9 g per year (95 % CI: -7.6, -6.2) (Table 2.3). Those conceived in Q3 (July–September) had the highest estimated mean weight at birth, 11.9 g (95 % CI: 9.0, 14.7) more than infants conceived in Q1 (January–March), the referent time period. Infants conceived in Q1 weighed the least.

Using an alternate model with seasonal effects parameterized as a cosinor, the magnitude of the seasonal effect was comparable (11.6 g; 95 % CI: 7.7, 15.5), as was the relative timing (i.e., phase) of highest birth weight, with the maximum occurring on 4 August (95 % CI: 29 July, 7 August) (Table 2.4).

Goodness-of-fit and residuals

The adjusted R^2 for the full model was 0.109. Residuals were plotted versus fitted values, and a quantile probability plot was constructed to verify that the residual distribution was normal. No heteroskedasticity of the residuals was apparent (data not shown).

2.4 Discussion

A slight reduction in estimated mean birth weight was evident among term infants exposed in utero to the 2003 California wildfires. The strongest estimated effect was observed for second-trimester exposure, followed by third-trimester exposure.

Climate change scientists predict that wildfires will increase in frequency and magnitude as global temperatures increase and rainfall patterns change (Westerling and Bryant, 2008; Westerling et al., 2006). These increases in wildfire events are projected to add to atmospheric pollution in the western United States under various climate change scenarios (Spracklen et al., 2009). In California, smoke impacts are already a required consideration in the planning and execution of preventive wildfire management activities, such as prescribed burns. For example, forest management professionals are required to assess the likely direction of smoke plumes and gauge their potential for impact on smoke sensitive areas (State of California 2001). Kochi et al. (2010) make the case that optimal wildfire management policy should explicitly include estimates of health-related and economic costs of wildfire smoke exposure.

Potential etiologic pathways

At least two categories of etiologic pathways plausibly link maternal wildfire exposure with lower birth weight: biological (exposure to air pollution from the fires) and psychosocial (stress caused by direct or indirect consequences of wildfires). A combination of the two is also plausible. This study could not differentiate the contributions of these two pathways, because daily air pollution exposures for each birth, and individual or ecological indicators of maternal stress, could not be accurately quantified. Nevertheless, the results may reflect the potential conjoint effect of these two pathways.

Among the biological mechanisms hypothesized as having a possible effect on intrauterine growth rate are: hypoxia and/or oxidative stress resulting from exposure to woodsmoke constituents, including carbon monoxide and PM (Siddiqui et al., 2008); alteration of maternal-placental exchanges; endocrine disruption; and oxidative stress pathways leading to alteration of maternal host-defense mechanisms and elevated infection risk (Slama et al., 2008). Reviews have found limited applicable research from animal and toxicological studies to distinguish these possible mechanisms (Ritz and Wilhelm, 2008; Slama et al., 2008; Woodruff et al., 2009). Human studies of the acute effects of wildfire smoke exposure on firefighters have demonstrated inflammatory responses and pulmonary function test declines (e.g. Swiston et al., 2008). Human experiments in which healthy non-smokers were exposed to woodsmoke under controlled conditions, with concentrations of $PM_{2.5} > 240\,\mu g\,m^{-3}$ for up to 4 hr, resulted in elevated levels of blood and urine biomarkers indicating oxidative stress and pulmonary inflammation in the lower airways (Barregard et al., 2006; Barregard et al., 2008; Sällsten et al., 2006). More recent experiments confirmed biomarkers of systemic and pulmonary inflammation in blood and lavage, but found no effect on pulmonary function or self-reported symptoms, and minimal effects on indices of heart rate variability (Ghio et al., 2011).

Psychosocial aspects of wildfire exposure may also contribute to adverse health outcomes, although this is an understudied topic (Kumagai, Carroll, and Cohn, 2004). Several studies have observed signs of fetal stress and adverse birth outcomes in the aftermath of disasters such as earthquakes (Weissman et al., 1989), shipwrecks (Catalano and Hartig, 2001), and terrorist attacks (Catalano et al., 2005). Plausible causes of stress in the wake of wildfires include loss of property, shelter, money, and other basic individual resources; physical incapacitation or injury; and disruption of sharing and support networks (Fowler, 2003).

Further analyses with methods that better characterize individual-level pollution exposures and psychosocial stress would be required to distinguish the relative contribution of the two pathways.

Exposure misclassification

This study captured temporal variation in wildfire exposure, but was limited in its ability to account for spatial variation. The SoCAB includes areas that were likely not directly exposed to heavy smoke plumes or to significant concentrations of diffused smoke. Because of its reliance on administrative vital statistics records, this study could not assess whether mothers resided within the air basin throughout their pregnancies, or determine how much time they spent at their primary residence. Meteorology, time-activity patterns, and variations in the built environment likely all contributed to variations in individual exposures, and therefore to exposure misclassification. Because this study did not capture variations in exposure among the exposed, it was not possible to quantify dose-response relationships. A relatively small number of highly exposed mothers in this region may have been affected to a greater degree than the marginal estimates would predict.

When a sensitivity analysis was conducted in an attempt to distinguish between births located in higher versus lower PM_{10} tracts during the wildfire event, the decrease in birth weight associated with gestational wildfire exposure was comparable between the two populations. This result may be attributable to the fact that monitoring results could not adequately capture differences in ambient PM_{10} levels. Improved analysis with PM_{10} as a continuous variable or modeling of the PM exposure using satellite data or chemical transport models might reveal a relationship between wildfire-related PM exposure and birth weight. Alternatively, it is also possible that the associations with decreased birth weight were mediated not by air pollution but by some other mechanism, such as stress.

Several factors could explain the finding of stronger associations with exposure during the second and third trimesters, compared to exposure during the first trimester. First, there is the issue of exposure misclassification. Given that the date of conception is less certain than the date of delivery, it is possible that some infants were categorized as exposed in the first trimester, when in fact their conception date occurred after the fire was over. This misclassification bias is unlikely to affect exposure assessment in the third or second trimester, but may lead to an underestimate of effects during the first trimester. Overestimation of the length of the wildfire event would also have resulted in some unexposed births being misclassified as first-trimester

exposures. However, reducing the length of the wildfire event did not substantively alter the main effects.

Exposure could also have increased the risk of preterm birth or fetal loss. Because preterm births and fetal losses were excluded by design, excess preterm delivery or fetal loss among the first-trimester exposed could have differentially eliminated the most vulnerable from the study population. When Breton, Park, and Wu (2011) examined prenatal exposure to high $PM_{2.5}$ levels from the same wildfires among eight counties in Southern California, using vital statistics records for 2003–2004, they did not estimate a significant effect on preterm birth, but they also did not assess fetal loss. The effects of wildfire exposure on birth weight could also be stronger among those exposed in the second or third trimesters for reasons that are not yet understood. Further examination of the effects of trimester-specific exposures in other studies may help to resolve this question.

Seasonal confounding

Controlling for seasonal variation in time-series studies of air pollution can be a challenge (Slama et al., 2008; Woodruff et al., 2009). For example, both temperature and ambient (non-wildfire) air pollution exhibit seasonal patterns, and these patterns themselves vary geographically due to differences in regional characteristics. In this study, when quarterly indicators were used to control for seasonality, 87.6 % of the infants exposed in the third trimester were conceived in Q1 (January–March), and 94.8 % of those exposed in the second trimester were conceived in Q2 (April–June) (Table 2.1, Figure 2.2). This raised the possibility of confounding between trimester-specific wildfire exposure and conception in the first half of the year.

To address this, a sensitivity analysis was conducted, in which the seasonal component of the model was instead parameterized as a smooth, continuous, and periodic function of time: the cosinor (Barnett and Dobson, 2010). The general form of the cosinor is sinusoidal, like many natural seasonal phenomena, and has only two degrees of freedom, amplitude and phase (see Appendix B.1). As such, it is readily interpretable, and it has been widely applied to the analysis of seasonal and circadian rhythms (Barnett and Dobson, 2010).

The cosinor-based analysis yielded effect estimates consistent with the pattern described by the primary model, increasing confidence in the results. The peak-to-peak amplitude (11.6 g, Table 2.4) in seasonal variation was similar to the difference between the minimum and maximum seasonal coefficients from the model using indicator terms (11.9 g, Table 2.3). The phase was also consistent with the primary model's seasons of lowest and highest average birth weight [January–March (Q1) and July–September (Q3), respectively].

Other potential confounders

This study adjusted for several individual-level covariates known to be associated with birth weight, but data on other potential confounders were not available. For example, maternal smoking is not reported on most California birth records, and its inclusion in the study may have changed the results. However, recent studies suggest that, although smoking during

pregnancy has a large effect on birth weight, it does not significantly confound the association between ambient air pollution exposure and adverse perinatal outcomes in studies of ambient air pollution (Basu et al., 2003; Darrow, Woodruff, and Parker, 2006).

In previous research of wildfire health effects, few studies have attempted to separate the fraction of smoke attributable to wildfire from that attributable to background air pollution (for a review, see (Dennekamp and Abramson, 2011). In areas with significant sources of other pollution, such as the SoCAB, apportionment can be a challenge. Observations from the nearest monitor, which are often used to characterize background air pollution, can be missing during a wildfire episode—sometimes due to the fire itself. To obtain ecologic or individual-level estimates of smoke exposure, several methods can be employed: satellite imagery; dispersion or chemical transport modeling; and/or spatiotemporal interpolation. However, each of these has associated difficulties in implementation and interpretation, especially during a short time window with such atypical meteorology as the Santa Ana winds that fanned the 2003 fires.

To the extent that variation in wildfire-attributable pollution and background pollution are independent, including background pollution in the model could improve the precision of effect estimates, but should not affect the central tendencies. On the other hand, insofar as background concentrations are correlated in space or time with wildfire smoke concentrations (e.g., to the extent that they are similarly determined by physical geography), including background pollution could induce confounding just as including seasonality can. Without access to detailed measurements of both fractions, this study elected to consider a strictly temporal contrast, reserving spatiotemporal refinements of exposure for future work.

Previous studies that have attempted to isolate the contribution of wildfire-generated smoke have also compared health effects to a reference period (e.g. Delfino et al., 2009). However, in any interrupted time-series study, there is always the possibility of an unmeasured confounder with a similar temporal profile to that of the exposure. For example, if a foodborne illness outbreak happened at the same time as the wildfires, and had a negative impact on birth weight, it could conceivably explain part or all of the observed effect. The fact that unexposed births were drawn from both before and after the exposure window, and from other years at the same time of year, helps to reduce such threats to validity, but cannot eliminate them.

2.5 Conclusion

This study indicated that maternal exposure to wildfire events may result in modestly lower infant birth weight. A small decline in birth weight is unlikely to have clinical relevance for individual infants, and there is debate about whether a small shift in the population distribution of birth weight has broader health implications (e.g. Wilcox, 2001). Although the effects estimated are much smaller than for many other exposures, such as smoking, the extent of exposures during wildfire events and their increasing frequency suggests potentially important implications for infant health and development. Finally, future research should also assess alternative mechanistic pathways besides air pollution (such as stress) for understanding the adverse health effects of wildfire events.

Table 2.3: Binary (left) and trimester-specific (right) exposure classifications, with quarterly terms for season.

	Effect (g)	95 % **CI**	**Effect (g)**	95 % **CI**
Exposure				
All trimesters before/after	(ref)		(ref)	
Wildfire during any trimester	-6.1	(-8.7, -3.5)		
Wildfire during first trimester			-3.3	(-7.2, 0.6)
Wildfire during second trimester			-9.7	(-14.5, -4.8)
Wildfire during third trimester			-7.0	(-11.8, -2.2)
Fetal sex				
Male	(ref)		(ref)	
Female	-119.0	(-120.8, -117.1)	-119.0	(-120.8, -117.1)
Gestational age (weeks)				
37	(ref)		(ref)	
38	143.3	(138.2, 148.4)	143.3	(138.2, 148.4)
39	273.3	(268.7, 278.0)	273.3	(268.7, 278.0)
40	368.9	(364.3, 373.5)	368.9	(364.3, 373.5)
41	441.9	(437.3, 446.6)	441.9	(437.3, 446.6)
42	460.0	(454.8, 465.3)	460.0	(454.8, 465.3)
Parity				
1	(ref)		(ref)	
2	90.5	(88.3, 92.8)	90.5	(88.3, 92.8)
3 or more	131.7	(130.5, 133.0)	131.7	(130.5, 133.0)
Maternal age (years)				
Less than 18	(ref)		(ref)	
18–34	46.4	(40.7, 52.0)	46.4	(40.7, 52.0)
35–50	71.8	(65.6, 77.9)	71.8	(65.6, 77.9)
Maternal education				
Less than high school	-19.3	(-21.9, -16.8)	-19.3	(-21.9, -16.8)
Completed H.S. or equivalent	(ref)		(ref)	
1–3 years postsecondary	23.6	(20.8, 26.5)	23.6	(20.8, 26.5)
$\geq$ 4 years postsecondary	35.3	(32.3, 38.3)	35.3	(32.3, 38.3)
Maternal race/ethnicity				
Hispanic	-42.0	(-44.7, -39.3)	-42.0	(-44.7, -39.3)
Non-Hispanic White	(ref)		(ref)	
Non-Hispanic Black	-175.9	(-179.3, -172.5)	-175.9	(-179.3, -172.5)
Non-Hispanic Asian	-166.8	(-171.2, -62.4)	-166.8	(-171.2, -62.4)
Non-Hispanic other/unknown	-31.2	(-47.9, -14.5)	-31.2	(-47.9, -14.5)
Season conceived				
Q1 (January–March)	(ref)		(ref)	
Q2 (April–June)	3.4	(0.7, 6.1)	3.9	(1.0, 6.8)
Q3 (July–September)	12.5	(9.8, 15.2)	11.9	(9.0, 14.7)
Q4 (October–December)	3.1	(0.5, 5.7)	2.7	(0.0, 5.4)
Trend				
Per year	-6.9	(-7.6, -6.2)	-6.9	(-7.6, -6.2)

Table 2.4: Trimester-specific exposure classification, with cosinor terms for season.

	Effect (g)	95 % **CI**
Exposure		
All trimesters before/after	(ref)	
Wildfire during first trimester	-3.2	(-5.2, -1.1)
Wildfire during second trimester	-11.6	(-14.0, -9.1)
Wildfire during third trimester	-6.4	(-8.8, -3.9)
Fetal sex		
Male	(ref)	
Female	-118.9	(-119.9, -118.0)
Gestational age (weeks)		
37	(ref)	
38	143.3	(140.7, 145.9)
39	273.4	(271.0, 275.7)
40	368.9	(366.5, 371.2)
41	441.9	(439.6, 444.3)
42	460.0	(457.4, 462.7)
Parity		
1	(ref)	
2	90.5	(89.4, 91.7)
3 or more	131.7	(130.5, 133.0)
Maternal age (years)		
Less than 18	(ref)	
18–34	46.4	(43.5, 49.3)
35–50	71.8	(68.7, 74.9)
Maternal education		
Less than high school	-19.3	(-20.6, -18.1)
Completed H.S. or equivalent	(ref)	
1–3 years postsecondary	23.6	(22.2, 25.1)
$\geq$ 4 years postsecondary	35.3	(33.8, 36.8)
Maternal race/ethnicity		
Hispanic	-42.0	(-43.4, -40.6)
Non-Hispanic White	(ref)	
Non-Hispanic Black	-175.9	(-177.7, -174.2)
Non-Hispanic Asian	-166.8	(-69.0, -164.6)
Non-Hispanic other/unknown	-31.3	(-39.8, -22.7)
Seasonality (by date of conception)		
Peak-to-peak amplitude	11.6	(7.7, 15.5)
Acrophase (date of maximum birthweight)	Aug 4	(Jul 29, Aug 7)
Trend		
Per year	-6.8	(-7.2, -6.5)

Table 2.5: Binary exposure classification, stratified by proximity to monitors reporting highest PM_{10} during wildfire.

	Effect (g)	95% **CI**	**Effect (g)**	95% **CI**
Exposure				
All trimesters before/after	(ref)		(ref)	
Wildfire during any trimester	-6.6	(-11.0, -2.2)		
Fetal sex				
Male	(ref)		(ref)	
Female	-118.2	(-121.3, -115.1)	-119.4	(-121.7, -117.1)
Gestational age (weeks)				
37	(ref)		(ref)	
38	149.4	(141.0, 157.9)	139.9	(133.5, 146.3)
39	273.5	(265.8, 281.3)	273.3	(267.5, 279.2)
40	367.1	(359.5, 374.7)	369.7	(363.9, 375.4)
41	436.0	(428.2, 443.8)	445.1	(439.2, 450.9)
42	448.4	(439.7, 457.0)	466.5	(460.0, 473.1)
Parity				
1	(ref)		(ref)	
2	88.5	(84.7, 92.2)	91.8	(89.0, 94.6)
3 or more	126.6	(112.6, 130.7)	134.9	(131.8, 138.0)
Maternal age (years)				
Less than 18	(ref)		(ref)	
18–34	48.0	(38.5, 57.5)	45.4	(38.4, 52.5)
35–50	72.1	(61.8, 82.4)	70.7	(63.1, 78.4)
Maternal education				
Less than high school	-14.5	(-18.7, -10.3)	-22.4	(-25.6, -19.3)
Completed H.S. or equivalent	(ref)		(ref)	
1–3 years postsecondary	25.8	(21.3, 30.3)	22.3	(18.7, 26.0)
$\geq$ 4 years postsecondary	34.8	(30.0, 39.6)	33.8	(30.0, 37.5)
Maternal race/ethnicity				
Hispanic	-30.0	(-34.1, -25.9)	-52.0	(-55.5, -48.4)
Non-Hispanic White	(ref)		(ref)	
Non-Hispanic Black	-167.4	(-173.3, -161.6)	-184.0	(-188.2, -179.8)
Non-Hispanic Asian	-159.2	(-166.8, -151.7)	-175.2	(-180.6, -169.8)
Non-Hispanic other/unknown	7.1	(-19.5, 33.7)	-57.7	(-79.2, -36.3)
Season conceived				
Q1 (January–March)	(ref)		(ref)	
Q2 (April–June)	3.7	(-0.8, 8.2)	3.2	(-0.2, 6.6)
Q3 (July–September)	11.7	(7.2, 16.1)	12.9	(9.5, 16.3)
Q4 (October–December)	-0.8	(-5.1, 3.5)	5.2	(2.0, 8.5)
Trend				
Per year	-7.1	(-8.2, -6.0)	-6.8	(-7.6, -5.9)

Chapter 3

Field calibrations of a low-cost aerosol sensor at a regulatory monitoring site in California

3.1 Introduction

This chapter[1] begins to explore possibilities for the next wildfire, the next industrial release, or the next study of the more mundane, yet much more costly, chronic PM exposures that occur in the world today. It demonstrates the possibility of generating useful and accurate estimates of hourly and daily $PM_{2.5}$ concentrations at a regulatory monitoring site by combining a newly available low-cost sensor with other low-cost, readily available hardware, and by calibrating it against the same continuous $PM_{2.5}$ monitoring equipment that is widely relied upon in urban-scale studies of $PM_{2.5}$ health effects today.

Previous studies of lower-cost aerosol measurement techniques have used observational and experimental methods to characterize instruments incorporating repurposed smoke-detector components (Chowdhury et al., 2007; Edwards et al., 2006; Litton et al., 2004) and consumer-oriented, laser-based particle counters (Northcross et al., 2013; Smith, 2011). Previous studies have also characterized short-term responses of relatively inexpensive optical instruments, both custom-built and commercially available, to particle-generating activities in indoor environments (Budde, Busse, and Beigl, 2012; Nafis, 2012; Olivares, Longley, and Coulson, 2012). A larger body of scientific work has compared commercially available nephelometers, particle counters, and other light-scattering instruments to reference methods (Burkart et al., 2010; Watson et al., 1998; Wilson et al., 2002). A peripheral subset has focused on "citizen scientists" constructing and using their own low-cost air pollution instrumentation (Demuth et al., 2013; Smith and Clark, 2013), as well as efforts to support this kind of innovation and to integrate it with established pollutant monitoring infrastructures (CITI-SENSE, 2012; US EPA, 2013).

Guided by the prior work of Watson, Wilson, Chow and colleagues (Watson, 2002; Watson

[1] First published as Holstius et al. (2014).

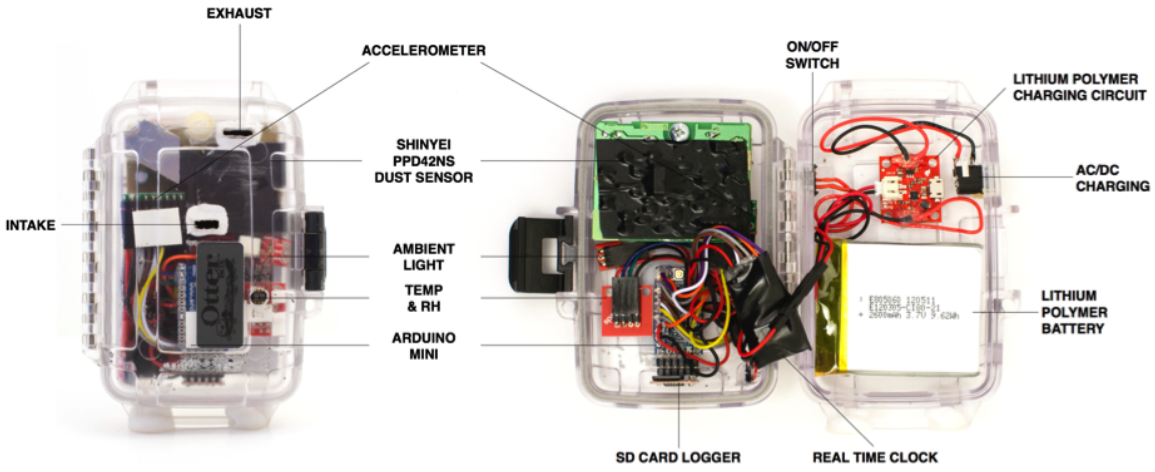

Fig. 3.1: Elements and design of a PANDA prototype.

et al., 1998; Wilson et al., 2002; Wilson et al., 2005; Wilson and Suh, 1997), who extensively analyzed and discussed issues in the augmentation of the then-current Federal Reference Method (FRM) $PM_{2.5}$ network with continuous PM monitors, this chapter concentrates first and foremost on demonstrating a *predictive* relationship between (a) the output of the sensor and (b) regulatory monitoring data that is widely relied upon in air quality regulation and epidemiology. (Given a predictive relationship, further work is still required to establish *equivalency* with $PM_{2.5}$ or any other measures of concentrations or properties.) The intent is to demonstrate "proof of concept" in a natural environment of interest, so that the findings and methodology can be extended, critiqued, and replicated (or refuted) by independent researchers interested in the utility of this class of sensors. It is apparently the first published work to evaluate such a low-cost sensor (approximately USD 10) under ambient conditions at a United States regulatory monitoring site, and the first to calibrate it using 24 h averages of $PM_{2.5}$ from a reference instrument with Federal Equivalent Method (FEM) status.

3.2 Methods

The PANDA platform

To conduct field studies, a small, portable, and reconfigurable platform was designed around a low-cost, off-the-shelf optical sensor: the Shinyei PPD42NS. (Shinyei Corp, 2010). Hereafter, this platform is referred to as the PANDA (Portable and Affordable Nephelometric Data Acquisition) system. Inspiration for the selection of the PPD42NS is credited to Nafis (2012), who freely published figures on his personal website showing relationships between high-frequency PPD42NS output and readings from a commercially available Dylos^{TM}particle counter (see Sec 3.2 and Appendix C.1).

Part	Description	Approx cost ($USD)
Arduino Pro Mini 5V	Microcontroller	10
DS3234	Real-time clock	20
SparkFun OpenLog	MicroSD datalogger	25
2600 mA h battery	Power system	25
Charging circuit	Power system	20
OtterBox	Enclosure	10
Shinyei PPD42NS	Aerosol concentration	10
SHT15	Temperature and RH	40
TEMT6000	Ambient light	5
ADXL335	3-axis acceleration	25
	Approx total cost:	< 200 $USD

Table 3.1: Components of PANDA prototypes. Prices are indicative of June 2013 from popular online electronics retailers, excluding taxes and shipping.

The Shinyei PPD42NS sensor has a partially enclosed chamber with a single light-emitting diode, a plastic lens, and an optical receiver at a forward angle of approximately 45°. A removable cap makes it possible to swab residue off the lens. Air is drawn through the sensing volume by means of a convection current established by a small 0.25 W resistor. The resulting absence of noise from fans or pumps is an attractive feature for possible applications in household settings, but the convective mechanism makes the airflow sensitive to orientation. The flow rate and maximum size of lofted particles are not specified. Signals resulting from the detection of scattered light are passed through filtering and amplification circuitry that are externally visible on the PPD42NS, resulting in 0 V to 5 V pulses of approximately 10 ms to 100 ms in length. Documentation posted online by the manufacturer indicates that the 30 s integrated duty cycle of this PWM signal increases monotonically with "cigarette smoke", with a zero intercept and a slightly sub-linear response at higher concentrations (Shinyei Corp, 2010). Hereafter, the uncalibrated 30 s integrated duty cycle is referred to as "percent full scale" (% FS).

A microcontroller was programmed to measure % FS by sampling the PWM signal at approximately 1 MHz, and to record the timestamped measurement to a microSD card with the aid of a real-time clock. To investigate the effects of temperature, humidity, and ambient light on the performance of the PPD42NS sensor, and to verify that instruments remained undisturbed, upright, and unexposed to extreme conditions, auxiliary sensors for light, temperature, and relative humidity were added to the PANDAs described in this paper. All components were housed in a $12 \times 9 \times 4$ cm, 250 g polycarbonate case, along with a charging circuit and a 2600 mA h lithium-polymer battery, which was charged continuously from a USB cable supplying 5 V power. Manufacturer part identifiers and approximate costs for all components are listed in Table 3.1; the physical design is shown in Fig 3.1. The components were easily procured from

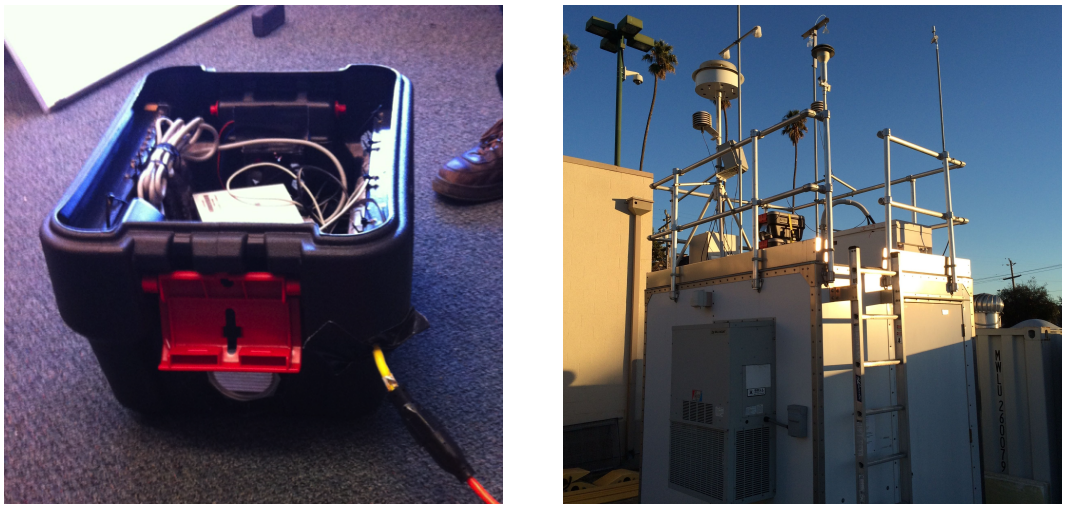

(a) Instrument chamber **(b)** West Oakland trailer

Fig. 3.2: Packaging and deployment.

online electronics retailers with a total materials cost under $200 (USD) per PANDA. A minimal variant, relying on a host device (e.g., a computer or phone) for power and datalogging, could be constructed for less than $25 (USD) in electronic parts.

Reference instruments

The primary standard used in this study was a Federal Equivalent Method (FEM) β-attenuation monitor (BAM-1020, Met One Instruments) that the Bay Area Air Quality Management District (AQMD) uses to monitor continuous $PM_{2.5}$ mass concentrations. 1 h FEM $PM_{2.5}$ data reported by this instrument were downloaded from the AQMD website. Commercially available optical instruments were also deployed by the authors at the regulatory monitoring site: a 16-channel particle sizer (GRIMM OPC, Model 1.108, GRIMM); a nephelometer (DustTrak™II model 8530, TSI) equipped with a 2.5 µm impactor and programmed with the default correction factor for ISO 12103-1 A1; and a consumer-oriented, laser-based optical particle counter (DC1700, Dylos™Corp). These instruments are typical of those that would be used in a human exposure study, though the number that could be deployed would be greatly constrained by the per-unit cost. With the exception of the last, all of these instruments report data in $\mu g\,m^{-3}$ after using proprietary algorithms to filter and transform optical measurements into mass-concentration equivalents. Only the BAM-1020 and DustTrak have a physical size cut mechanism.

Packaging and deployment

The Bay Area AQMD granted permission to co-locate equipment at their West Oakland regulatory monitoring site in Oakland, California. Instruments were placed in two 30 L chambers

within 2 m of the inlet to the AQMD's β-attenuation monitor, approximately 5 m a.g.l., on the roof of the Air District's air-conditioned trailer in a parking lot, from 15 April 2013 to 23 April 2013 (Fig 3.2). Chambers were constructed from 30 L plastic containers, with 10 cm diameter holes cut into the front and rear. A 10 cm 12 V DC fan flush with the rear (exhaust) vent served to draw in ambient air. Zip-ties were used to secure five PANDAs devices, a Dylos DC1700, a GRIMM v1.108, and a laptop inside the chamber, along with AC power supplies. Due to space limitations, a second chamber was constructed to house a DustTrak II Aerosol Monitor. Tubing (1/4 inch) was run from the first chamber to the DustTrak, which has an active inlet and a 2.5 μm impactor, and 120 V AC power was run from an outlet on the trailer to a surge protector in each chamber.

Study location

West Oakland has previously been the subject of targeted air pollution modeling, emission inventories, mobile monitoring, saturation monitoring, and chemical speciation and source apportionment studies (Fujita and Campbell, 2010; Pingkuan, 2008; Reid, 2007; Fujita et al., 2013) as well as a locus for community-based participatory research concerning transportation-related emissions (Gonzalez et al., 2011). The West Oakland site is close to the Port of Oakland, the fourth largest container shipping port in the United States, and proximate to considerable sources of truck and railroad diesel, as well as light-duty vehicle traffic on the Bay Bridge toll plaza and the surrounding freeways. The previous monitoring, speciation, and apportionment studies indicate that elemental carbon is concentrated near traffic routes, indicative of the influence of diesel truck traffic to primary PM, while organic carbon and $PM_{2.5}$ exhibit a more uniform spatial distribution in the area, reflecting the importance of secondary aerosol formation and nitrate and sulfate particles (Fujita and Campbell, 2010; Fujita et al., 2013).

Analytical methods

Pairwise plots of data collected from the different instruments were augmented with loess smoothers and examined for linearity. Coefficients of determination (R^2) from ordinary least-squares (OLS) regression models fit to each pairwise dataset were used to quantify and compare the strengths of correlations. To provide perspective on the range of R^2 values expected with 1 h integration times, empirical and simulated R^2 values were calculated for two colocated BAM-1020s. Root mean squared errors (RMSE) were used to assess the accuracy of linear calibrations. Sensitivity analyses, designed to assess the effects of temperature, relative humidity, and ambient light on instrument performance, were also conducted.

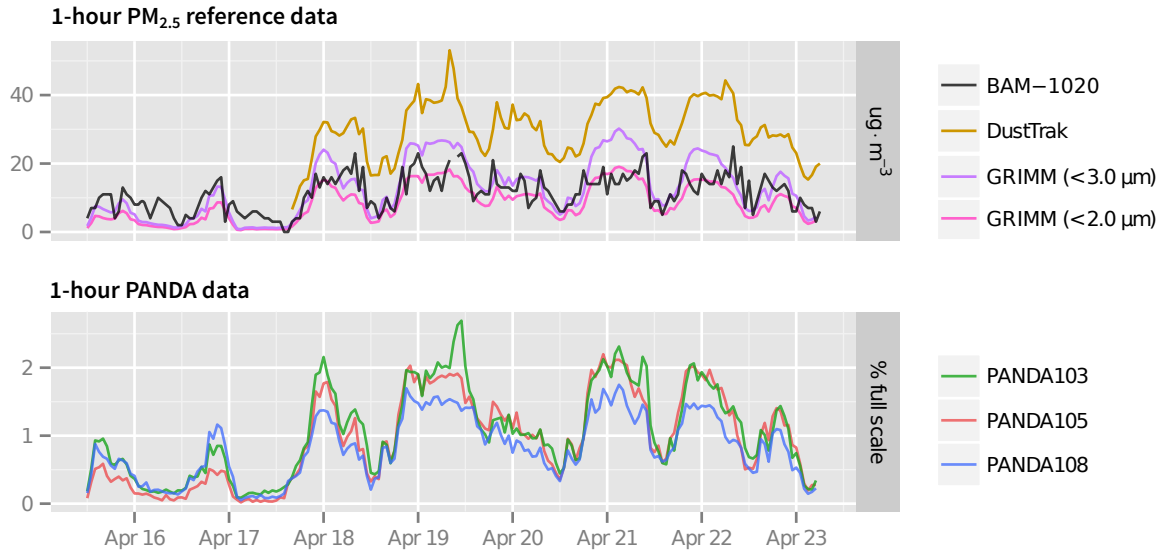

Fig. 3.3: Hourly data collected between 15 April 2013 and 23 April 2013 at the West Oakland regulatory monitoring site. Top: $PM_{2.5}$ measurements reported by BAM-1020, DustTrak, and GRIMM. Bottom: output (% full scale) from three Shinyei PPD42NS sensors (see Table S1 and Figs. S1, S2, and S3, Supplement, for configuration details).

3.3 Results

Time series at 1 h scale

Hourly PM concentrations

Figure 3.3 shows time-series data from a range of instruments deployed during the 8 day interval in April 2013. Nighttime $PM_{2.5}$ concentrations were higher than daytime concentrations, consistent with a nighttime descent of the boundary layer. Smaller ranges and means were seen in the first 48 h. Concentrations reported by the DustTrak were consistently higher than β-attenuation measurements, which may be accounted for by the use of the default DustTrak correction factor. (This does not affect the primary statistic of interest, R^2.) Mass concentrations were also reported by the GRIMM OPC in size ranges from 0.3 µm to 30 µm. Since the GRIMM OPC does not report data corresponding exactly to $0 < d_p < 2.5$ µm (i.e. $PM_{2.5}$), Fig 3.3 instead shows data for both $0.3 < d_p < 3.0$ µm and $0.3 < d_p < 2.0$ µm. Number concentrations, as reported by the Dylos for "small" particles (approximately $0.3 < d_p < 2.5$ µm), also followed the same diurnal and synoptic patterns as the other instruments (Fig 3.3).

Hourly temperature, relative humidity, and ambient light

Fig 3.5 charts temperature, relative humidity, and ambient light inside the chamber. The intake for the chamber was located within 2 m of the BAM-1020 intake. However, the electronics

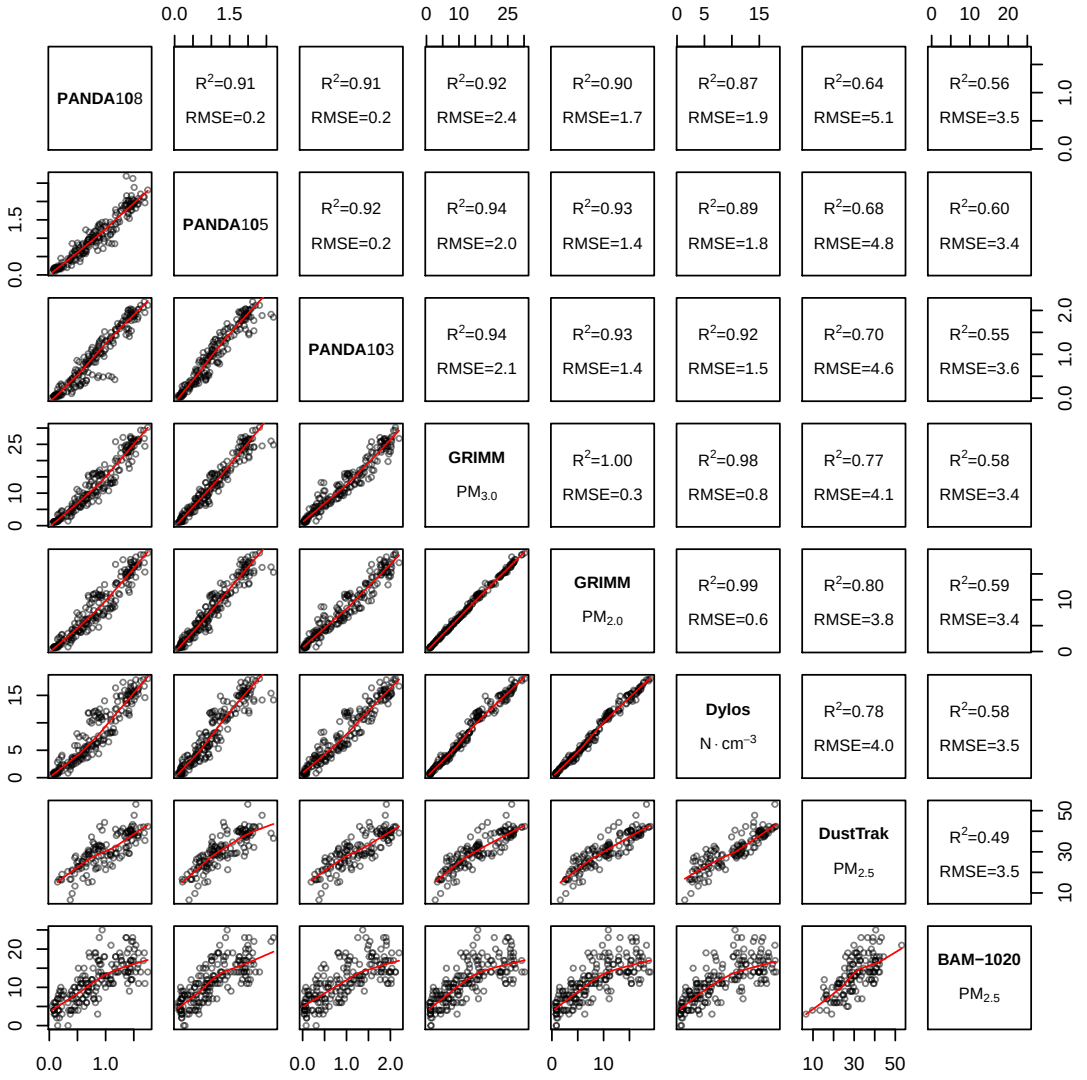

Fig. 3.4: Intercomparisons between hourly data from all instruments deployed at the West Oakland site from 15 April 2013 to 23 April 2013. Upper-right set of panels: R^2 and RMSE for linear models fit using ordinary least squares (OLS). Lower-left set of panels: loess smoothers superimposed on pairwise plots of the hourly data.

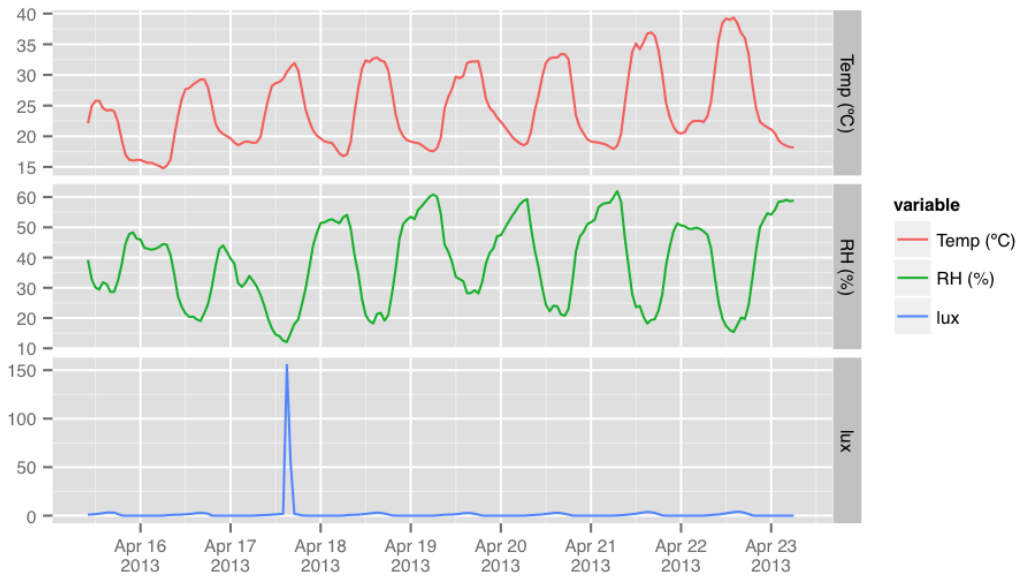

Fig. 3.5: Inside the chamber, relative humidity varied between 20 % to 60 %. Temperature was elevated relative to ambient temperature, presumably due to heat generated by the electronics. Ambient light was consistent across the study, save during the 1 h spot check when the lid of the chamber was removed to evaluate the operational status of equipment.

housed in the chamber contributed a small amount of excess heat, raising the temperature and lowering the relative humidity. Mean daily temperatures trended from approximately 20 °C to 30 °C, with diurnal variations of approximately 8 °C. Except for the 1 h period when the chamber lid was removed to conduct a spot check, Ambient light remained below 1×10^1 lux. Relative humidity in the chamber ranged between 10–60 % over the course of each day, well within the operating range of the PPD42NS and well under the 80 % level at which light-scattering efficiency begins to substantially affect the quality of nephelometric measurements (Chow et al., 2002).

Correlations at 1 h scale

Correlations between PANDAs and other optical instruments

Figure 3.4 shows statistical and graphical summaries of pairwise correlations between 1 h data from all instruments. High correlations were found between individual PANDAs (R^2 = 0.91–0.92) and between PANDAs and the Dylos (R^2 = 0.87–0.92). These data are consistent with previous pilot data from a 6 week experiment testing the longer-term stability and inter-device variability of PPD42NS sensors (see Appendix C.1, Figs C.1 and C.2). Correlations between PANDAs and GRIMM $PM_{2.0}$ and $PM_{3.0}$ were high as well (R^2 = 0.90–0.93 and 0.92–

0.94, respectively). Correlations of the DustTrak with the other optical instruments were more moderate ($R^2 = 0.64$–0.80).

Correlations of PANDAs and other optical instruments with the reference instrument (regulatory β-attenuation monitor)

Using 1 h β-attenuation data as a reference, coefficients of determination (R^2) calculated for 1 h PANDAs, GRIMM $PM_{2.0}$ and $PM_{3.0}$, Dylos, and DustTrak data were 0.55–0.60; 0.59 and 0.58; 0.58; and 0.49, respectively (Fig 3.4). The accuracies of linear models based on each device were essentially equal (RMSE = 3.4–3.6; 3.4 and 3.5; 3.5; and 3.5 $\mu g\,m^{-3}$, respectively). A slight non-linearity, common to all except the DustTrak, is suggested by the loess smoother superimposed on the lowest row of panels in Fig 3.4.

At first glance, an R^2 of 0.55–0.60 may seem low, but it can be explained by the measurement error inherent in the reference instrument, which is specified as $\sigma = 2.0\,\mu g\,m^{-3}$ to $2.4\,\mu g\,m^{-3}$ for a 1 h integration time (Met One Instruments, n.d.). This σ was used to simulate paired observations of a "true" $PM_{2.5}$ distribution with independent Gaussian errors, resulting in a range of expected R^2 estimates centered at 0.59 (95 % CI 0.50–0.67) (Fig. S7, Supplement). In other words, this is as correlated as one would expect 1 h measurements from two such reference instruments to be. Empirical data corroborated this expectation; although only one BAM-1020 is in operation at the West Oakland site, Fig 3.6 shows 3 weeks of contemporaneous 1 h data from a pair of colocated BAM-1020s at a nearby Air District site in Vallejo, 40 km away. The R^2 for these 1 h β-attenuation measurements ($R^2 = 0.58$) differs negligibly from (a) the simulated expectation, as well as the empirical R^2 between the BAM-1020 at West Oakland and (b) each of the three PANDAs, (c) the GRIMM, and (d) the Dylos. (The DustTrak exhibited slightly less agreement, $R^2 = 0.49$.)

Effects of ambient light, temperature, and humidity

No convincing associations with light (L), temperature (T), or relative humidity (RH) were observed. Tables 3.2a and 3.2b show that neither 1 h data from the BAM nor 1 h data from the PANDAs could be explained by L or T. Though 1 h RH measurements had some ability to predict 1 h BAM responses ($R^2 = 0.24$), 24 h averages did not ($R^2 = 0.02$). This can be explained as a simple case of confounding at the 1 h timescale, rather than a causal association. Both $PM_{2.5}$ and RH were elevated at night; moreover, since the intake air for the BAM-1020 is actively dried by heating, there is no mechanistic explanation for the observed association between 1 h RH and 1 h BAM responses. Correlations of RH with PANDA responses at 1 h and 24 h timescales were not appreciably different ($R^2 = 0.27$ and 0.01, respectively). Accordingly, L, T, and RH were omitted from subsequent models.

	PANDA			
Model	**#103**	**#105**	**#108**	**Combined**
BAM $= B_0 + B_1 \cdot L$	0.06	0.03	0.03	0.04
BAM $= B_0 + B_1 \cdot T$	0.02	0.02	0.03	0.02
BAM $= B_0 + B_1 \cdot$ RH	0.23	0.23	0.26	0.24

(a) BAM vs covariates

	PANDA			
Model	**#103**	**#105**	**#108**	**Combined**
PPD42NS $= B_0 + B_1 \cdot L$	0.02	0.01	0.00	0.01
PPD42NS $= B_0 + B_1 \cdot T$	0.01	0.01	0.02	0.01
PPD42NS $= B_0 + B_1 \cdot$ RH	0.25	0.25	0.28	0.27

(b) PPD42NS vs covariates

	PANDA			
Model	**#103**	**#105**	**#108**	**Combined**
BAM $= B_0 + B_1 \cdot$ PPD42NS	0.54	0.60	0.56	0.58
BAM $= B_0 + B_1 \cdot$ PPD42NS $+ B_2 \cdot$ RH	0.56	0.61	0.58	0.59

(c) BAM vs PPD42NS

Table 3.2: Adjusted R^2 for linear regressions including combinations of BAM ($PM_{2.5}$ µm), PPD42NS, and covariates L = light (lux), T = temperature (Celsius), RH = relative humidity (%). Each PANDA has its own RH/T sensor. R^2 statistics were calculated on a per-PANDA basis (columns 2–4) as well as for a "combined" model (column 5). Note: The "combined" R^2 values are not the means of R^2 in columns 2–4, but were obtained by fitting the specified model form to the means of the regressands (L, RH, or T) averaged across all 3 PANDAs at each point in time.

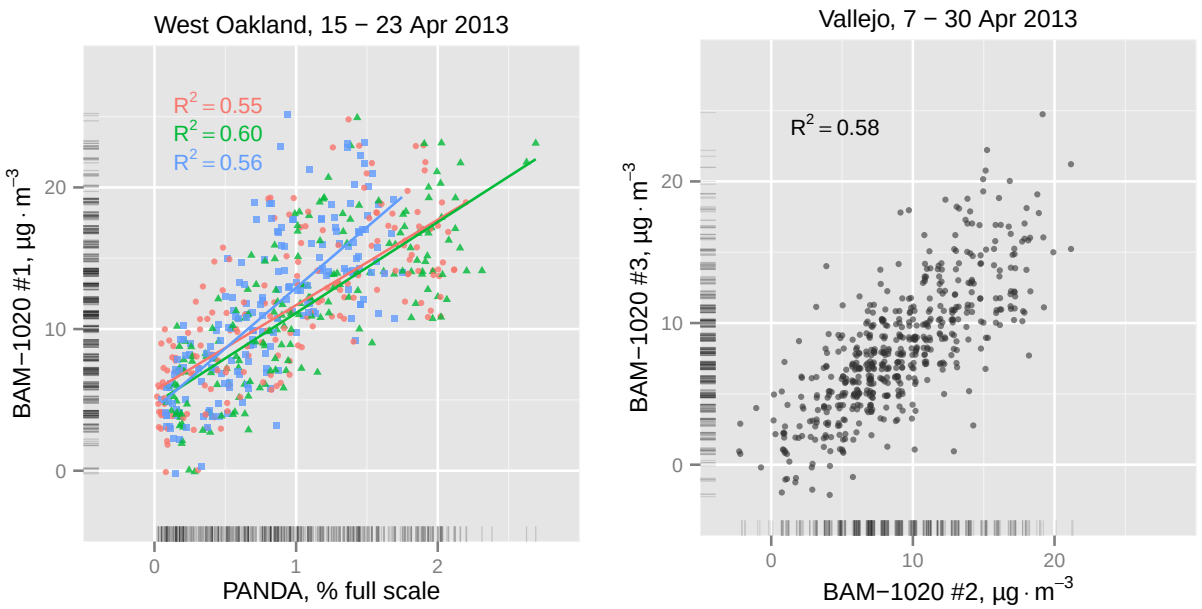

Fig. 3.6: Left: 1 h data collected between 15–23 April 2013 from three PANDAs and a reference (β-attenuation) $PM_{2.5}$ instrument at the regulatory monitoring site in Oakland. Right: approximately the same level of agreement ($R^2 \approx 0.6$) was found between 1 h data from a pair of β-attenuation instruments at a nearby regulatory monitoring site in Vallejo, California (40 km away), 7–30 April 2013. The original 1 h BAM data were available only at 1 $\mu g\,m^{-3}$ resolution; points are jittered to reduce overplotting. Superimposed lines represent linear regressions of unjittered 1 h data.

Correlations at 24 h scale

Following initial observations with 1 h data, a longer-term deployment was conducted to examine 24 h averages (arithmetic means) from a single sensor at the same site from 1 August 2013 through 15 November 2013. Figure 3.7 shows a scatterplot of these 24 h data, superimposed by a linear regression fit by ordinary least squares. This linear model yielded an R^2 of 0.72, an improvement compared to the R^2 of 0.60 found with 1 h data from the previous study (Sec 3.3).

3.4 Discussion

Findings

The overall objective of this study was to determine whether a low-cost aerosol sensor like the PPD42NS could be used to generate adequately resolved measurements of urban $PM_{2.5}$. The first specific aim was to assess the utility of the PPD42NS by custom-building portable instruments (the PANDAs platform) and comparing them to commercially available optical

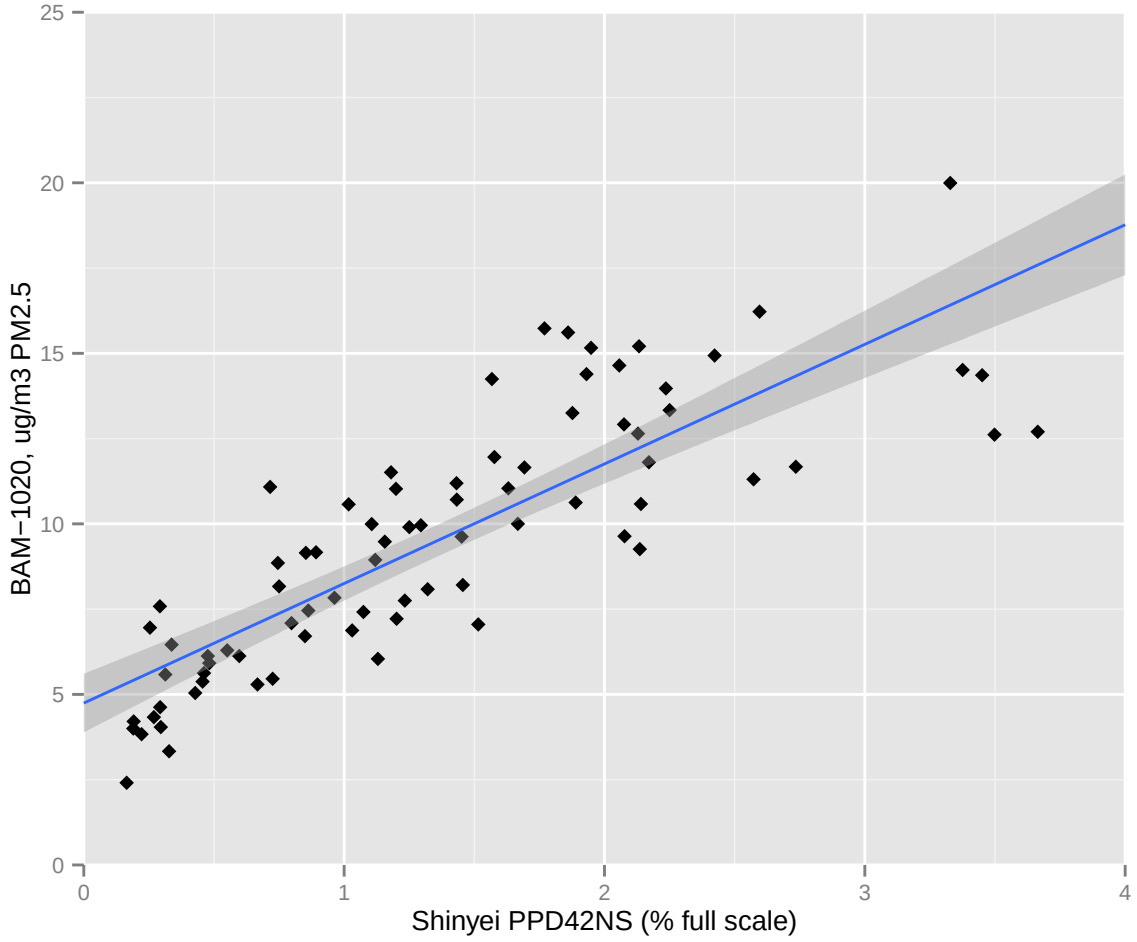

Fig. 3.7: 24 h arithmetic means of 1 h data collected between 1 August 2013 and 15 November 2013 at the West Oakland site. The superimposed line and shading represents a linear regression, fit by ordinary least squares ($R^2 = 0.72$), along with its 95 % pointwise confidence intervals.

instruments. Given the substantial differences in cost (material vs. retail), the agreement observed between PANDAs and commercially available instruments was remarkably good (Figs 3.3 and 3.4). In addition, PANDAs essentially matched the precision and accuracy (R^2 and RMSE, respectively) of these more expensive instruments in predicting hourly $PM_{2.5}$ from the reference instrument, a β-attenuation monitor (Fig 3.4). While commercially available instruments may perform better in more extreme or varied environments, or in measuring other aerosols, or when faster response times are desired, within the context of this 1 h dataset there was little, if any, practical difference.

Conditional on the success of the first aim, the second aim was to use 24 h $PM_{2.5}$ data from the reference instrument (the Met One BAM-1020) to conduct a calibration over a longer period of time, on health-relevant scales. During the 3 month deployment, 24 h averages of reference measurements at the West Oakland site ranged from approximately 2 $\mu g\,m^{-3}$ to 21 $\mu g\,m^{-3}$ $PM_{2.5}$, with a substantial amount of variability explained by a simple linear correction to the sensor data ($R^2 = 0.72$). Obtaining this level of agreement with such a low-cost sensor suggests that, at least in urban areas with similar aerosols and concentrations, additional deployments and calibrations may help to usefully enhance the resolution of $PM_{2.5}$ datasets. Moreover, the sensor's apparent effectiveness at resolving differences between relatively low 24 h concentrations suggests that it may be useful in more polluted regions, if can be shown to resist saturation and wear. For reference, the 24 h ambient $PM_{2.5}$ concentration standard has been set by the US EPA (US EPA, 2012) at 35 $\mu g\,m^{-3}$, while the World Health Organization has established a 24 h guideline (World Health Organization, 2005) of 25 $\mu g\,m^{-3}$. Annual standards/guidelines set by the US EPA, WHO, and EU are now 12, 10, and 25 $\mu g\,m^{-3}$, respectively (European Union, 2008; US EPA, 2012; World Health Organization, 2005). Exceedances of these health-related benchmarks frequently occur in many populous cities and regions worldwide (Brauer et al., 2012).

Limitations and tradeoffs

Two major limitations are relevant to the aim of this work, i.e. increasing the availability of $PM_{2.5}$ data through the use of lower-cost sensors. The first has to do with calibration requirements. In the United States, the reference instrument selected for calibration carries FEM (Federal Equivalent Method) status for 24 h measurements of $PM_{2.5}$ (though not for 1 h measurements). Observational calibration, of the kind we employed, requires access to a site that is sufficiently close to such an instrument for a sufficient length of time; these parameters are conditional on the desired quality of the calibration, which is in turn conditional on the evidentiary standards that the resulting data need to meet. This kind of calibration has particular importance in the domain of $PM_{2.5}$ measurement. While bottled standards are available to calibrate many gas instruments, the creation and circulation of $PM_{2.5}$ transfer standards is problematic. The composition of $PM_{2.5}$ is not universal, and it is impractical to create stable atmospheric suspensions of the $PM_{2.5}$ mixtures to which urban populations are actually exposed. At the same time, the key parameters for calibration by co-location (closeness and duration) are bounded by serious practical and logistical constraints, including scarcities of time and trusted

personnel. Working out these boundaries and relationships is an interesting and important task that is beyond the scope of this paper. For practical purposes, it seems possible that at least some professional air quality managers, urban planners, community-based organizations, and academics could coordinate co-location campaigns with relatively few resources, thereby developing calibration curves specific to neighborhoods and aerosols of interest.

The second limitation is intrinsic to the use of optical techniques as proxies for gravimetric measurements. When a difference in measured values is observed, one cannot be certain whether it is attributable to a difference in the total mass, size distribution, or optical properties—or some combination of all three—of the measured aerosols (Watson et al., 1998; Wilson et al., 2002). Conversely, a lack of difference can obscure real differences in sub-micron or ultrafine particle concentrations, or in other aerosol properties, such as composition or size distribution, that may have real toxicological significance (Lighty, Veranth, and Sarofim, 2000; Wilson and Suh, 1997). Ambient aerosols typically have a trimodal size distribution, with a certain proportion of the respirable mass, and a much higher proportion of the total count, distributed in such sub-micron or "accumulation-mode" particles (John, 2011; Whitby, 1978). In urban atmospheres, these particles can generally be traced to emissions from internal combustion engines. They are more likely to deposit in the deep lungs or be absorbed through the nasal cavity, and are thus of considerable public health concern (Lighty, Veranth, and Sarofim, 2000). The error from these technical limitations can be approximately bounded, however, and a rough 95 % bound on the uncertainty associated with nephelometric estimates of $PM_{2.5}$ has been estimated (Molenar, 2003) as ± 40 %, close to that associated with replicate gravimetric analyses (Lighty, Veranth, and Sarofim, 2000).

Continuing work with more sensors under varying environmental and experimental conditions will be needed to more precisely characterize the influence of variations between low-cost optical aerosol sensors, aerosols, and operating conditions. However, it is instructive to compare the expected magnitude cited above (± 40 %) with the specified variance of the β-attenuation method ($2\sigma = 4.0\,\mu g\,m^{-3}$ to $4.8\,\mu g\,m^{-3}$ for 1 h integration times) and the accuracy of predictive $PM_{2.5}$ models (RMSE $= 3.4\,\mu g\,m^{-3}$ to $3.6\,\mu g\,m^{-3}$, again for 1 h estimates). When true concentrations are in the range of $2\,\mu g\,m^{-3}$ to $25\,\mu g\,m^{-3}$, then in absolute terms these errors are roughly comparable. More importantly, measurement error of $1\,\mu g\,m^{-3}$ to $10\,\mu g\,m^{-3}$ may be much less than the error associated with interpolations of sparse data from a few expensive instruments. This leads to the consideration of tradeoffs in methodology—or, from a complementary perspective, to the optimal design of hybrid approaches (National Research Council, 2012).

For exposure scientists, a larger number of less precise instruments may be especially useful in studies where both intra-subject and between-subject variability cannot be adequately sampled with a smaller number of higher-quality monitors, for example in monitoring household kitchens burning solid fuels (McCracken et al., 2009). In community monitoring or near-roadway contexts, a dense network or gradient with deliberate oversampling could provide high-quality estimates of spatiotemporally resolved concentrations. More flexible saturation monitoring, based on less expensive and more portable instruments, could also respond more readily to changing land use, enable more timely empirical verifications of emission-reduction

policies, facilitate rapid responses to natural or accidental releases of observed aerosols, and support more efficient screening campaigns for urban "hot spots", with follow-up measurements made by reference techniques.

3.5 Conclusion

The next steps of this work involve the continuing deployment of a larger number of aerosol sensors within the context of an established neighborhood-scale multi-pollutant network in the Bay Area (Teige et al., 2011), the coverage of which overlaps with neighborhoods identified by the Bay Area AQMD over the past decade as having high levels of air pollution and vulnerable populations (Martien, 2014). It complements efforts by other scientists to develop and refine emission inventories, screening methods, and exposure assessments. It is also germane to the relatively new phenomenon of "citizen scientists" constructing and using their own low-cost air pollution instrumentation (Demuth et al., 2013; Smith and Clark, 2013) as well as to recent efforts to support this kind of innovation and to integrate it with established pollutant monitoring infrastructures (CITI-SENSE, 2012; US EPA, 2013). It is informed by the work of research-engineers in related fields, including atmospheric science (Mead et al., 2013; Teige et al., 2011), networked sensor calibration (Hasenfratz, Saukh, and Thiele, 2012; Balzano, 2007; Xiang et al., 2012) and mobile/participatory air quality sensing (Aoki et al., 2009; DiSalvo et al., 2012; Dutta et al., 2009; Honicky et al., 2008; Jiang et al., 2011; Mun et al., 2009; Nikzad et al., 2012; Paulos, Honicky, and Goodman, 2007; Willett et al., 2010). Finally, it suggests new prospects for collaborative environmental health research with community residents. Community-engaged participatory research projects have deployed fixed-site monitors (Brugge et al., 2010; Hedges, 2002; Loh et al., 2002) and surveyed intra-urban variations in $PM_{2.5}$ using portable nephelometers (Kinney et al., 2000; Pastor Jr. Morello-Frosch, and Sadd, 2010). This study indicates that device-specific and site-specific calibrations may help low-cost sensors yield data of comparable quality. To increase the value of collected data, protocols for calibration might be profitably incorporated into research on user interfaces and scaffolding (Willett et al., 2010, see) for non-professional users and groups interested in gathering, organizing, and collectively interpreting localized air quality measurements.

Despite their limitations, trends in the development and deployment of low-cost air pollution monitoring technologies are likely to continue (Snyder et al., 2013). A significant but little-explored vein of research concerns the impacts that a proliferation of low-cost air quality instrumentation will have on structures of participation in air pollution monitoring and air quality management (*cf* Harrison, 2011; Ottinger, 2009). Although collaborations between new and established stakeholders may improve mutual awareness and engagement, the manner in which new monitoring data generated from low-cost instrumentation should be incorporated into regulatory decision-making remains an important open question.

Chapter 4

Observing urban plumes

4.1 Introduction

Exposures are characterized by two dimensions: intensity and time. In outdoor urban settings, at timescales on the order of 0.01 h to 1 h, substantial variation can be observed in measurements of ambient PM concentrations to which appropriately sensitive instruments are exposed. Variation on these scales can be found in the presence of plumes from important urban sources, such as highways, as well as in the presence of an accidental release or natural disaster. The mobility of receptors can contribute to observed variation, but variation on these scales can also be observed at fixed locations under the influence of shifting winds, as well as transient increases or decreases in emission intensities.

Empirical observations of such variation stand to improve practical and theoretical understandings of relevant sources and transport mechanisms, thereby improving exposure science and control. Such observations can, for example, be used to improve constraints on mobile-source emission inventories. In turn, these improved inventories can benefit exposure estimates derived from forward modeling. Micro-scale and neighborhood-scale observations can also aid in identifying and characterizing uninventoried sources ("ground truthing"). Finally, when coupled with appropriate disease-process models and epidemiological cohorts (e.g. acute reversible effects on sub-hourly timescales in a school-based study), such observations can be used to support epidemiological analyses. But, variation on these scales is not adequately captured by existing monitoring infrastructure.

In this chapter, a larger sample ($n = 48$) of the low-cost sensors described in Chapter 3 is used to estimate an appropriate lower bound on integration time T, and then to explore features revealed in the sub-hourly data. This chapter also replicates previous 24 h and 1 h calibrations (against FEM $PM_{2.5}$; see Chapter 3) at new sites, addressing the question of whether calibrations at a regulatory monitoring site might generalize to different locations. Finally, this chapter quantifies and compares distributions of calibration parameters among sub-samples of the sensors, culminating in a demonstration of the viability of a statistical approach to remotely transferring calibrations. This approach can remove a nominal barrier to broader participation

in neighborhood-scale PM monitoring campaigns.

4.2 Methods

Study locations

Measurements for this study were produced at three routine air quality monitoring sites in western Alameda County, CA, during a 10 week interval from Jan 14 to Mar 26, 2014. Meteorological records were obtained from a fourth location, the Oakland Sewage Treatment Plant ("Oakland STP"), approximately 1.5 km NW of the Oakland West monitoring site. Site characteristics for Oakland West were described in Chapter 3. Oakland East is similarly situated, approximately 12.5 km SE of Oakland West and 2 km NE of the heavily trafficked I-880 corridor (downwind). The third site, Laney College, is located less than 100 m from the downwind edge of I-880, approximately 3 km SE of Oakland West and 10 km NW of Oakland East. Laney College is a newly established routine monitoring site, intended to capture "near-roadway" rather than traditionally monitored "background" concentrations.

Reference data

Reference data for wind speed, direction, ambient temperature and humidity, and FEM $PM_{2.5}$, as well as co-pollutants (CO, NO, NO_2, NO_X, O_3, and black carbon) were obtained from the Bay Area Air Quality Management District (AQMD) Data Management System (DMS) at 1 h resolution for all three routine monitoring sites. Not all co-pollutants were monitored at all sites. For example, black carbon (BC) was not monitored at Oakland East during the course of our study, and ultrafine particles (UFP) were only monitored at Laney College. Table 4.1 lists the reference instruments producing 1 h reference data at each site.[1]

Parameter(s)	**Instrument(s)**	**Site(s)**
$PM_{2.5}$	Met One BAM-1020 (FEM)	(all)
CO	Thermo 48i, API300	(all)
NO, NO_2, NO_X	Thermo 42i	(all)
O_3	Thermo 49i	Oakland East, Oakland West
BC_{UV}, BC_6	Aethalometer	Laney College
UFP	TSI 3783	Laney College

Table 4.1: Reference instruments and sites producing 1 h reference data.

[1] Because the Laney College site was established in 2014, reference data from that location were only available from Jan 26 onward. Some analyses and figures are therefore restricted to the common timeframe of Jan 26 to Mar 26 (e.g. Fig 4.5).

A composite meteorological profile was computed from 1 h data from the Oakland STP meteorological site (Fig 4.3). All metrics except wind speed and direction were aggregated using arithmetic means. Resultant vectors for wind speed and direction were calculated at supra-hourly scales to support the identification of sources to which the experimental apparatus might be more or less sensitive (Figs 4.5 and 4.4; for the analysis of residuals, see Sections 4.3 and D.1). For the same reason, since urban sources and prevailing winds are known to vary by time of day, diurnal profiles of air quality and meteorology were also constructed.

Apparatus

This study required the construction of new instrumentation, consisting primarily of 12 replicates of an enhanced version of the PANDAs described in Chapter 3. The new instruments featured the same models of temperature, relative humidity, and light sensors described in Chapter 3. They were also equipped with GPS. During this study, GPS location data were not used, but GPS timestamps were used as an absolute time reference. Elapsed time was tracked by the integrated Arduino microprocessor at high resolution and logged with every sensor reading, while GPS timestamps were interleaved with the logs approximately every 5 min.

The enhanced versions were equipped with three PPD42NS sensors, rather than one, that were sampled continuously and in parallel at approximately 1 MHz by new firmware.[2] Sampling sensors in triplicate increased the odds of detecting and mitigating individual sensor failures; the failure rates and failure modes of these sensors had not previously been characterized. It was also envisioned that this approach would provide the potential to increase signal-to-noise in the absence of failures. Timeseries resulting from parallel sampling by a single microprocessor did not need to be resampled (to align sampling intervals) before aggregation.

Groups of four instruments each were connected to four Raspberry Pis (small Linux-based computers retailing for approximately USD $35). The Raspberry Pis mirrored captured data on their own SD cards and independently timestamped the captured data with high-resolution hardware clocks. The redundant records and timestamping were found to be in excellent agreement, with all interpolated clock times differing by 1 s or less.

The material cost per unpackaged instrument was approximately $150 (USD). The marginal cost, per instrument, for triplicate PPD42NS sensors was approximately USD $20.

Packaging and deployment

Four 30 L plastic containers having the same dimensions, flow-through design, and fan described in Chapter 2 were constructed to serve as “hosts” to four instruments apiece. Hence, each host contained 12 PPD42NS sensors, 4 SHT15 sensors, 4 GPS modules, and one Raspberry Pi. A 10 cm, 12 V DC fan, flush with the rear exhaust vent, served to draw in ambient air. Figure 4.1 shows the physical configuration of apparatus within a host, while Fig 4.2 shows a schematic of host deployments. Two hosts, “springer” and “ironhide”, were deployed at West

[2]The source code is freely available for inspection or reuse: `http://github.com/holstius/PANDAs`

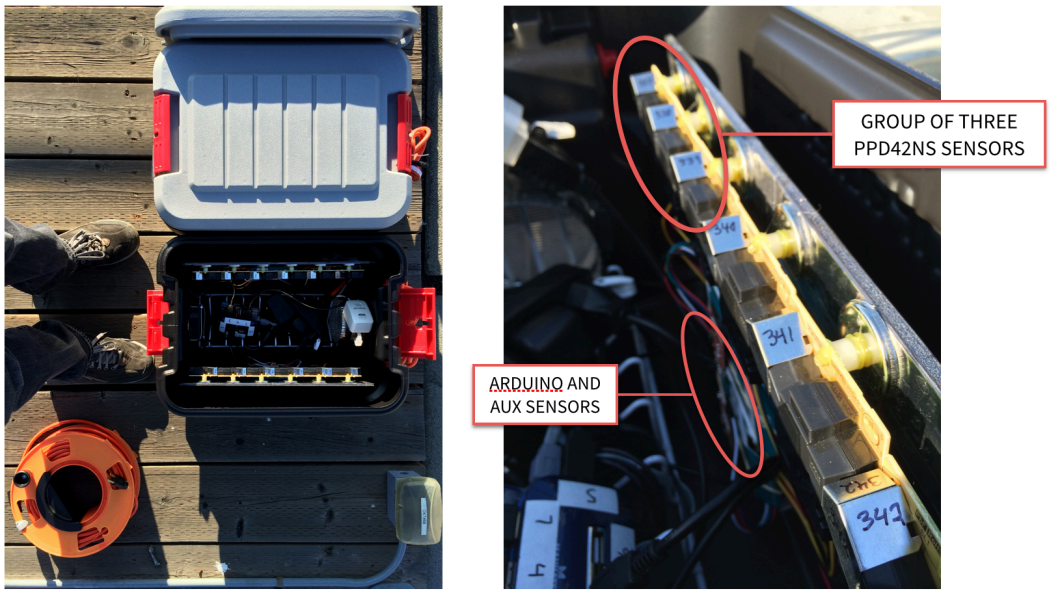

Fig. 4.1: Physical packaging of apparatus inside a host chamber. Each chamber contained 12 PPD42NS sensors, 4 SHT15 sensors, 4 GPS modules, and one Raspberry Pi. A 10 cm, 12 V DC fan, flush with the rear exhaust vent, served to draw in ambient air.

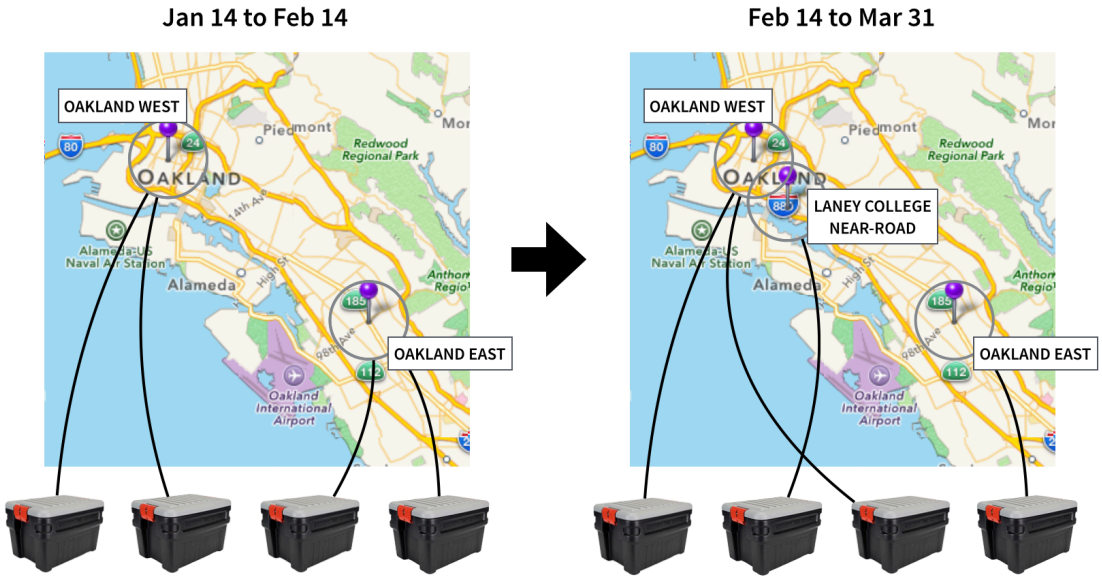

Fig. 4.2: Schematic depicting deployment and subsequent rotation between sites. Two hosts, “springer” and “ironhide”, were deployed at West Oakland on Jan 14 2014. On Jan 23, two additional hosts, “sunstreaker” and “wheelie”, were deployed at Oakland East. On Feb 14 – 15, “wheelie” was rotated from Oakland East to Oakland West, and “ironhide” was rotated from West Oakland to Laney College.

Oakland on Jan 14 2014. On Jan 23, the remaining two hosts, “sunstreaker” and “wheelie”, were deployed at Oakland East. On Feb 14 – 15, “wheelie” was rotated from Oakland East to Oakland West, and “ironhide” was rotated from West Oakland to Laney College.

Cross-calibration

Prior to calibrations against other instruments, the 48 PPD42NS sensors were cross-calibrated against each other. Three weeks near the midpoint of the study were selected to serve as the basis for cross-calibration (Feb 17 to Mar 10). Pairwise scatterplots of unadjusted 30-second PPD42NS data (Fig 4.6) revealed strong correlations between all pairs of sensors, so Principal Components Analysis (PCA) was used to construct a sparse linear representation of these correlations that appropriately minimized orthogonal error. One sensor per host was nominated as a reference, thereby defining its offset as zero and gain as unity. This was the sensor for which the median of the geometric means of the estimated gains for other sensors was closest to unity. The offsets and gains for the other sensors were then fully determined.

First-order calibrations

Cross-calibrated 30-second data were binned and aggregated at 24 h, 12 h, 8 h, 6 h, 4 h, 3 h, 2 h, 1 h, 30 min, 10 min, 3 min, and 1 min scales using arithmetic means. Reference data were also binned and aggregated at timescales from 24 h to 1 h. The same three weeks used for cross-calibration (Feb 17 to Mar 10) were used for calibrations against reference data.

To assess the influence of different timescales and estimators, calibrations against reference equipment were generated at 24 h to 1 h timescales using (a) ordinary least squares (OLS) with a forced intercept through the origin, as well as L_1 minimizations of (b) mean absolute error (MAE) and (c) mean absolute relative error (MARE). In all cases, the primary regression model had a linear form, with i indexing the sensors, and β_0 forced to zero:

$$Y_{i,t} = \beta_0 + \beta_1 X_{i,t} + \epsilon \tag{4.1}$$

Residuals from the OLS calibrations at 3 h scale were subsequently examined with respect to available covariates, including co-pollutants and meteorological parameters.

For commensurability with the site- and host-specific calibration at 24 h scale reported in Chapter 3, an intercept term was re-introduced to the OLS regressions. These models had the following form, allowing for deployment-specific intercepts and slopes (defined by appropriate pairings of host h and site s):

$$Y_{h,s,t} = \beta_{0,h,s} + \beta_{1,h,s} X_{h,s,t} + \epsilon \tag{4.2}$$

Sub-hourly analyses

To estimate an approximate lower bound for the effective temporal resolution of the PPD42NS sensor, binned and aggregated timeseries $\boldsymbol{X}_i$ from sensors $i = \{1, 2, \ldots 48\}$ were examined with

integration times T from 0.05 h to 0.5 h (3 min to 30 min). Given a series of regular intervals $\boldsymbol{t} = \{0, T, 2T, \dots\}$ over which to integrate, when T was small it was more common to observe time-integrated values within $\overline{\boldsymbol{X}} = \{\overline{x_{it_1}}, \overline{x_{it_2}}, \dots\} = \frac{1}{T}\{\sum_{j=1}^{T} x_{ij}, \sum_{j=T+1}^{2T} x_{ij}, \dots\}$ that were equal to exactly zero. These distorted the overall distribution of $\overline{\boldsymbol{X}}$. From inspection of the proportion $P(\overline{\boldsymbol{X}} = 0)$ as a function of T (Fig D.2, Appendix D), it became evident that integration times of 5 min or longer consistently produced $P(\overline{\boldsymbol{X}} = 0) < 0.01$. This was taken as a reasonable lower limit on T for individual sensors under the observed field conditions.

Aggregation across triplets of sensors $j = \{(1,2,3),(4,5,6),\dots(46,47,48)\}$ reduced $P(\overline{\boldsymbol{X}} = 0)$ by a factor of approximately $\sqrt{3}$, equivalent to increasing T by a factor of 3 (data not shown). Thus, for triplets of sensors, a reasonable lower limit for T was taken to be 1 min to 2 min.

Having established approximate lower limits for T, calibration coefficients were examined at 1 h to 24 h scale (Table 4.3). No evidence of scale dependence was found, so calibrations from 1 h data were applied to sub-hourly data. An exploratory analysis of this calibrated sub-hourly data focused on features evident at the near-roadway site (Laney College) that were absent or attenuated at corresponding background sites (Oakland West and Oakland East).

4.3 Results

Meteorology and pollutant concentrations

Figure 4.3 depicts temperatures and resultant wind vectors at Oakland STP throughout the course of the study. Although the week-to-week variation in Fig 4.3 is considerable, aggregating these parameters on a diurnal scale suggested that morning winds were generally from the SE, with warmer afternoon and evening winds from the WSW (Fig 4.4).

Figure 4.5 summarizes the diurnal patterns of pollutant concentrations observed during Jan 26 to Mar 26, during which data were available from all three air quality monitoring sites. At the near-roadway site (Laney College), BC concentrations tended to peak at approximately 0900h LST, and were mirrored by a similar pattern in UFP concentrations. Elevated NO concentrations, relative to the nearest background site (Oakland West), were also evident. O_3 data were not available at Laney College. These observations are consistent with an expected deficit of O_3 and elevation of other primary and secondary mobile source emissions ($PM_{2.5}$, NO_X, BC, UFP) less than 100 m downwind of a major goods movement corridor (I-880).

Federal Equivalent Method (FEM) $PM_{2.5}$ measurements were highest at Oakland West during the first 10 days, with a 95th percentile of 40 $\mu g\,m^{-3}$. In contrast, the 95th percentile was 17 $\mu g\,m^{-3}$ during the remainder of the study.

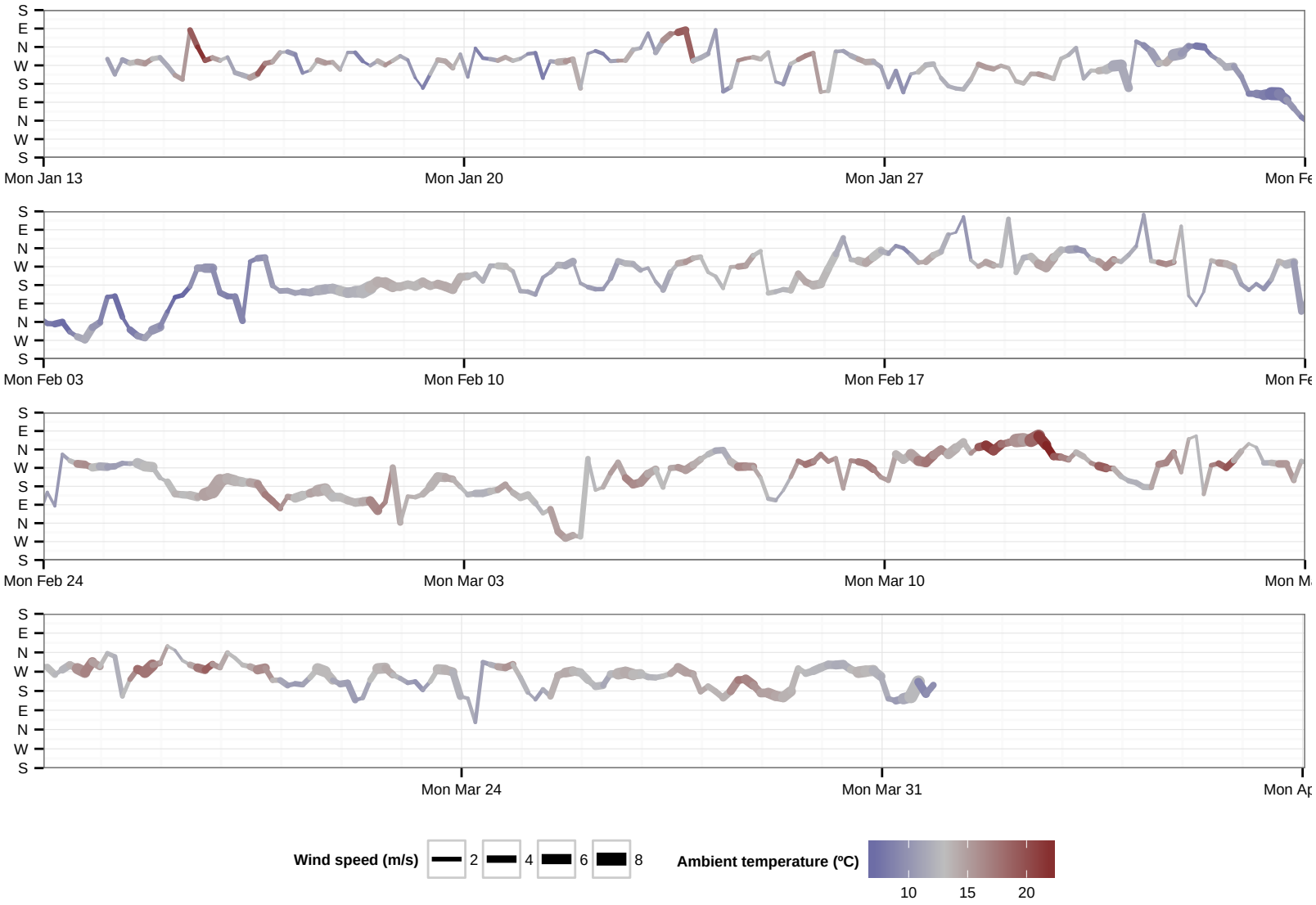

Fig. 4.3: Resultant wind vectors and ambient temperature at Oakland STP during the study (3 h scale).

id	gain	offset
01	1.00	0.00
02	1.06	−0.05
03	0.98	−0.02
04	1.26	0.03
05	1.04	0.01
06	0.80	0.01
07	1.06	−0.04
08	1.19	−0.01
09	1.31	−0.01
10	0.86	0.02
11	0.95	0.02
12	0.84	0.01

(a) springer

id	gain	offset
13	0.80	0.02
14	1.21	0.01
15	1.00	0.00
16	1.28	0.02
17	1.28	−0.01
18	0.89	0.02
19	0.93	−0.01
20	0.74	−0.03
21	0.91	−0.02
22	1.12	0.02
23	0.83	0.02
24	1.07	0.02

(b) ironhide

id	gain	offset
25	1.18	0.00
26	1.13	0.02
27	0.85	0.05
28	0.90	0.00
29	0.87	−0.02
30	0.77	−0.01
31	1.13	0.00
32	0.83	0.00
33	1.04	0.01
34	1.07	0.02
35	1.02	0.00
36	1.00	0.00

(c) sunstreaker

id	gain	offset
37	1.09	0.00
38	1.00	0.00
39	1.06	0.00
40	1.09	−0.02
41	1.12	−0.02
42	1.18	0.00
43	1.11	−0.02
44	1.04	−0.02
45	0.82	−0.01
46	0.93	−0.02
47	0.73	−0.01
48	0.82	0.01

(d) wheelie

Table 4.2: Linear cross-calibration coefficients estimated using Principal Components Analysis (PCA). Offsets (% FS) and gains were estimated separately for groups of sensors in each host ("springer", "ironhide", "sunstreaker", and "wheelie"). For reference, an offset of 0.01 % FS is approximately equivalent to 0.1 $\mu g\,m^{-3}$ after applying calibrations from Sec 4.3.

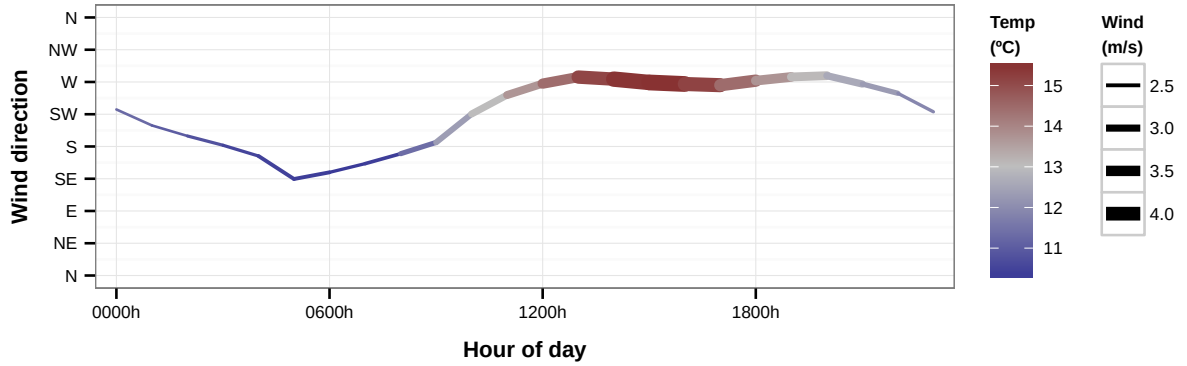

Fig. 4.4: Diurnal profile of wind and temperature at Oakland STP during the study.

Cross-calibration

Figure 4.6 illustrates the expected correlation between data from pairs of sensors. From inspection, it was evident that inter-sensor agreement would be improved by simple linear corrections. Principal Components Analysis (PCA) was used to estimate linear (additive and multiplicative) cross-calibration coefficients for all sensors, using data from Feb 17 to Mar 10 at 24h as a basis.

Cross-calibration coefficients obtained with PCA are reported in Table 4.2. Hereafter, the additive coefficients are referred to as "offsets", and the multiplicative coefficients as "gains".

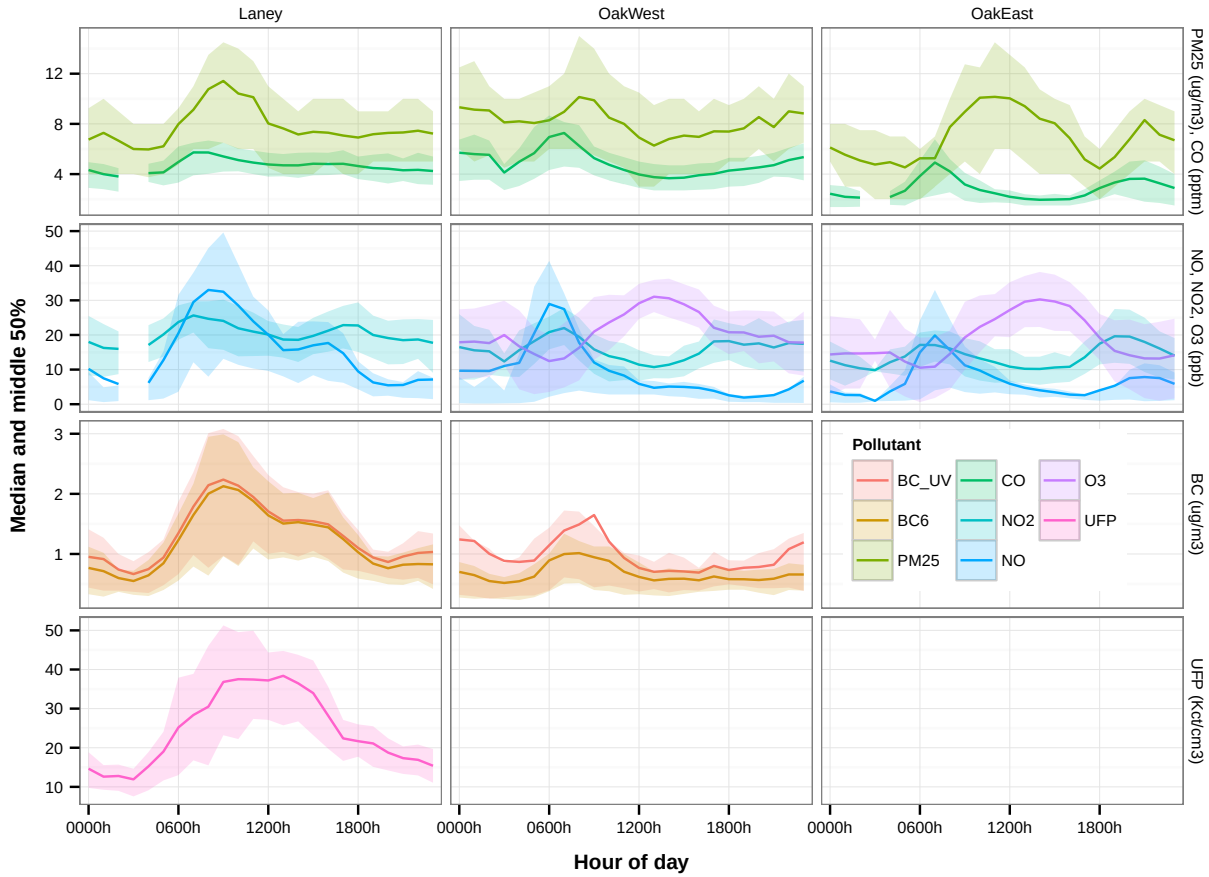

Fig. 4.5: Diurnal profiles of 1 h air quality data during the study.

(These may be regarded as equivalent to β_0 and β_1 in a typical linear regression.) Estimated offsets ranged from −0.05 to 0.05 %FS, equivalent to 2.9 % of the full range of uncalibrated data, or less than $\pm 1\,\mu g\,m^{-3}$ after applying the calibrations described in Sec 4.3. These offsets were considered negligible; only the gains were used in subsequent corrections. 95% (n=46) of estimated gains were between 0.7 and 1.3, and 50% (n=24) were between 0.9 and 1.1.

First-order calibrations

Figures 4.8–4.10 illustrate the results from an ordinary least squares (OLS; equivalently, MSE) calibration based on 1 h cross-calibrated data from Feb 17 to Mar 10. From Figs 4.8 and 4.9, it is evident that the 48 sensors tracked very well with each other over the course of the study. No examples of sensor failure or drift are observable at a glance. Figures 4.8 and 4.10 also show that most of the 24 h means were within a factor of 2 of the 24 h average indicated by the reference instrument (a Met One BAM-1020). Finally, good agreement is shown between pairs of hosts colocated at the same site. (This last point will be revisited in Sec 4.4.)

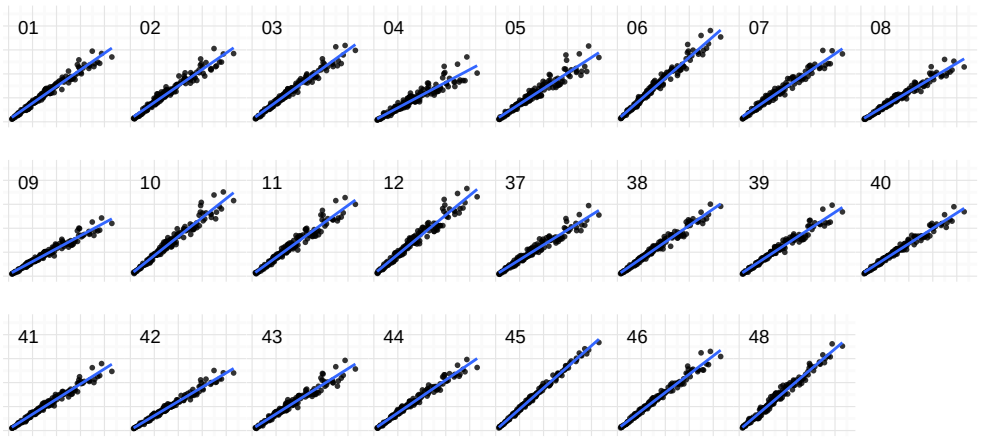

Fig. 4.6: Unadjusted 3 h data from PPD42NS sensors, illustrating differences in sensitivity. For clarity, only data from the calibration timeframe are shown. Superimposed lines represent linear regressions (OLS). The number in the upper left of each panel is the unique ID of the sensor whose data are plotted as the dependent variable (y-axis) in that panel. The x-axis in all panels corresponds to a reference sensor chosen at random for this figure (ID 47).

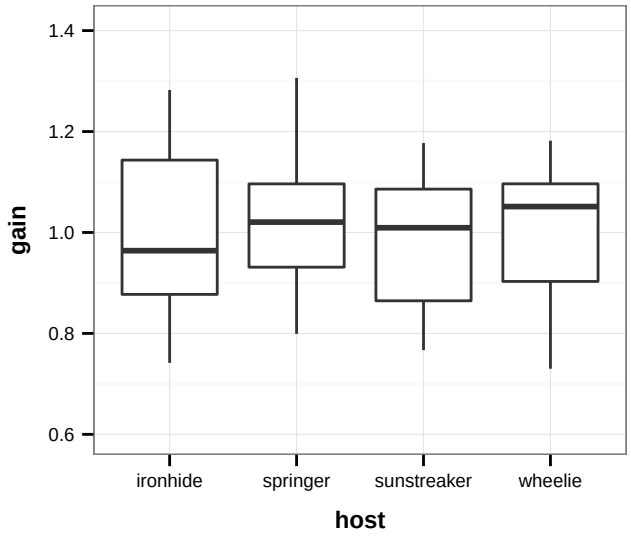

Fig. 4.7: Distributions of multiplicative correction factors ("gains") estimated by cross-calibrating the sensors within each host. Hinges are 1st and 3rd quartiles.

Simplified models, omitting the intercept, produced consistent results when applied to within-sample and out-of-sample data at different sites and times. Table 4.3 presents estimates for the parameter β_1 when β_0 was forced to zero, conditional on (a) the timescale T used for aggregation and (b) minimizations of selected L_1 and L_2 measures of error (see Appendix A for definitions). Results did not suggest substantial dependencies on T or on the choice of loss function, except for a single anomaly (MAE with T of 3 h to 4 h). The reason for this anomaly is not known.

No substantial differences were observed between within-sample and out-of-sample performance of calibrations from the selected calibration timeframe. For example, sensors inside hosts "sunstreaker" and "springer", which remained at Oakland East and Oakland West for the duration of the study, yielded reasonable predictions at their respective sites both before and after the calibration window (Fig 4.8, blue and green lines). Similary, calibrations for sensors in host "wheelie" (Fig 4.8, purple line) appeared to yield consistent results before and after the host was moved from Oakland West to Oakland East, and calibrations for sensors in host "ironhide" (Fig 4.8, red line) yielded consistent results before and after the host was moved from Oakland West to Laney College.

As operationalized by correlations with reference instruments (R^2) at 24 h and 1 h scale, this study observed nearly the same performance reported in Chapter 3. OLS regressions were run at 24 h and 1 h scale, as described in Section 4.2. The respective coefficients of determination (R^2) were 0.68 and 0.53. For reference, the 24 h and 1 h R^2 values from the previous deployment (Chapter 3) were 0.72 and 0.55–0.60, respectively.

Table 4.3: L_1 and L_2 minimizations of B_1 given T.

T	**MSE**	**MARE**	**MAE**
24h	1192	1210	1321
12h	1160	1162	1330
8h	1145	1171	1340
6h	1147	1177	1325
4h	1134	1166	1601
3h	1140	1155	1098
2h	1138	1150	1444
1h	1149	1159	1448

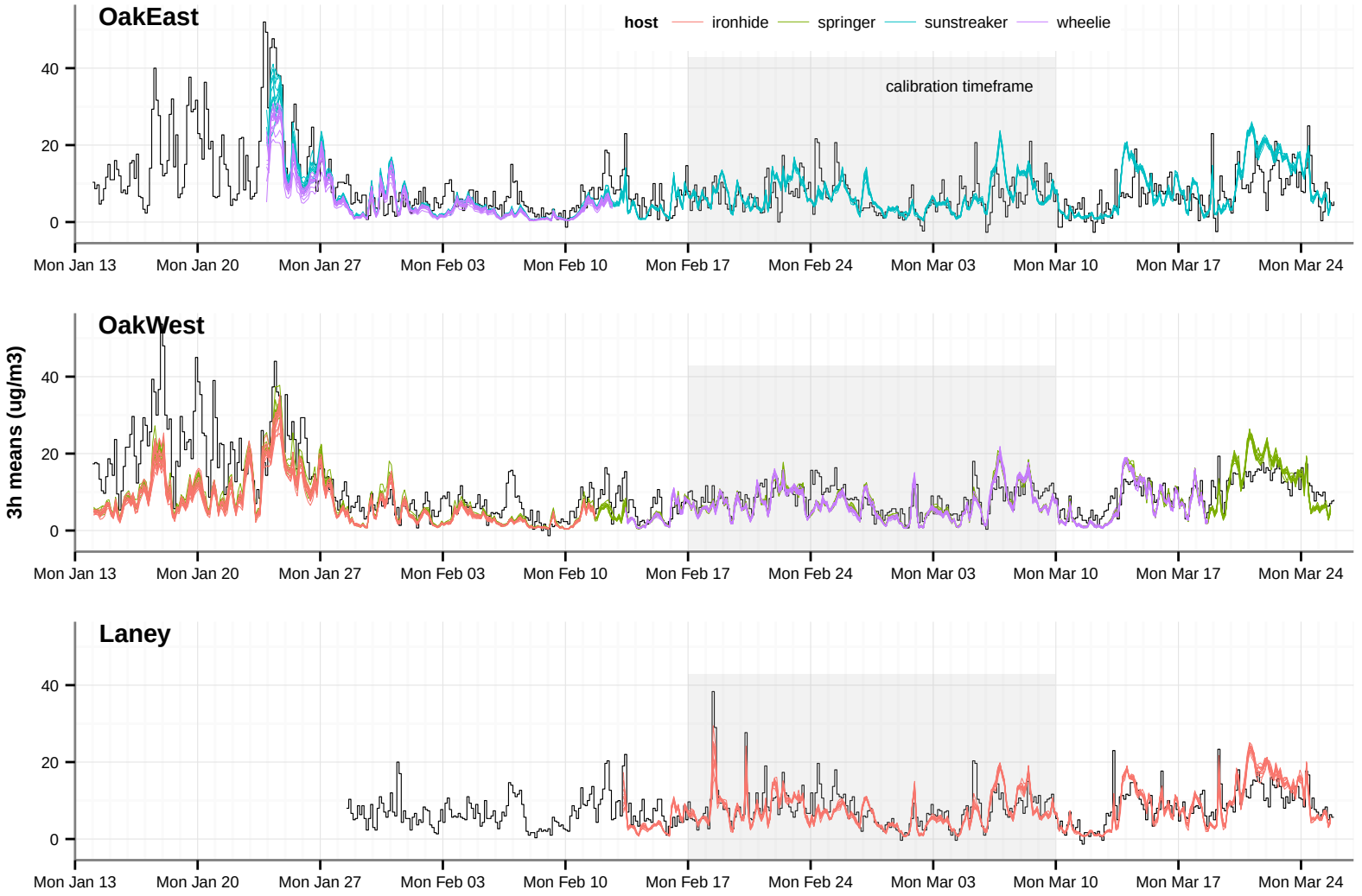

Fig. 4.8: First-order calibration at 3 h scale. Colored lines are calibrated data from PPD42NS sensors; black stairstep is FEM PM2.5.

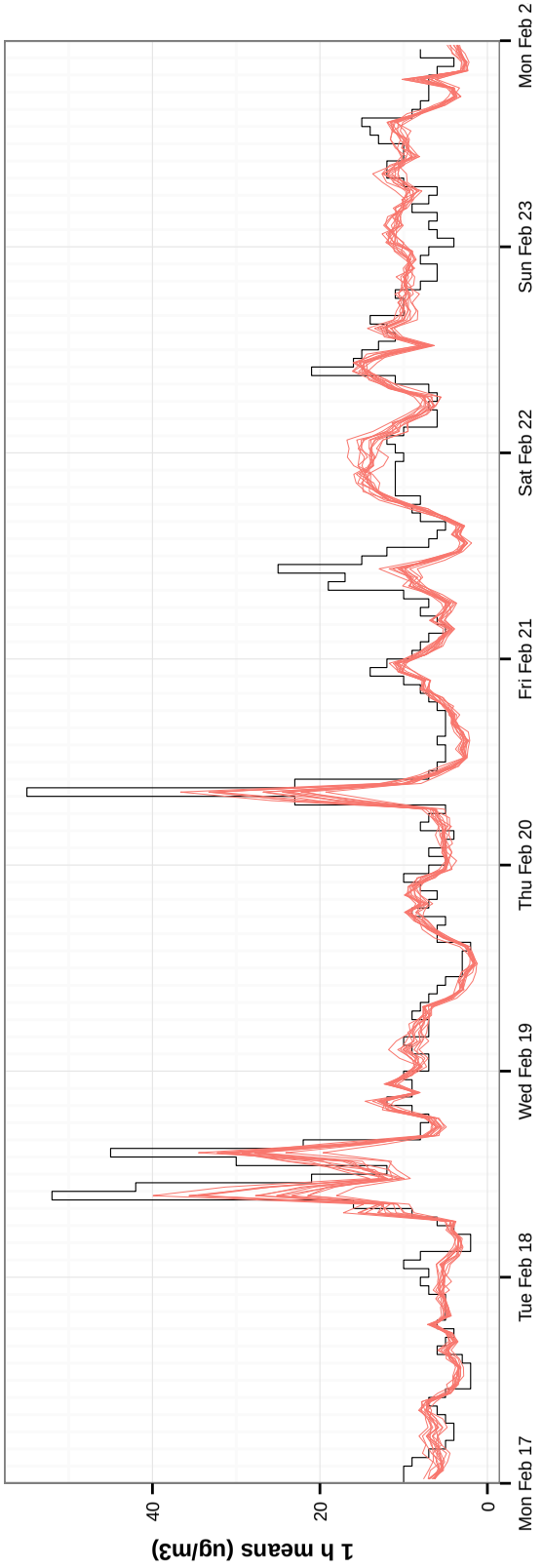

Fig. 4.9: Detail of Laney College data at 1 h scale. Larger maxima and more variation are revealed.

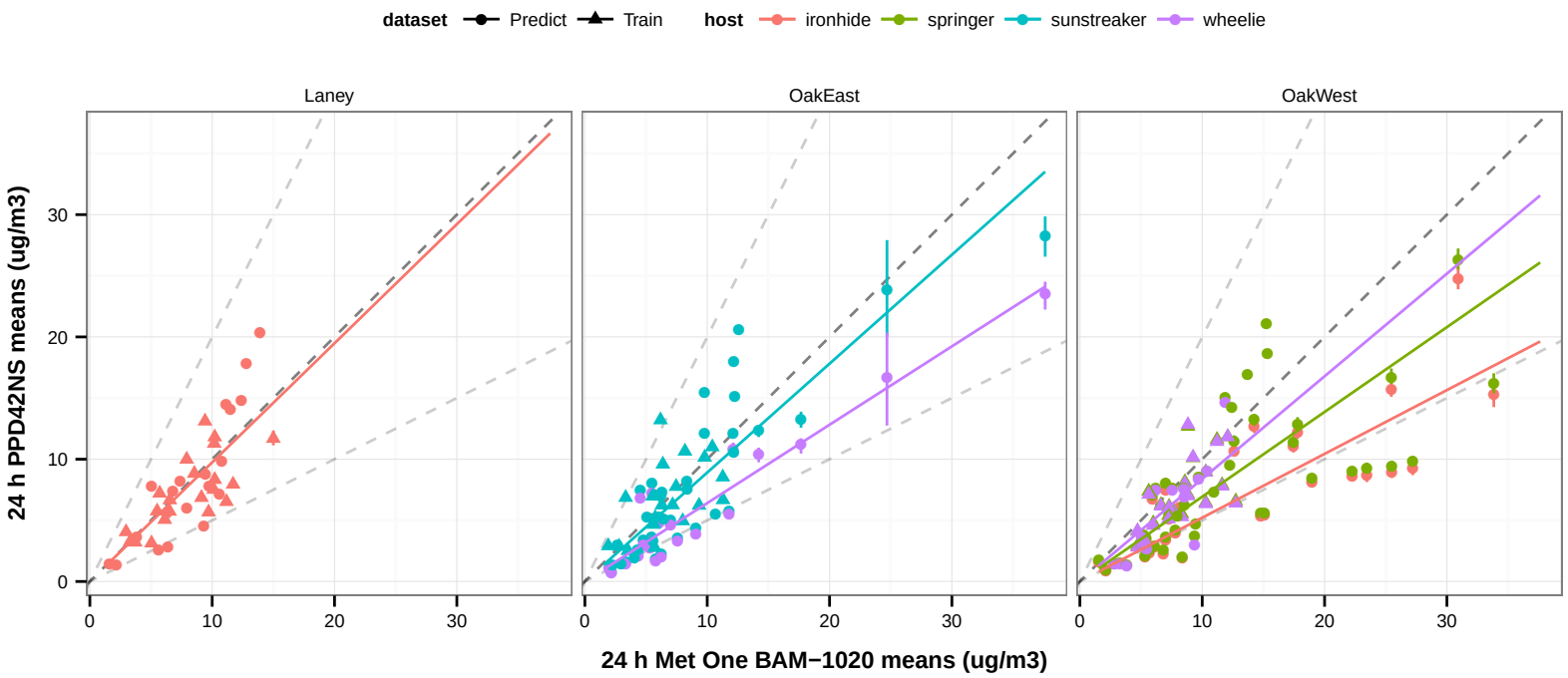

Fig. 4.10: First-order calibration from 24 h data (Feb 17 to Mar 10) applied to full dataset (Jan 14 to Mar 26). Points and associated error bars indicate groupwise bootstrapped means and confidence intervals for each datapoint consisting of twelve 24 h cross-calibrated PPD42NS means.

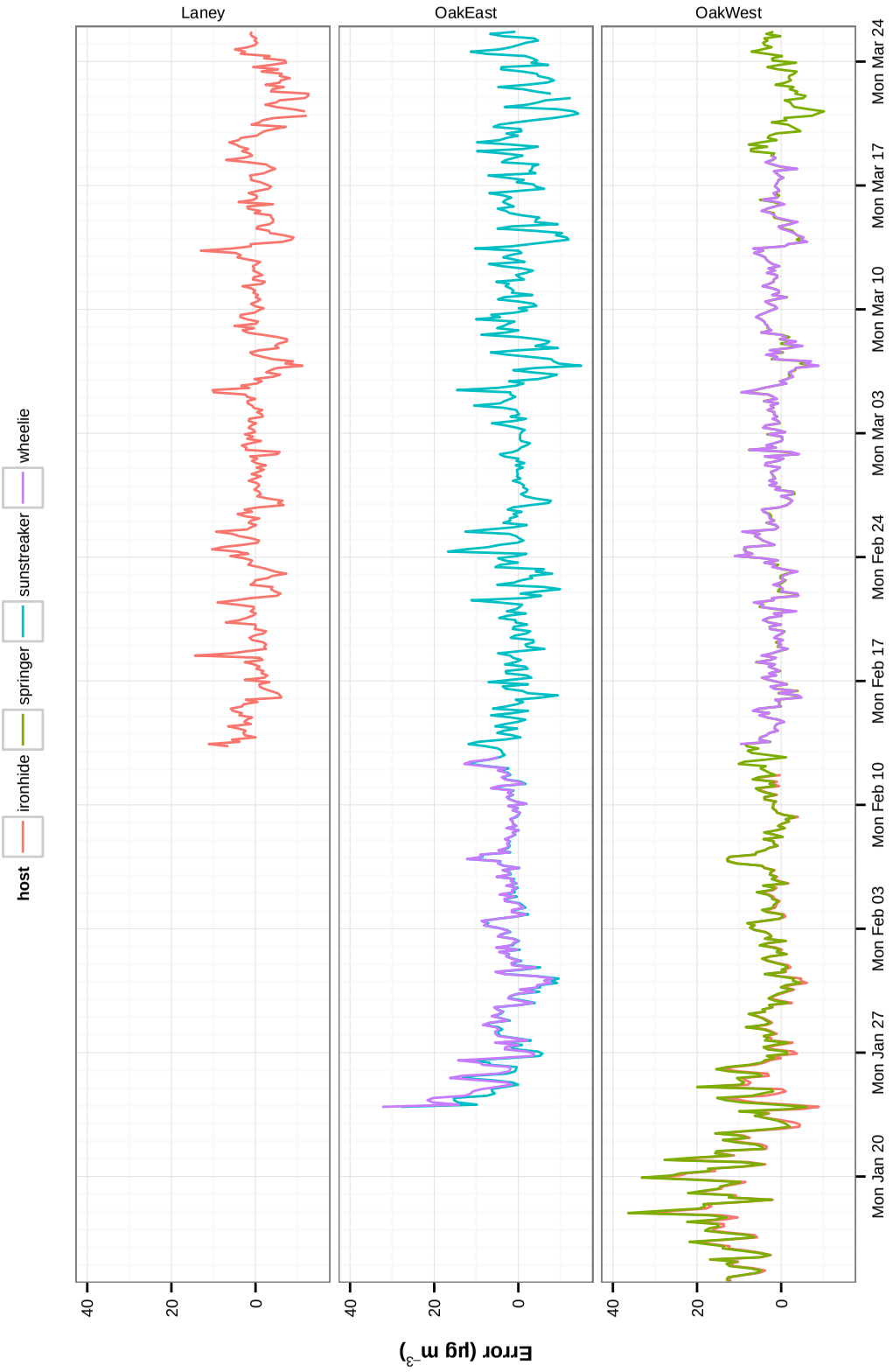

Fig. 4.11: Residuals vs time (3 h scale).

Residuals

Figure 4.11 shows that residuals were serially correlated, and at scales considerably longer than the characteristic response time of the PPD42NS. This suggests that the first-order regressions were failing to capture the influence of some environmental parameter(s) varying on scales from hours to days. Applying first-order calibrations from the chosen calibration timeframe to data from the first 10 days resulted in the largest residuals (more than 50 % underprediction). During this time, reported $PM_{2.5}$ concentrations were also considerably higher than during the rest of the study. Sensors had yet to be deployed at sites other than Oakland West, so it was not possible to determine if this underprediction was due to a site-specific or regional factor.

On occasion, the magnitude and direction of error exhibited remarkably similar patterns at multiple sites. For example, during Feb 2–3 and 6–7, sensors at Oakland East and Oakland West under-predicted similar rises and falls in reference $PM_{2.5}$ at both sites. A regional-scale difference in aerosol composition, rather than a site-specific factor, may have a role in explaining these anomalies.

More localized environmental factors may also have a role in explaining anomalies. For example, the latter half of the residuals from Oakland East appear to exhibit a periodic component not captured by the calibration—roughly on a 24 h cycle—that does not appear to be as pronounced at Oakland West or Laney College. This is corroborated by a plot of diurnal residuals (Fig D.3), in which time-of-day effects are apparent in the panel corresponding to the deployment of "sunstreaker" at Oakland East, but not in panels corresponding to other hosts or other sites.

A search for missing variables was conducted with the aid of graphical summaries. Data from the first and last 2 weeks were held out as test sets, in case potential explanatory factors were identified. Residuals were plotted against functions of time (calendar time, day-of-week, and hour-of-day), as well as metrics routinely reported at the colocation sites and neighboring weather station. Concentrations of co-pollutants (CO, NO, NO_X, and BC) were first divided by the reported concentration of $PM_{2.5}$. This analysis did not result in the confirmed identification of any explanatory factors from among the candidates, though weak inverse associations were noted between the magnitude of residuals and BC / $PM_{2.5}$ ratios, and larger residuals were generally observed at relative humidities above 75 %. Appendix D.1 presents the graphical summaries that were used.

Sub-hourly analyses

Reference $PM_{2.5}$ estimates were not available at timescales below 1 h. However, 1 h calibrations were applied to averages of data from triplicate sensors on scales from 3 min to 30 min, on the following grounds:

1. As shown in Table 4.3, estimates of β_1 were reasonably invariant to the timescale T for $1 \leq T \leq 24$ h (Table 4.3).

2. Within the context of this dataset, a reasonable lower limit to the effective temporal resolution of a single PPD42NS sensor was approximately 5 min (Fig D.2, Appendix D). Integrating across three PPD42NS sensors had the same effect as increasing T by a factor of three (data not shown).

3. Instruments were designed to sample three sensors in parallel, and no sensors exhibited failures.

Figures 4.12 and 4.13 show that important structure was revealed in sub-hourly data. At scales of 3 min to 30 min, consistent responses were observed from replicate instruments at the near-roadway site (Laney College), while similar responses were not observed at a nearby background site (Oakland West). Using a 1 h calibration, the amplitudes of these localized features were estimated to reach $100\,\mu g\,m^{-3}$ to $200\,\mu g\,m^{-3}$. Given their intermittent character, the total time-integrated exposure during a 1 h interval containing several such features would be lower, consistent with the levels indicated by the 1 h reference $PM_{2.5}$ data (black stepped line).

4.4 Discussion

Cross-calibration, first-order calibrations, and residuals

Cross-calibrations (Table 4.2) demonstrated that sensor-to-sensor variability was manageable, and that a substantial component of this variability could be removed through the application of a multiplicative correction factor. Additive corrections were negligible (less than $\pm 1\,\mu g\,m^{-3}$) These findings have practical implications for future calibrations and fieldwork with these instruments.

Compared to previous results reported in Chapter 3, the deployments reported here exhibited nearly the same level of agreement with FEM $PM_{2.5}$ at 24 h and 1 h scale (as measured by R^2). Good agreement was also found using a simplified model with a forced intercept through the origin. Moreover, host-specific calibrations appeared to be exchangeable between sites—even between a background site and a near-roadway site. This warrants further investigation. If independently confirmed, it would imply that the association between the PPD42NS's measurand and the BAM-1020's measurand (nominally $PM_{2.5}$) did not differ radically between near-road and background monitoring sites.

Residuals were serially correlated at scales considerably longer than the characteristic response time of the PPD42NS (Fig 4.11). Moreover, consistent errors were exhibited by sets of sensors at the same site, and (on occasion) by sets of sensors at different sites. These data are consistent with two interpretations:

- Some "nuisance" environmental parameter(s) influenced the PPD42NS; and/or
- The PPD42NS and the reference $PM_{2.5}$ instrument measured two related but distinct properties of urban aerosol.

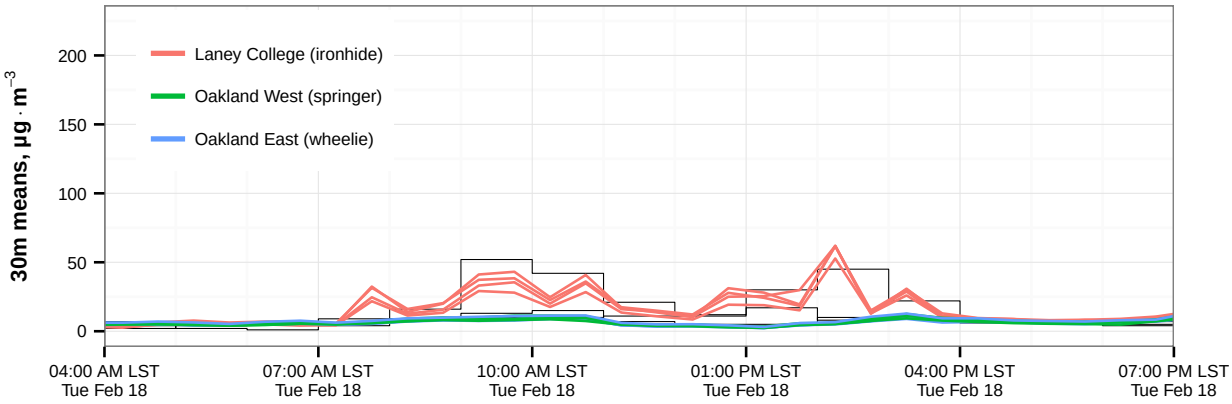

(a) 30 min scale

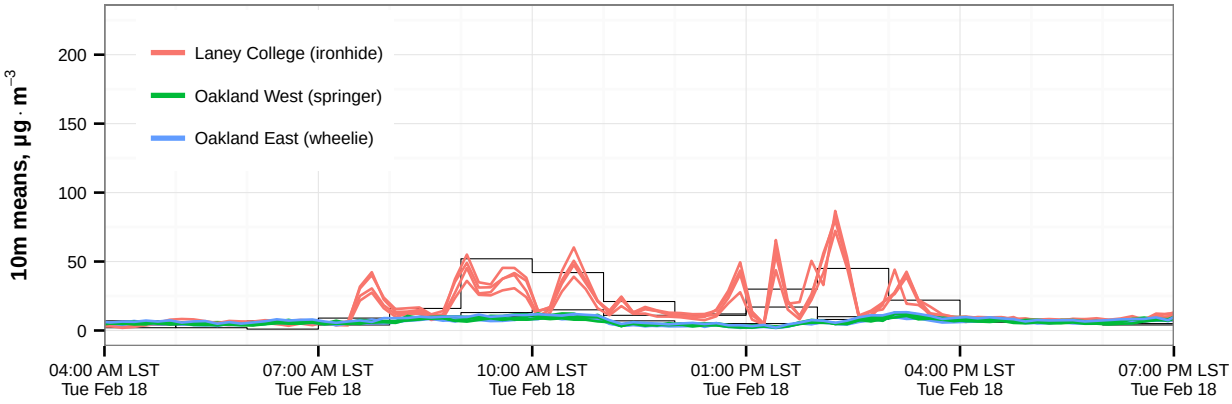

(b) 10 min scale

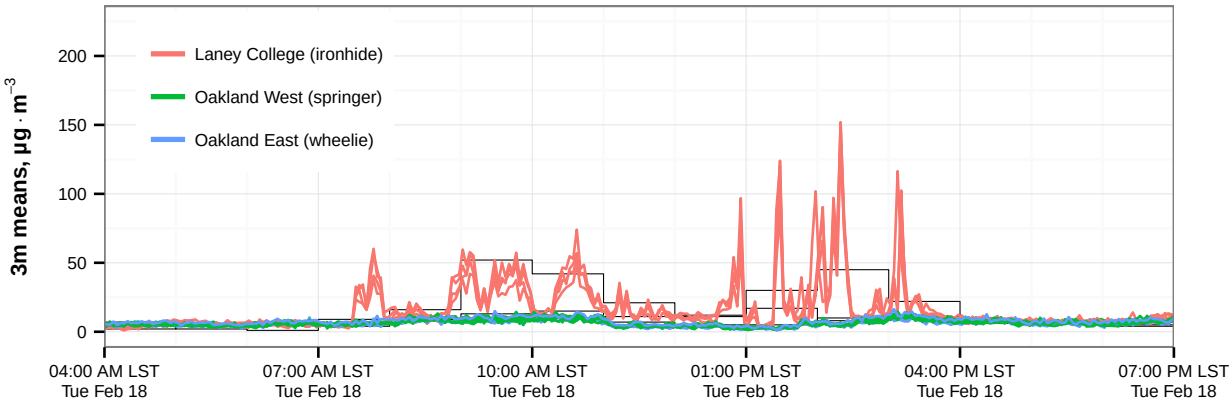

(c) 3 min scale

Fig. 4.12: Data aggregated to 30, 10, and 3 min scales. Substantial variation is evident at the near-roadway site (Laney College) and absent from background sites (Oakland West and East). Colored lines are data from triplicate PPD42NS sensors. Stepped lines are 1 h FEM $PM_{2.5}$.

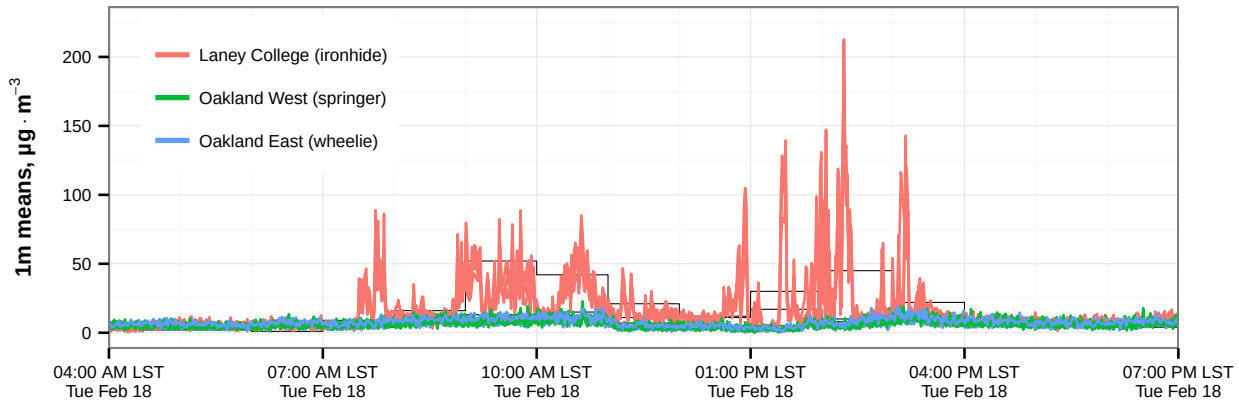

(a) 1 min scale

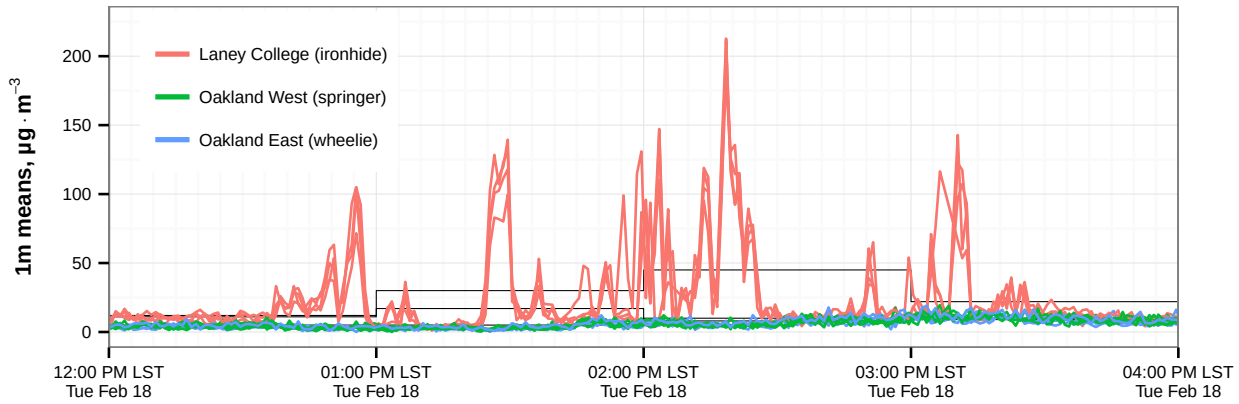

(b) 1 min scale (detail)

Fig. 4.13: Data aggregated to 1 min scale. Top: same timeframe depicted in the previous figures (4am–7pm LST, Feb 18 2014). Bottom: detail, noon–4pm LST, Feb 18 2014. Note the magnitudes, durations, and localized character of peaks evident in data at this scale. Since $PM_{2.5}$ reference data were not available at timescales below 1 h, the calibration applied to sensor output was obtained from 1 h data.

These interpretations are mutually compatible. It may be, for example, that the composition of the particles could explain some of the residuals, while an unmeasured or improperly modeled environmental parameter could also have altered the sensitivity of the PPD42NS.

Although no missing variables were identified from inspection of the residuals, a large set of data has been obtained that can be investigated with additional resources, including speciation data and predictions from air quality models. A weak time-of-day effect was apparent at Oakland East, but was not apparent at other sites. A weak inverse association was observed between BC / $PM_{2.5}$ ratios and the magnitudes of residuals. More sophisticated statistical techniques (e.g., G-computation, clustering, lasso, ridge regression) might also be brought to bear on the identification and parameterization of a calibration model with additional terms.

Sub-hourly analyses

Applying a 1 h calibration to data on scales of 0.05 h to 0.5 h (3 min to 30 min) revealed physically plausible structure on relevant scales (2 $\mu g\,m^{-3}$ to 200 $\mu g\,m^{-3}$). These observations should be compared to predictions from simple physical models, perhaps by using appropriate rescalings of existing emission inventories as a starting point. Such fine-scale obervations stand to improve the empirical foundation of our understanding of relevant sources (e.g. highways), as well as to aid in identifying and characterizing uninventoried sources ("ground truthing"). There are many practical consequences; for example, improving constraints on inventories of urban combustion stands to improve exposure science, atmospheric modeling, and accountability studies of policy implementations.

Traditional practice in air pollution exposure epidemiology is to use steady-state dispersion models to predict average concentrations at scales of weeks, months, or years. As researchers and regulators develop new knowledge and guidance concerning the health effects of urban pollutants at finer spatial and temporal scales, modelers must meet the challenge of forecasting and diagnosing micro-scale data. Although strong consensus on best practices at these scales has yet to emerge, it is technically possible for relatively simple gridded advection-dispersion models to be applied to this dataset on scales of 0.1 h to 1 h. Such an analysis is outside the scope of the present work.

Remotely transferring calibrations

In this study, hosts "sunstreaker" and "springer" remained at Oakland East and Oakland West, respectively, for the duration of the study. During the time that "wheelie" was colocated with "sunstreaker", the MARE between the 3 h averages (arithmetic means) of uncalibrated output from the 12 sensors in each host was 10 %, with an RMSE of 2×10^{-3} % FS, or approximately 2 $\mu g\,m^{-3}$. Had "wheelie" been observing a comparable environment elsewhere, it would therefore have been quite reasonable to transform its sensor outputs to $\mu g\,m^{-3}$ merely by multiplying the uncalibrated data by (a) an estimate of β_1 obtained for "sunstreaker", along with (b) the relative correction factors for "sunstreaker" obtained using PCA. Judging by the MARE reported above, this would have increased the expected multiplicative error by approximately $\pm$ 10 %

beyond a direct calibration against reference equipment. Had this been acceptable, and had a collaborator been operating and reporting the β_1 for "sunstreaker", there would not have been a need to install "wheelie" at Oakland East, nor at any other regulatory site. The expected agreement between measures of central tendency will increase with the number of sensors n, so if a figure of 10 % were unacceptable, n might be increased until practical tolerance requirements were met.

In essence, this demonstrates the viability of a statistical approach to remotely transferring calibrations between two sets of low-cost sensors. Arguments in favor of mass deployments of lower-cost sensors typically focus on other advantages, such as increased coverage or density. In general, for two sets of timeseries $\boldsymbol{X}_1, \boldsymbol{X}_2, \ldots \boldsymbol{X}_n$ and $\boldsymbol{X}^\star_1, \boldsymbol{X}^\star_2, \ldots \boldsymbol{X}^\star_m$, with each timeseries $\boldsymbol{X_i}$ having k observations $\{x_{i1}, x_{i2}, \ldots x_{ik}\}$, it is possible to use the same three-part decomposition: cross-calibrations $\boldsymbol{\gamma} = \gamma_1, \gamma_2, \ldots \gamma_n$ among the first set; cross-calibrations $\boldsymbol{\gamma}^\star$ among the second set; and a mapping $\boldsymbol{\beta}$ from $E[\boldsymbol{X}]$ to the reference standard $\boldsymbol{Y}$. With a suitable estimator θ for $E[\boldsymbol{X}]$, such as the mean, median, or geometric mean[3], the Law of Large Numbers entails that $\theta(\boldsymbol{X}) = \{\theta(x_{11}, x_{12}, \ldots x_{1k}), \theta(x_{21}, x_{22}, \ldots x_{2k}), \ldots \theta(x_{n1}, x_{n2}, \ldots x_{nk})\}$ will approach $\theta(\boldsymbol{X}^\star)$ as n and m grow sufficiently large. Only a small number of sensors may be necessary; here, $n = m = 12$.

This opens up interesting possibilities for collaboration. If the first set of n cross-calibrated sensors can be colocated with reference equipment (perhaps even managed by the operators of the reference monitoring site), the calibration $\boldsymbol{\beta}$ can be transferred remotely, at any time, to a second set of m cross-calibrated sensors. To the extent that the surplus error from the expected difference between $\theta(\boldsymbol{X})$ and $\theta(\boldsymbol{X}^\star)$ falls within stable and practical tolerances (above, it was $\pm 10\,\%$) in the context of the sensors' calibration model, there is in principle no need for collaborators to collocate a secondary set, or set(s), with any reference equipment at all.

This approach still depends on having good faith collaborators with physical access to reference equipment. It does not mitigate the threats to validity associated with extrapolation (or interpolation) of calibration parameters to conditions beyond those observed during calibration. But, as remarked in Chapter 3, scarcities of time and trusted personnel may be some of the most significant barriers to calibration of low-cost PM instruments. Therefore, reducing or eliminating the need for physical colocations in this manner could help to support broader participation in the production of valuable observational data in two ways. First, it could reduce the labor required to transport and set up instrumentation. Second, it could reduce certain liabilities—for example, the risk of accidental interference with reference equipment. In the United States, access to routine PM monitoring sites is heavily restricted, at least in part because of such risks.

Limitations

The design of this study could not address the generalizability of calibrations beyond the variation represented by the three selected sites. Due to its observational nature, this study was also

[3]More robust statistics than the mean might be preferred.

limited in its ability to identify and/or quantify the influence of environmental variables that might influence the sensitivity of PPD42NS sensors or the instruments constructed with them. Chapter 3 contained a discussion of several general caveats along these lines, but additional examples may serve to underscore the point:

- It is reasonable to expect that temperatures *outside of* the ranges observed would have an influence on the supporting electronics, and possibly on the airflow induced by the resistive heating element inside the PPD42NS module.
- The influence of temperature (or another variable) *within* observed ranges may have been masked by covariation with other uncontrolled variables.
- It is also reasonable to anticipate typical "cross-sensitivities" associated with optical instruments (e.g. relative humidity), as well as differential sensitivity to aerosols with different compositions and size distributions, especially under circumstances more extreme than investigated here.

4.5 Conclusion

The 24 h and 1 h calibrations of Chapter 3 conducted at West Oakland in 2013 were generally commensurate with calibrations at the same site during Spring 2014, and with calibrations at Oakland East, a regulatory site approximately 15 km away. Calibrations at a near-roadway site (Laney College) appeared to be applicable to data collected earlier at Oakland West. This warrants further investigation. Analysis of residuals did not reveal clear, consistent, and substantial associations between the residuals and any single variable examined within the scope of this study. However, this does not constitute strong proof, only a lack of disproof. Weak inverse associations were noted between the magnitude of residuals and BC / $PM_{2.5}$ ratios, and larger residuals were generally observed at relative humidities above 75 %. An experimental design, in addition to or instead of the application of more sophisticated statistical methods, could establish and quantify the importance of one or more missing variables. This work would be strongest if conducted independently.

Variation in sensitivity among a large sample of low-cost aerosol sensors ($n = 48$), as modeled by PCA, was almost entirely captured by a single, stable, sensor-specific correction factor (multiplicative gain). Relative offsets were less than $\pm 1\,\mu g\,m^{-3}$, based on calibrations against reference equipment. 95 % of relative gains were within 30 % of unity, and 50 % were within a factor of 10 % (see Sec 4.3). The MARE between the 3 h averages (arithmetic means) of uncalibrated output from $n = 12$ sensors in two hosts was 10 %, with an RMSE of 2×10^{-3} % FS, or approximately $2\,\mu g\,m^{-3}$. Had this surplus error been acceptable, and had a collaborator been operating and reporting the β_1 for the first host, there would not have been a need to colocate the second host with any reference instrumentation (neither the first host nor any regulatory monitors). The expected MARE (and MSE, etc.) between samples will decrease with

the number of sensors n, so if a figure of 10 % were unacceptable, n might be increased until practical tolerance requirements were met.

In the context of this dataset, a practical lower limit to the effective temporal resolution was on the order of 1 min to 5 min. This limit could be relaxed when examining averages of data from multiple sensors and/or higher PM concentrations. Simple averaging of triplicate sensors yielded 1 min data consistent with intermittent observations of localized plumes at the near-roadway site. Although the composition and character of such plumes would be expected to differ from the composition of emissions from the 2003 wildfires in Southern California (Chapter 2), time-weighted average concentrations at sub-hourly scales were roughly commensurate with the 1 h intensities observed during the wildfires ($100\,\mu g\,m^{-3}$ to $200\,\mu g\,m^{-3}$). A reference instrument capable of supplying sub-hourly reference data would be useful in confirming or refuting the accuracy of these estimates.

Chapter 5

Discussion

5.1 Overview

The central argument of this thesis has proceeded in two parts. Chapters 1 and 2 discussed and demonstrated the inadequacy of existing PM monitoring infrastructure for modern air pollution exposure assessment and epidemiology. Chapters 3 and 4 demonstrated the possibility of generating useful and accurate estimates of hourly and daily $PM_{2.5}$ concentrations in carefully chosen contemporary contexts (regulatory monitoring sites within selected urban neighborhoods) by combining a newly available low-cost sensor with other low-cost, readily available hardware. In so doing, this thesis raises, but cannot fully address, several lines of potential sociotechnical development that could be variously characterized as "progressive" or "disruptive". The unique contribution of this chapter is to discuss selected examples of such prospects, drawing out the ways in which they are connected to the methods and results of the previous four.

5.2 Progressive prospects

In the canonical model of environmental health, formal knowledge is established through research and risk assessments conducted by trained professionals. In turn, the products of these professionally guided activities influence action primarily through the mechanisms of social policy. Improvements to technical practices that establish the credibility, relevance, and usefulness of sensor systems stand to benefit these existing stakeholders in certain ways, notably by increasing the reach and efficiency of exposure science and related disciplines. (See Chapter 1.) Hereafter, prospects linked to such improvements are termed "progressive".

One progressive prospect was alluded to by the selection of a near-roadway site in Chapter 4. New EPA monitoring requirements are creating challenges for state and local air monitoring agencies, who are now required to operate monitoring stations near roadways in addition to regionally representative stations. Low-cost sensors like those employed in this project could form the basis of some near-roadway monitoring as well as future personal exposure instru-

mentation. Understanding their performance in short-term field deployments can serve as a stepping stone to wider use in ambient monitoring and personal exposure assessment studies. They can also be used to validate models and constrain emission inventories. New tools based on EPA-approved dispersion models and emission inventories are emerging to assist urban planners and policymakers in estimating near-roadway exposures at regional scale (Samaranayake et al., 2014; Holstius et al., 2013; Rioux et al., 2010). However, these tools require validation in contemporary urban contexts, as the vast majority of empirical observations historically used to validate the underlying dispersion models have been collected under conditions (i.e., terrain, meteorology, and emission intensities) insufficiently representative of contemporary usage.

A second progressive prospect concerns the scarcity of data from a more global perspective. Scientifically speaking, the bulk of the evidence base for the health effects of PM rests on studies of high doses (primarily from studies of tobacco smoking) and low doses (from ambient monitoring in wealthier countries). The middle regions of the integrated exposure-response (IER) curves that have been developed for relevant health outcomes are supported by relatively few observations (Burnett et al., 2014). These regions coincide with the bulk of exposures and health burdens borne by the world's poor, who largely rely on biomass burning or other high-emission combustion sources for cooking and heating. Solidifying the evidence base in these regions is important so that the shape of pertinent integrated exposure-response curves can be more firmly established. These curves in turn shape estimates of global burdens of disease, and can potentially guide policy-driven allocations of resources for mitigation and prevention.

5.3 Disruptive prospects

There are many more potential examples of how affordable $PM_{2.5}$ monitoring equipment could enable the collection of valuable data in poorly understood contexts. However, the ability to effectively monitor particulate matter with commodity hardware may also lead to proliferations of disruptive observations and claims.

If, as envisioned by many exposure scientists (National Research Council, 2012), it becomes easier for individuals and groups with relatively limited technical training and resources to produce trustworthy $PM_{2.5}$ measurements more-or-less autonomously, it is hard to see how this would not begin to play out in sparsely monitored yet highly contested spaces, such as near roadways or on the fencelines of industrial facilities. It is unclear how regulatory agencies and other established interests can, will, or should respond. Current regulatory practice generally observes certain cadastral boundaries, at least in the domain of air pollution; for example, central-site monitors may be more or less considered "representative" of cities, counties, regions, and states. With some exceptions, these geographies map fairly well to political units or aggregations thereof. The result is that constituents of counties and states are represented by elected officials and appointees in the political arenas where funding is allocated to mitigate air pollution problems. The possibilities afforded by low-cost instrumentation push attention in the direction of problems with different geographies. As an EPA representative expressed (personal communication, Chicago Air Quality Egg workshop, June 2013), "Suppose these

[new] near-roadway NO_2 monitors show high values. What is out of attainment? The entire highway?" Presently, no one speaks in the same arenas for constituents living near roadways, at least not in the same manner or from positions of comparable authority and power.

As low-cost sensors and open hardware become increasingly affordable and accessible, and as requisite skills and motivation grow and circulate among "expert amateurs" (Kuznetsov and Paulos, 2010), participation in the design of exposure assessment instrumentation, as well as its operation, stands to increase (Holstius and Seto, 2011). The methods and materials used in Chapters 3 and 4 were sourced from websites and vendors representative of those frequented by members of "expert amateur" communities, and are thus representative of the quality of measurements that one might expect from carefully executed campaigns conducted by persons or teams equipped with comparable technology and know-how. In most real-world contexts, it is unreasonable to expect any two commercially available environmental monitoring instruments to agree perfectly. How much more so, then, with fully customizable instrumentation? With a proliferating *variety*, as well as number, of instruments and techniques becoming possible, it is reasonable to expect interested parties to go "measurement shopping", selecting the techniques and instruments that produce the data that best support their interests. Studies of metrology have extensively documented the laborious practices required to "compare, standardize, and settle agreement" (Mallard, 1998) amongst the creators and users of one-of-a-kind or limited-run instrumentation, but so far these practices have been restricted to a fairly small number of mutually familiar experts. (By analogy, in the domain of computer modeling, a scarcity of officially sanctioned models, as well as a scarcity of resources needed to run them, somewhat mitigates the problem.)

Limiting the sheer volume of attention-worthy claims, which is in effect accomplished by limiting access to the means of producing them, has the side effect of limiting demands on regulatory agencies and regulated industries. Removing these barriers could result in an influx of claims that bureaucracies would have a vested interest in dismissing. Thus, although absences of adequate data have been rhetorically linked to the sticker prices of instruments accepted within certain communities of practice, there are reasons to suspect that causality may not flow solely in that direction. And, there is as yet no convincing evidence that the existence of comparable instruments at a substantially lower price point would be sufficient to promote envisioned changes.

Two other categories of disruptive prospects could follow from the commodification of personal monitoring technologies. First, when accurate individual-level or small-group exposure data are readily available, the responsibility for remediating problems, as well as perceptions of agency and blame, can shift to individuals—a process termed "responsibilization" (cf Rous and Hunt, 2004; LeBesco, 2011). The pooling of risk, in contrast, brings economies of scale to insurance and mitigation activities, and simplifies or obviates questions about equitable distributions of risks. Second, the easy availability of personal monitoring technologies with effective personal-feedback components is envisioned by many researchers to be a natural outcome of a proliferation of accurate and low-cost personal monitoring technologies. Insofar as study participants would alter their exposures based on the data available from such instruments, their provision or withholding constitutes an intervention. Inferences generalized from study

populations where the allocation of such instruments is not randomized or otherwise controlled may be biased. Statistical control would require unbiased estimates of the effect, and blinding research participants to real-time information that (it is claimed) would otherwise have the effect of reducing their exposures would be akin to withholding a beneficent treatment, which would require justification and, if possible, mitigation or compensation.

5.4 Summary and conclusion

This thesis has discussed and demonstrated the inadequacy of existing PM monitoring infrastructure for modern air pollution exposure assessment and epidemiology, and has demonstrated the possibility of generating useful estimates of daily, hourly, and sub-hourly estimates of $PM_{2.5}$ concentrations with a low-cost sensor and other commodity hardware in contexts of interest. Independent confirmation or refutation of these findings is warranted, and better characterization of the limitations of these sensors will be required if claims in other contexts are to be supported as well. Skepticism is warranted. It is reasonable to start from the premise that the calibrations reported in Chapters 3 and 4 will *not* generalize, and then to challenge that hypothesis by probing additional contexts to discover where and when they might.

Given the accelerating speed of sensor research and development, it is important to consider the demonstrations supplied in this thesis as contributions toward frameworks for rapid screening and evaluation of the next generation of aerosol sensors, rather than attempts to fully characterize this specific sensor. The development of a plethora of new sensors is likely to outpace present capacity for independent, resource-intensive, laboratory-based calibration practices. The invention and support of sustainable practices for collaborative calibrations and intercomparisons is naturally of interest. Chapter 4 showed how a single-parameter calibration could be remotely transferred between two sufficiently large sets of sensors, and quantified the surplus error in the case of the particular sensor and context considered here. Whether the technique is extensible and applicable to the needs of participants in real-world monitoring campaigns remains to be seen.

When data are missing, it is important to understand why. Absences of data, like absences of knowledge (Frickel et al., 2010), may signal the presence of countervailing causal factors. Previous scholarship has demonstrated that technological possibilities do not solely determine whether, or for whom, environmental monitoring instruments become trusted sources of data (Mallard, 2001; O'Rourke and Macey, 2003; Harrison, 2011; Ottinger, 2009; Shilton, 2011). It will be interesting to observe, and perhaps to influence, the dynamic interplays between publics and technologies that will shape the provenance and coverage of tomorrow's data. Establishing the relevance and credibility of newly affordable modes of participation in the production of that data is an obvious challenge for many stakeholders, and an area that future research should explore.

Appendix A

Abbreviations and definitions

AQMD Air quality management district

BC Black carbon

BEACON BErkeley Atmospheric CO_2 Network

CITRIS Center for Information Technology Research in the Interest of Society

CO Carbon monoxide

DMS Data management system

FEM Federal equivalent method

FRM Federal reference method

GPS Global positioning system

IUGR Intrauterine growth restriction

LBW Low birth weight; less than 2500 g

LMP Last menstrual period

LST Local standard time

MAE Mean absolute error $\frac{1}{n}\sum_{i=1}^{n}\left|Y_i - \hat{Y}_i\right|$

MODIS Moderate Resolution Imaging Spectroradiometer

MARE Mean absolute relative error $\frac{1}{n}\sum_{i=1}^{n}\frac{\left|Y_i - \hat{Y}_i\right|}{Y_i + \hat{Y}_i}$

MSE Mean squared error $\frac{1}{n}\sum_{i=1}^{n}(Y_i - \hat{Y}_i)^2$

PANDAs Portable and Affordable Nephelometric Data Acquisition [system]

PCA Principal components analysis

PM Particulate matter

$PM_{2.5}$ PM with aerodynamic diameter $d_p < 2.5\,\mu m$; also known as *fine PM*

PM_{10} PM with aerodynamic diameter $d_p < 10\,\mu m$

NO Nitric oxide

NO_2 Nitrogen dioxide

NO_X Nitrogen oxides ($NO + NO_2 = NO_X$)

OLS Ordinary least squares

RMSE Root mean square error $\sqrt{\frac{1}{n}\sum_{i=1}^{n}(Y_i - \hat{Y}_i)^2}$

SoCAB South Coast Air Basin

SES Socioeconomic status

SGA Small for gestational age

TLS Total least squares

USD United States Dollars

Appendix B

Supplement to Chapter 2

B.1 Modeling seasonality with a cosinor

The temporal term $f(t_i)$ is constructed from a modified cosine function having phase P, frequency ω, and amplitude A:

$$f(t_i) = \alpha_0 t_i + A cos(\omega t_i - P) \tag{B.1}$$

The additive term $\alpha_0 t_i$ models the secular trend, since t_i represents the last LMP for birth i. The frequency ω is chosen according to the length of the modeled cycle; in this case, we are interested in modeling an annual cycle, so $\omega = (2\pi/365.14)$ days.

The following expression is equivalent to Eq B.1, but is linear in t_i, and so can be fit using standard techniques such as least squares:

$$f(t_i) = \alpha_0 t_i + c\, cos(\omega t_i) + s\, sin(\omega t_i) \tag{B.2}$$

In terms of the coefficients c and s, the amplitude A then corresponds to:

$$A = \sqrt{c^2 + s^2} \tag{B.3}$$

While the phase P (in radians) corresponds to:

$$P = \begin{cases} arctan(s/c), & \text{if } c \geq 0 \\ arctan(s/c) + \pi, & \text{if } c < 0 \text{ and } s \geq 0 \\ arctan(s/c) - \pi, & \text{if } c < 0 \text{ and } s < 0 \end{cases}$$

Appendix C

Supplement to Chapter 3

C.1 Pilot study

As a pilot study, 5 Shinyei PPD42NS sensors were colocated in a 70 m^3 office environment, located on the 5th floor of a building in downtown Berkeley, CA, for 6 weeks (Jul 16 – Aug 30 2012). All windows were left open to promote extensive infiltration of outside air. Aims for the pilot study were: (a) to assess whether previously reported high-frequency (1 min) correlations between a PPD42NS and a consumer-grade optical counter (OPC) could be reproduced with a longer integration time (1 h) at the much lower concentrations characteristic of ambient urban aerosol; and (b) to assess variations in response among a sample of PPD42NS sensors. Reference data at 1 min scale were collected from a consumer-grade OPC (Dylos DC1700) positioned within 30 cm of the sensors. All data were subsequently binned and analyzed using 1 h arithmetic means.

During our pilot study, we observed very high pairwise correlations (R^2) of 0.98–0.99 between all sensors (Figure C.2). The data were left-skewed, with 99 % of observations between 0.013–1.623 and 95 % between 0.023–1.362 (% FS; see Methods for an explanation of the metric). The mean and median were 0.366 and 0.215 % FS, respectively. The overall correlation between PANDAs and the OPC was slightly lower but still high, with $R^2 = 0.85$–0.87. We did not observe any obvious signs of an upper or lower detection limit in either PANDAs or OPC data (Fig C.1).

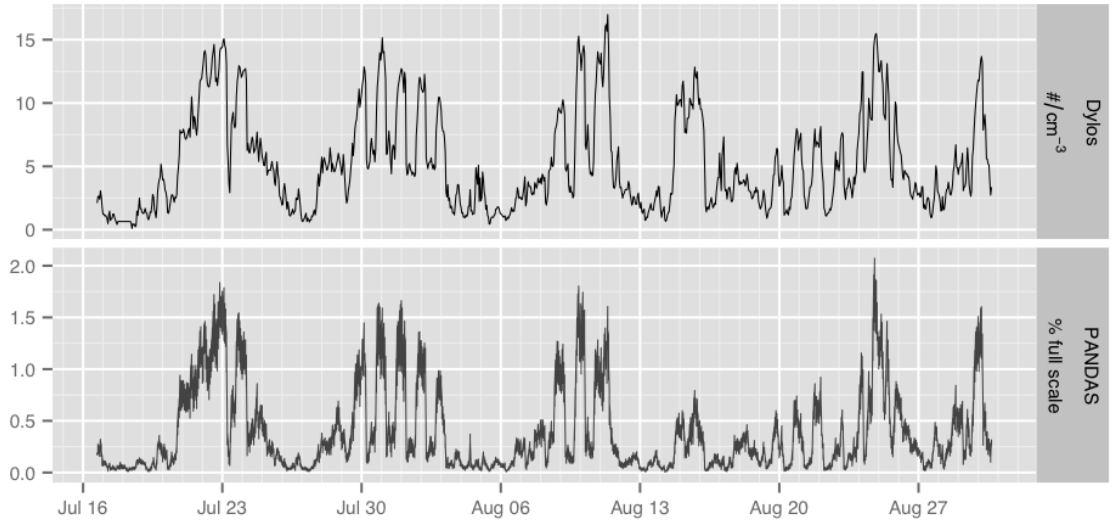

Fig. C.1: Temporal patterns (pilot study). Top: number concentration ($d_p < 2.5\,\mu m$) from optical particle counter (Dylos DC1700). Bottom: 5 colocated PPD42NS sensors (sensor used in PANDAs). .

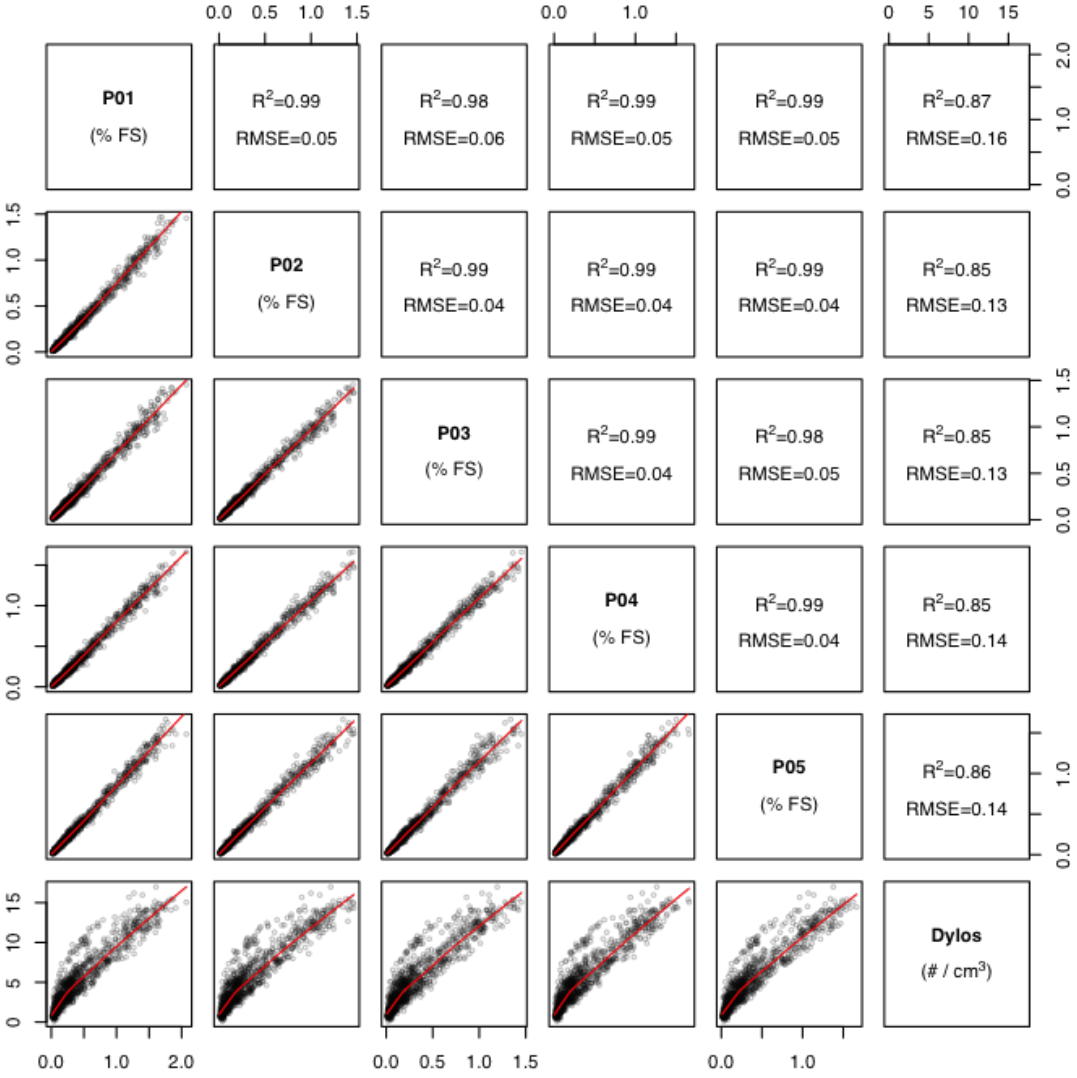

Fig. C.2: Pairwise associations between 1 Dylos DC1700 and 5 PPD42NS sensors deployed in a pilot study. Lower panels: 1-hour data smoothed by loess (red lines). Top panels: coefficient of determination (R^2) and root mean squared error (RMSE) for linear models fit to the corresponding pairwise datasets.

Appendix D

Supplement to Chapter 4

D.1 Apparatus

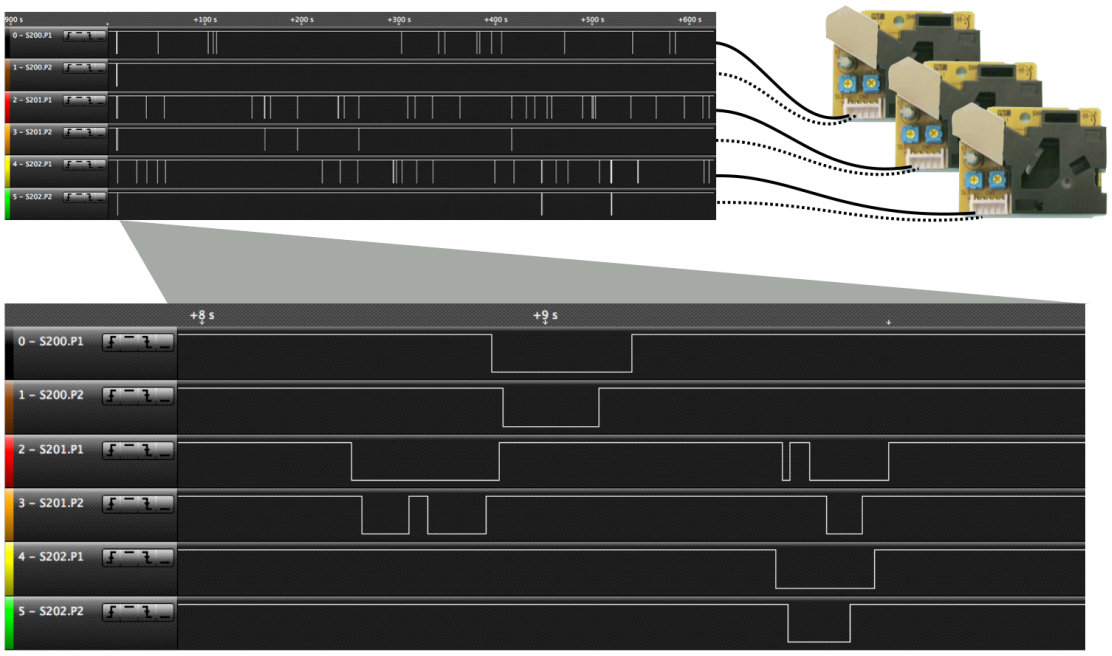

Fig. D.1: Raw signals acquired from from P1 and P2 channels.

Figure D.1 shows the character of the pulse-width modulated digital signal[1] coming from two channels of the PPD42NS, P1 and P2. Relatively long stretches of time can go by without the signal being pulled low. This can distort the distribution of the statistic of interest, which is taken to be the time-integrated average. When the signal is time-integrated, these stretches are transformed into exact zeros, while the remaining data approximate a continuous, positive, and (typically) long-tailed distribution.

Figure D.2 shows that, as the integration time T was increased, the proportion of aggregated data exactly equal to zero decreased, as expected. Because the number of averaged intervals per unit time is inversely proportional to T, the *rate* (per unit time) of exact zeros diminishes less quickly than the proportion (but still quickly). With $T = 3$ minutes, the proportion is about 1.0 %; hence, the rate is about $0.1\,\mathrm{h}^{-1}$.

Source code for the firmware is available at `http://github.com/holstius/PANDAs`.

[1] Acquired with a Salae Logic digital probe.

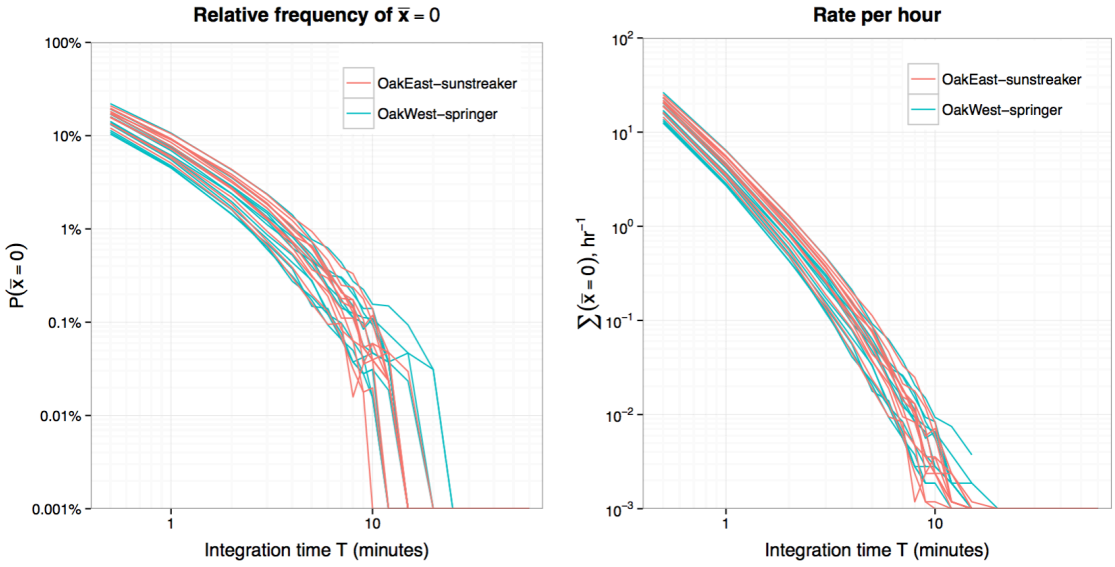

Fig. D.2: Proportion and rate of "exact zeros" in time-integrated signals from the P1 channel of PPD42NS sensors as functions of integration time T.

D.2 Residuals

The following figures depict residuals, at 3 h scale, from the first-order calibration reported in Section 4.3. The first and last two weeks of the study were held out as test sets, in case the analysis of residuals yielded candidates for additional explanatory factors.

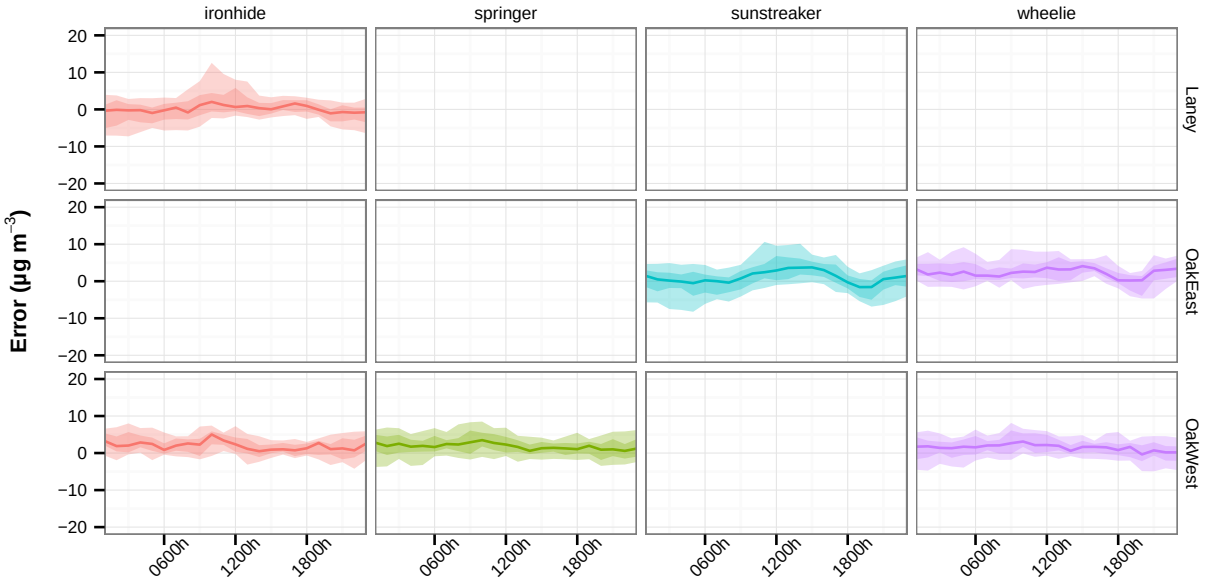

(a) Absolute scale ($\mu g\, m^{-3}$)

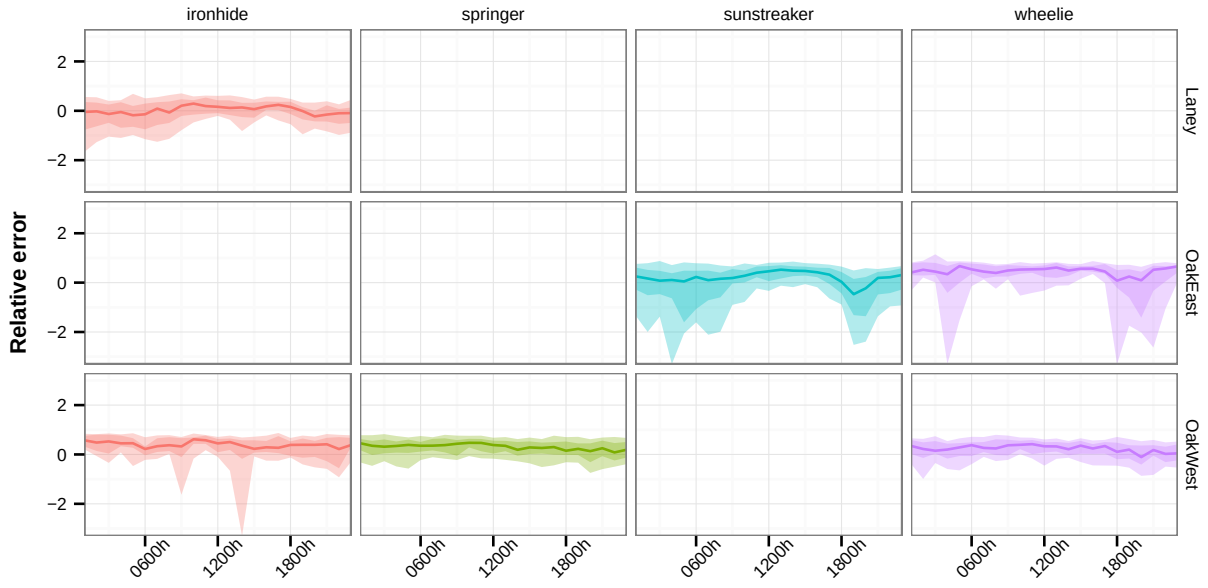

(b) Relative scale

Fig. D.3: Residuals vs hour of day. Panels are conditioned by host (left to right) and host (top to bottom). Light and dark colored ribbons indicate middle 90 % and 50 % of residuals; lines represent the medians.

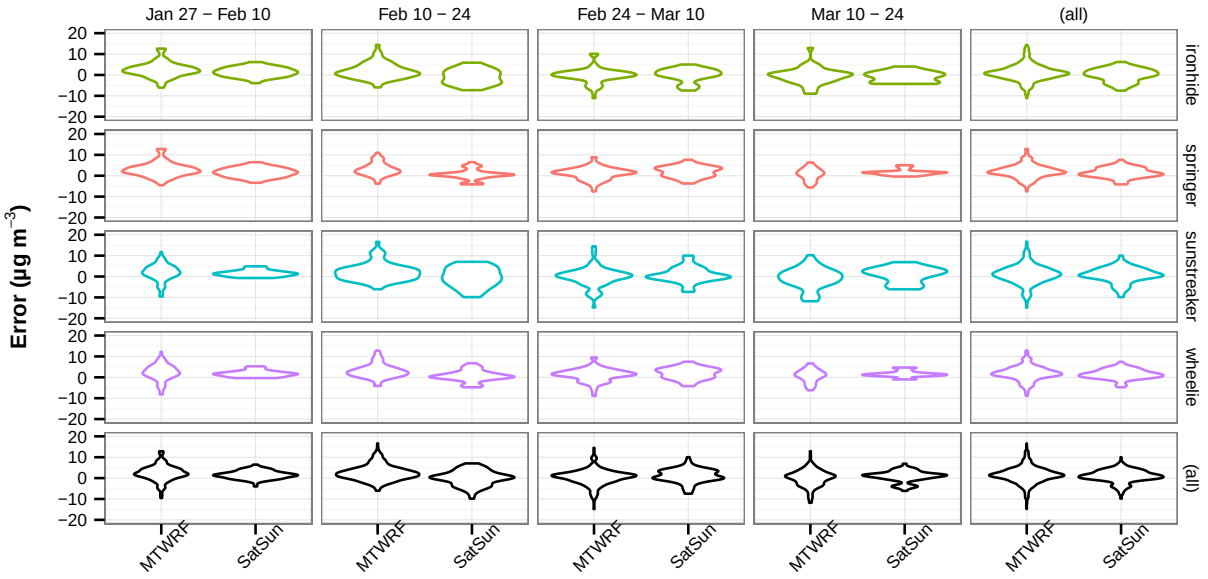

(a) Absolute scale ($\mu g\, m^{-3}$)

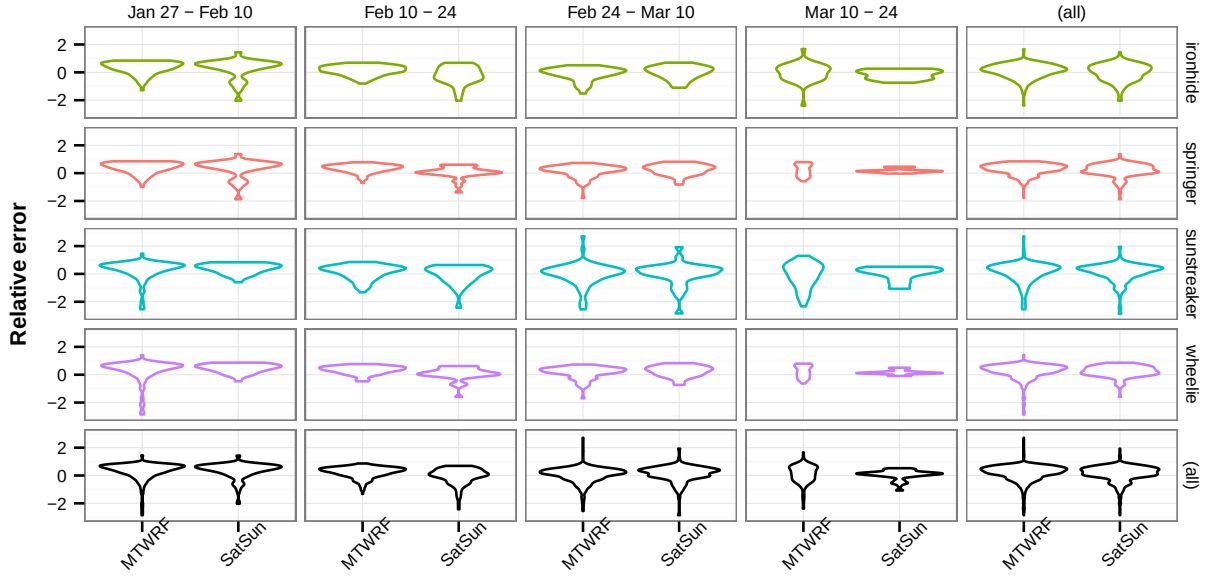

(b) Relative scale

Fig. D.4: Residuals vs weekend/weekday. Panels are conditioned by host (top to bottom) and biweekly intervals (left to right).

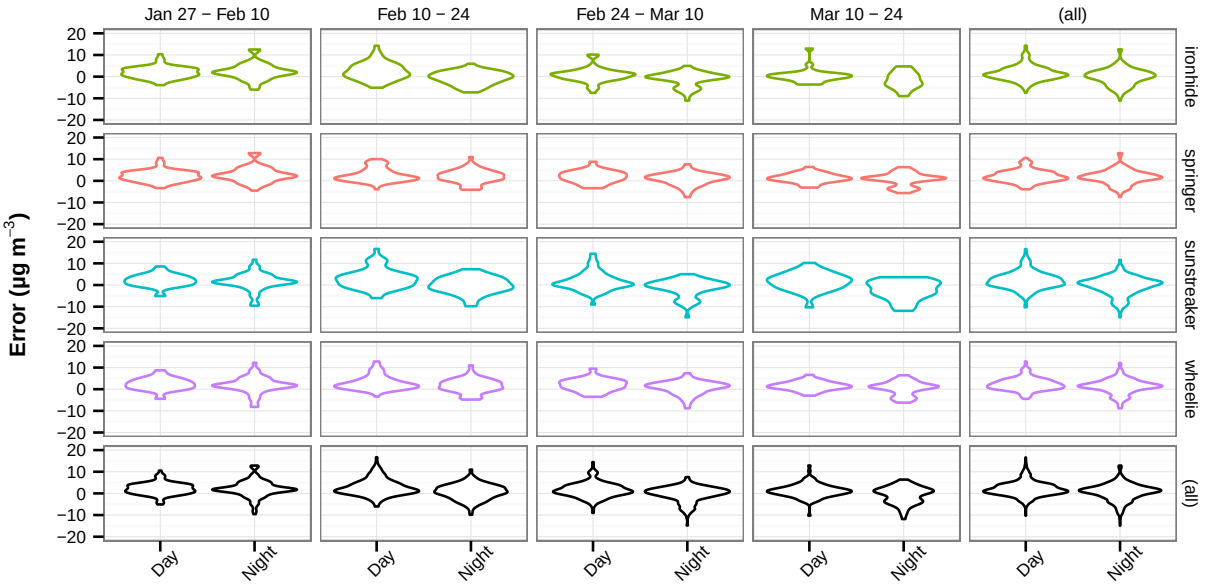

(a) Absolute scale ($\mu g\, m^{-3}$)

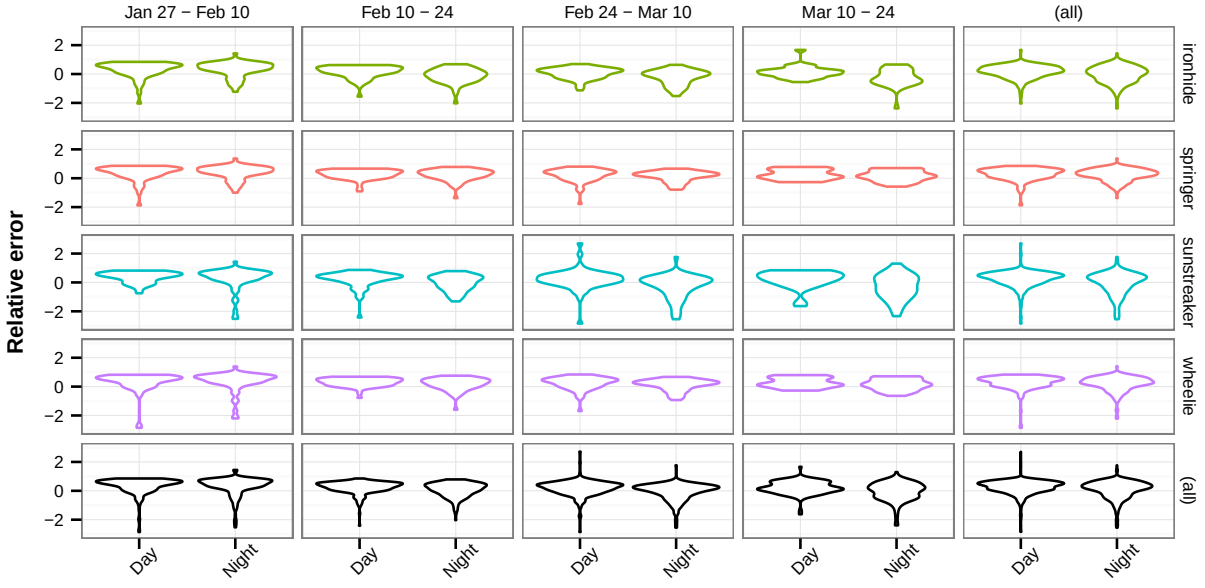

(b) Relative scale

Fig. D.5: Residuals vs solar day/night. Panels are conditioned by host (top to bottom) and biweekly intervals (left to right).

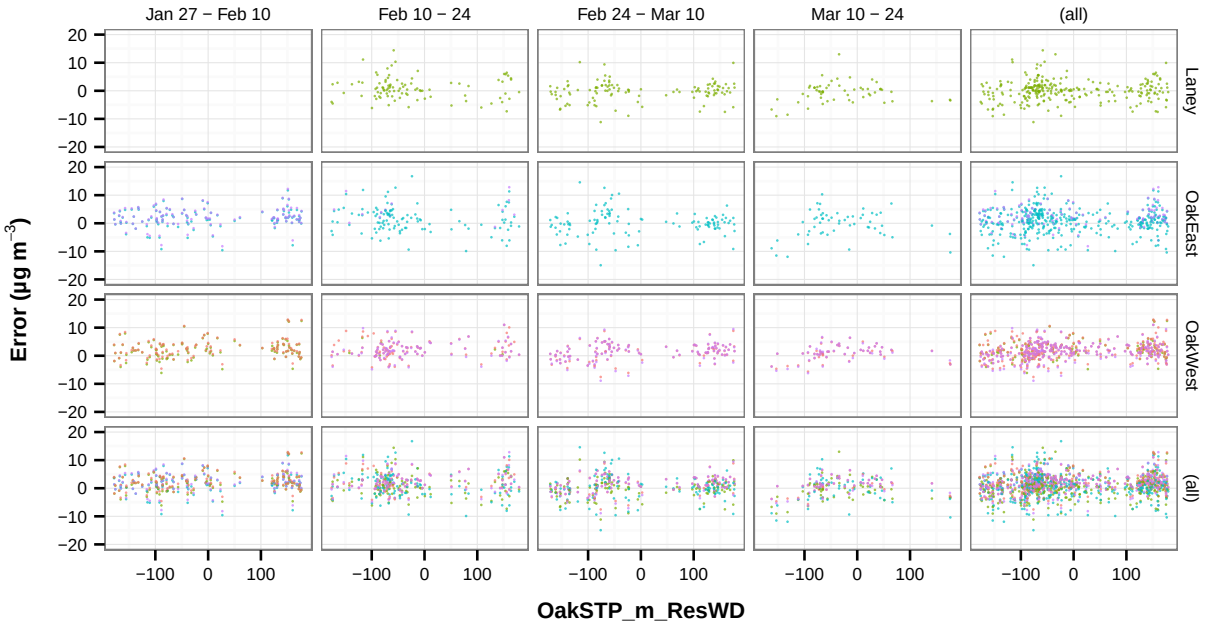

(a) Absolute scale ($\mu g\, m^{-3}$)

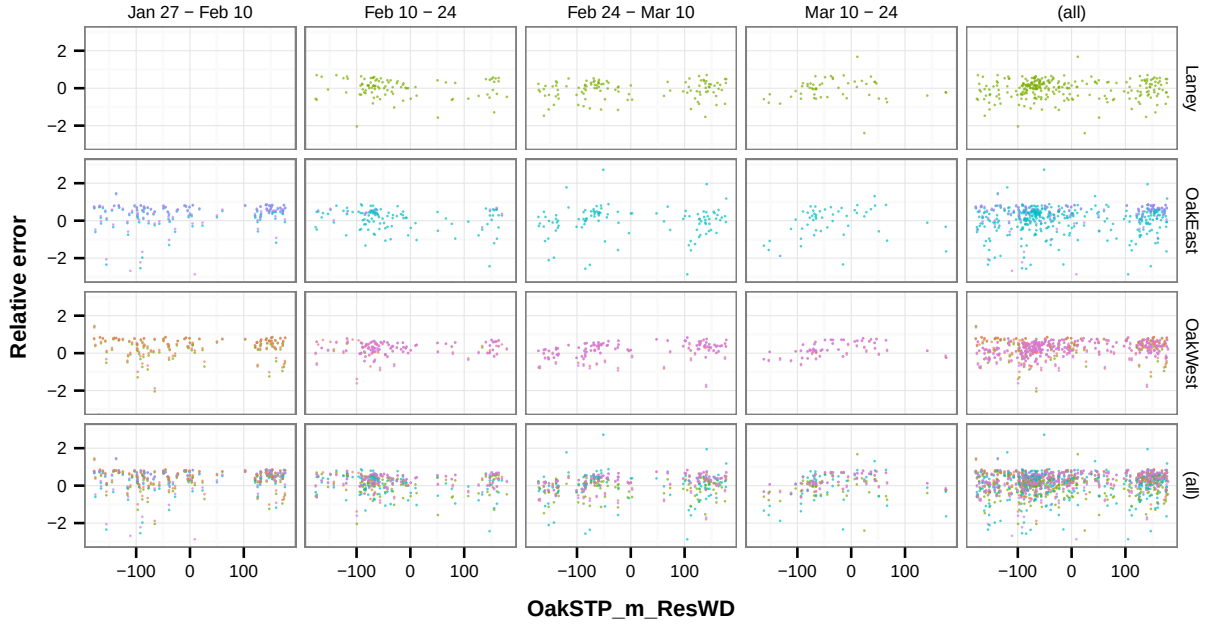

(b) Relative scale

Fig. D.6: Residuals vs wind direction (0 = North). Panels are conditioned by site (top to bottom) and biweekly intervals (left to right).

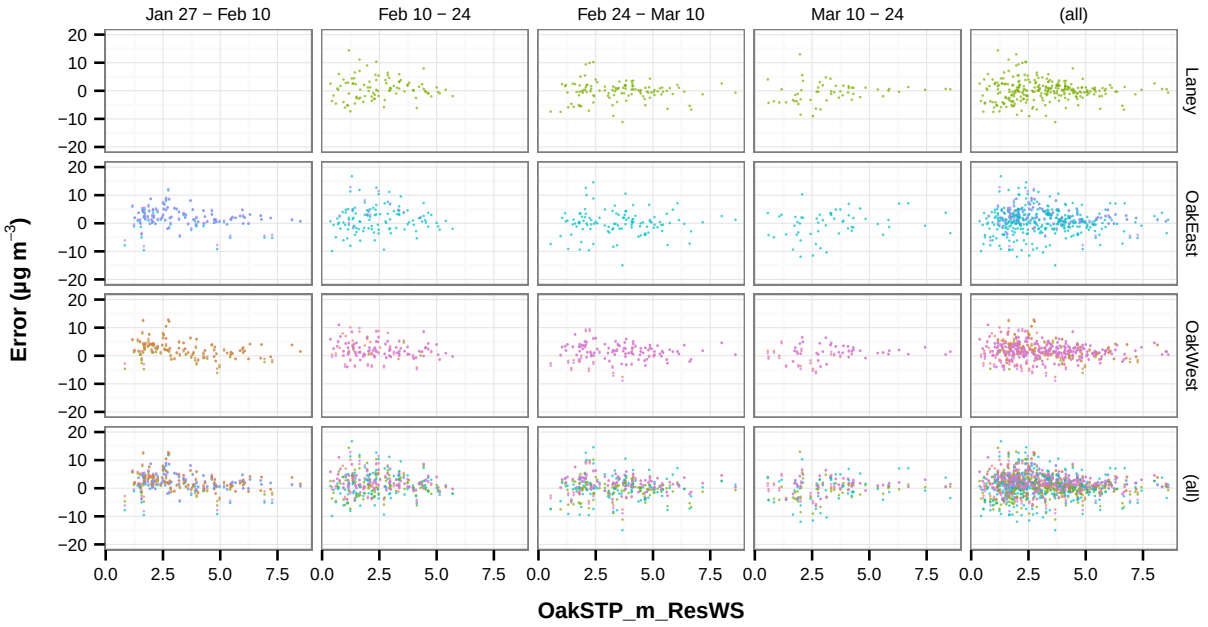

(a) Absolute scale ($\mu g\, m^{-3}$)

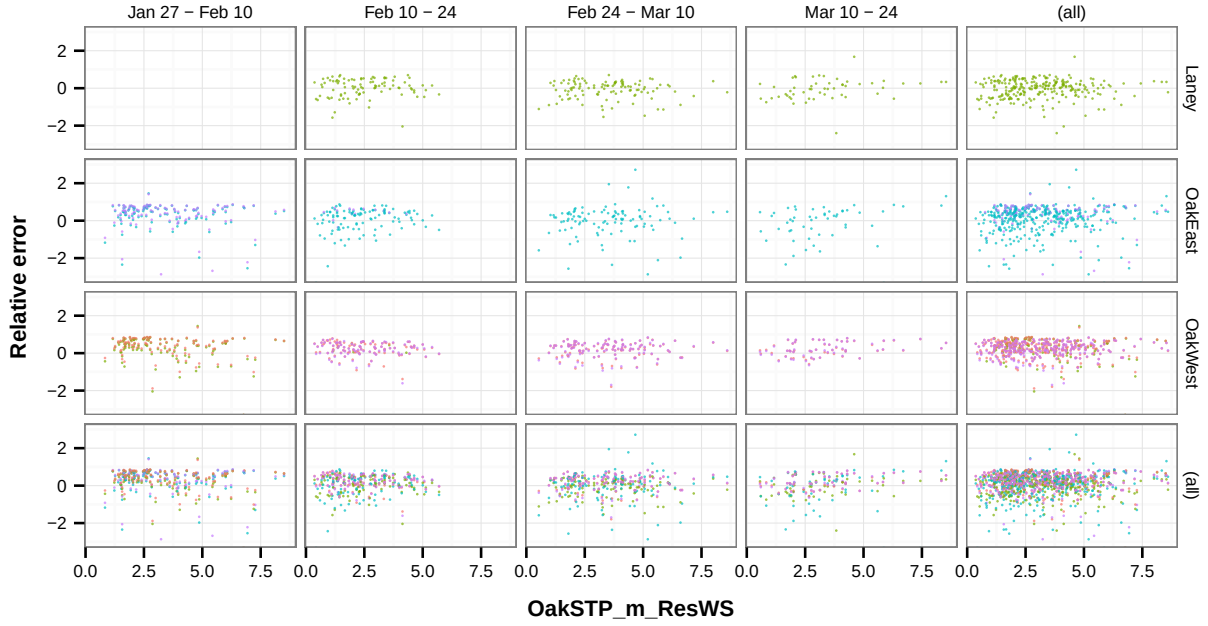

(b) Relative scale

Fig. D.7: Residuals vs wind speed (m/s). Panels are conditioned by site (top to bottom) and biweekly intervals (left to right).

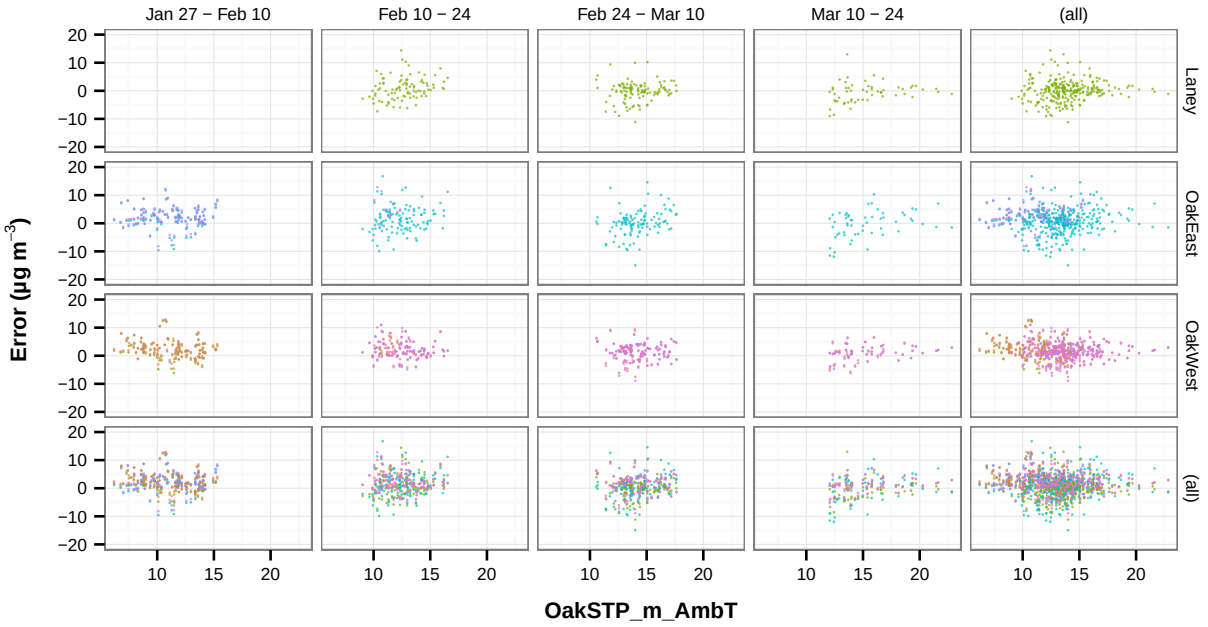

(a) Absolute scale ($\mu g\, m^{-3}$)

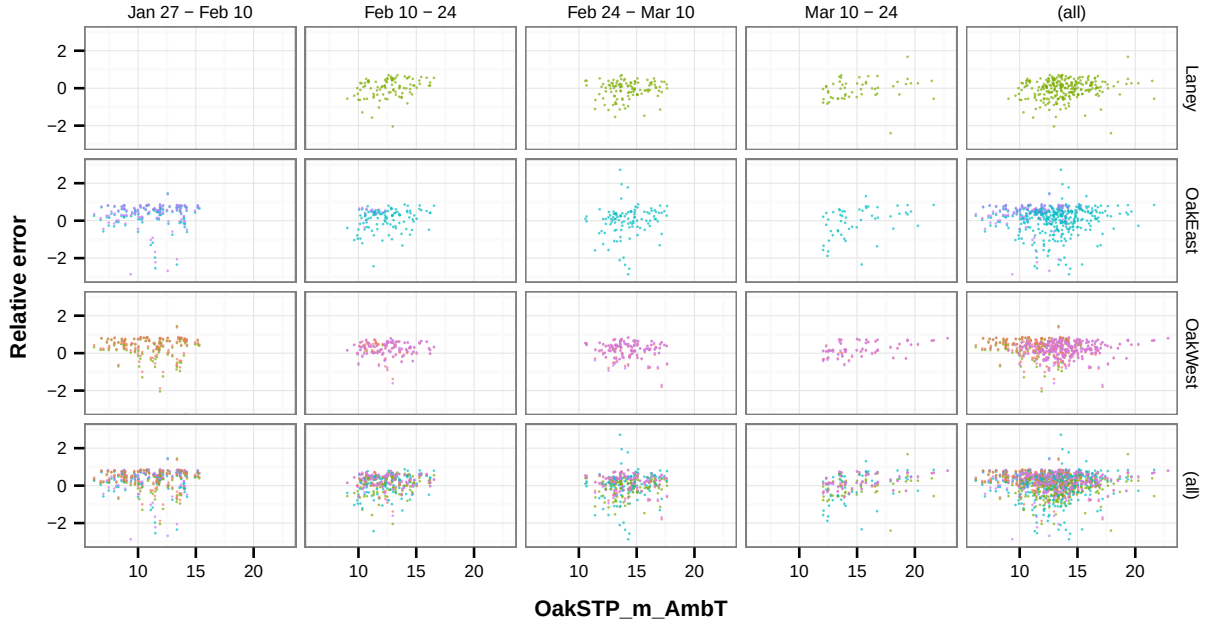

(b) Relative scale

Fig. D.8: Residuals vs ambient temperature. Panels are conditioned by site (top to bottom) and biweekly intervals (left to right).

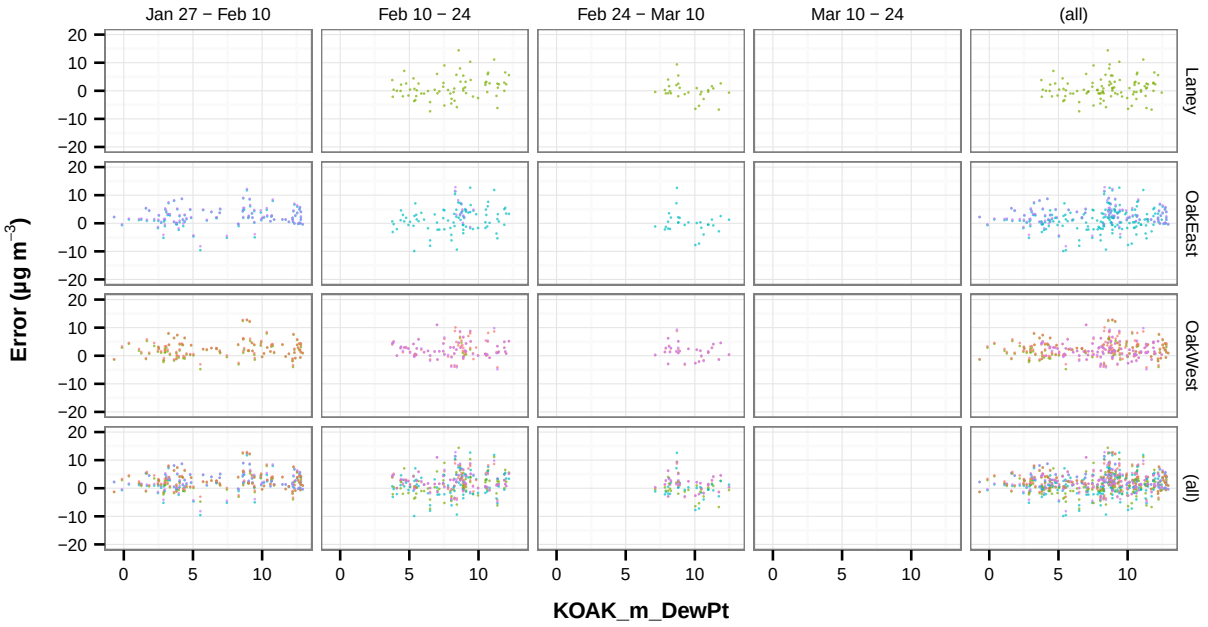

(a) Absolute scale ($\mu g\, m^{-3}$)

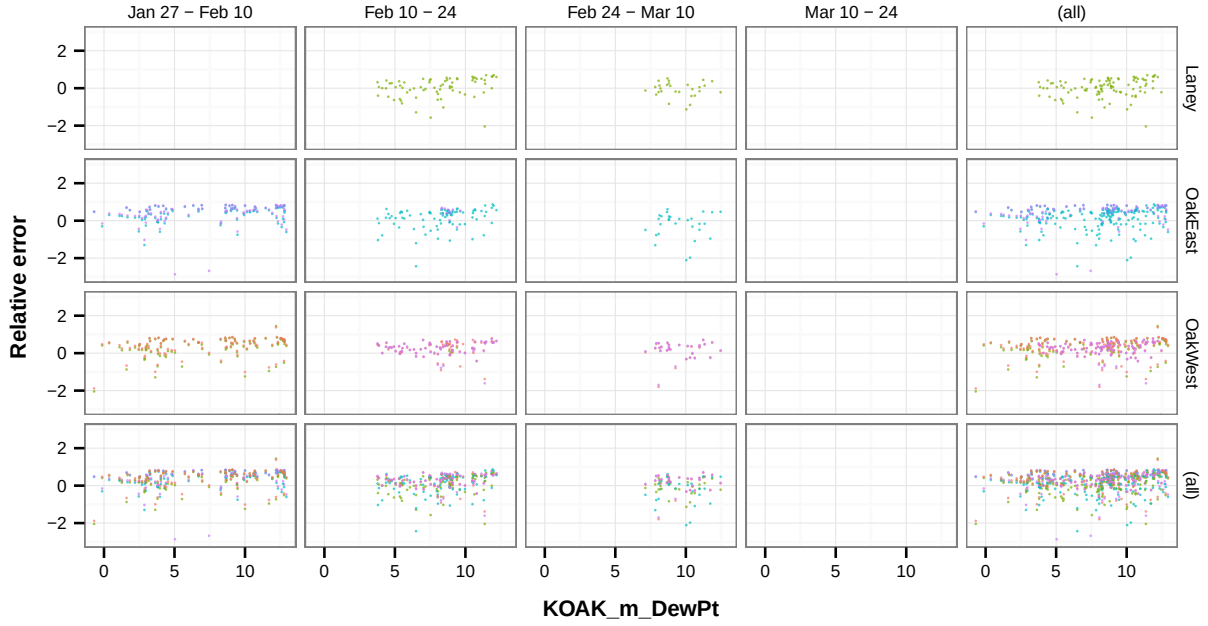

(b) Relative scale

Fig. D.9: Residuals vs dew point (KOAK). Panels are conditioned by site (top to bottom) and biweekly intervals (left to right).

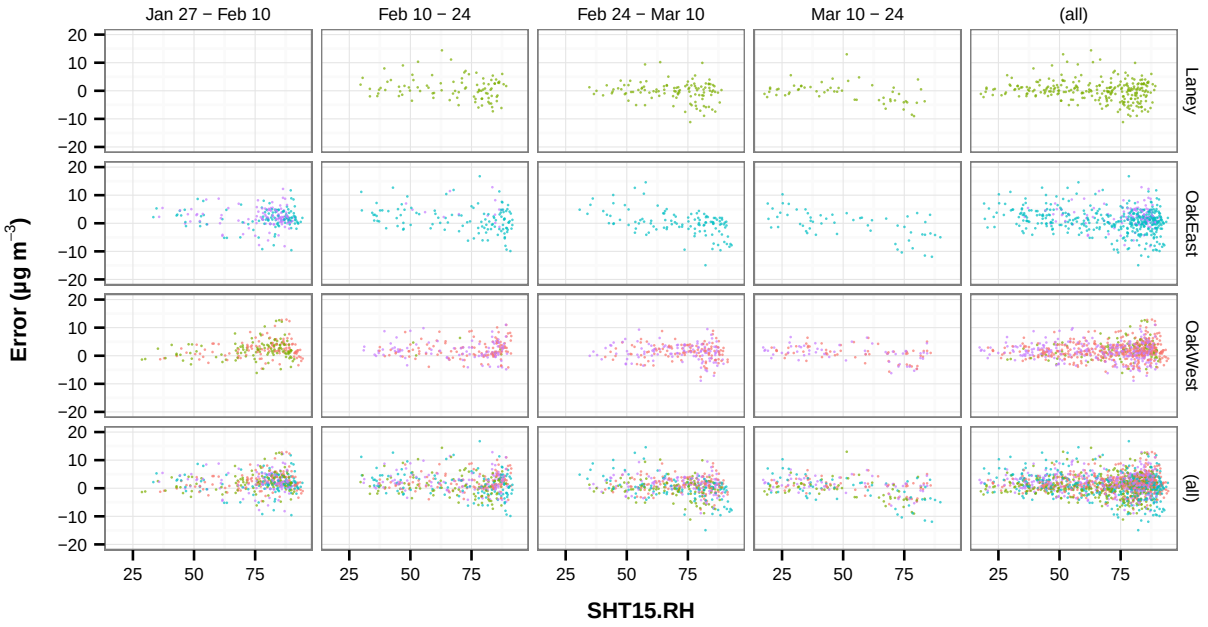

(a) Absolute scale ($\mu g\, m^{-3}$)

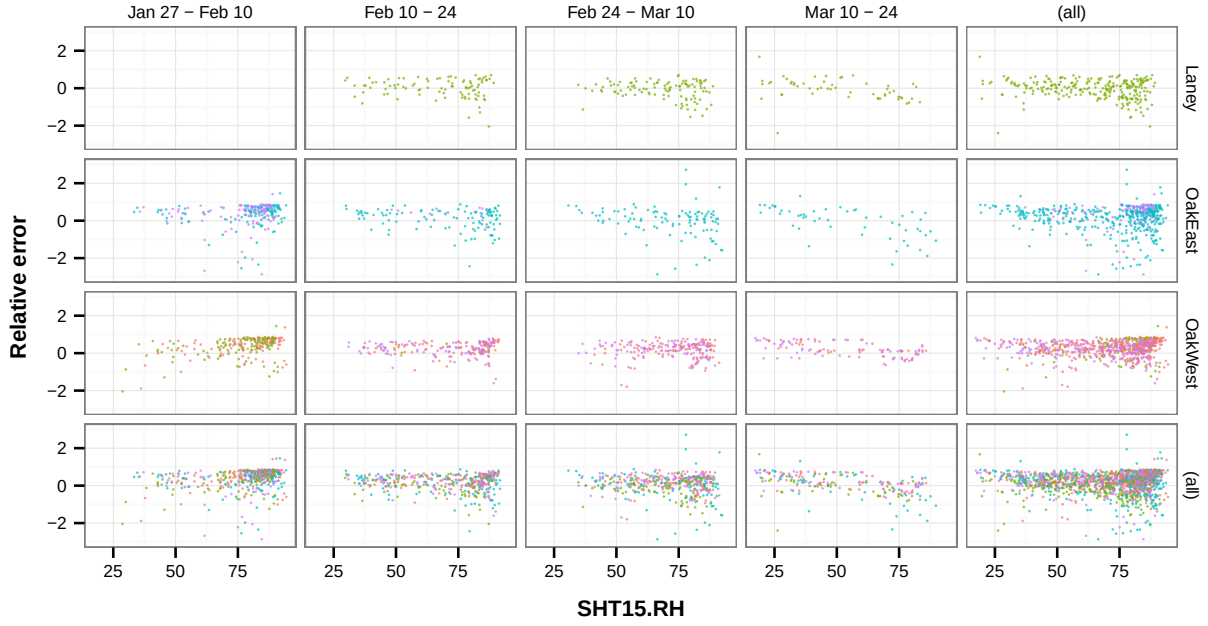

(b) Relative scale

Fig. D.10: Residuals vs chamber RH. Panels are conditioned by site (top to bottom) and biweekly intervals (left to right).

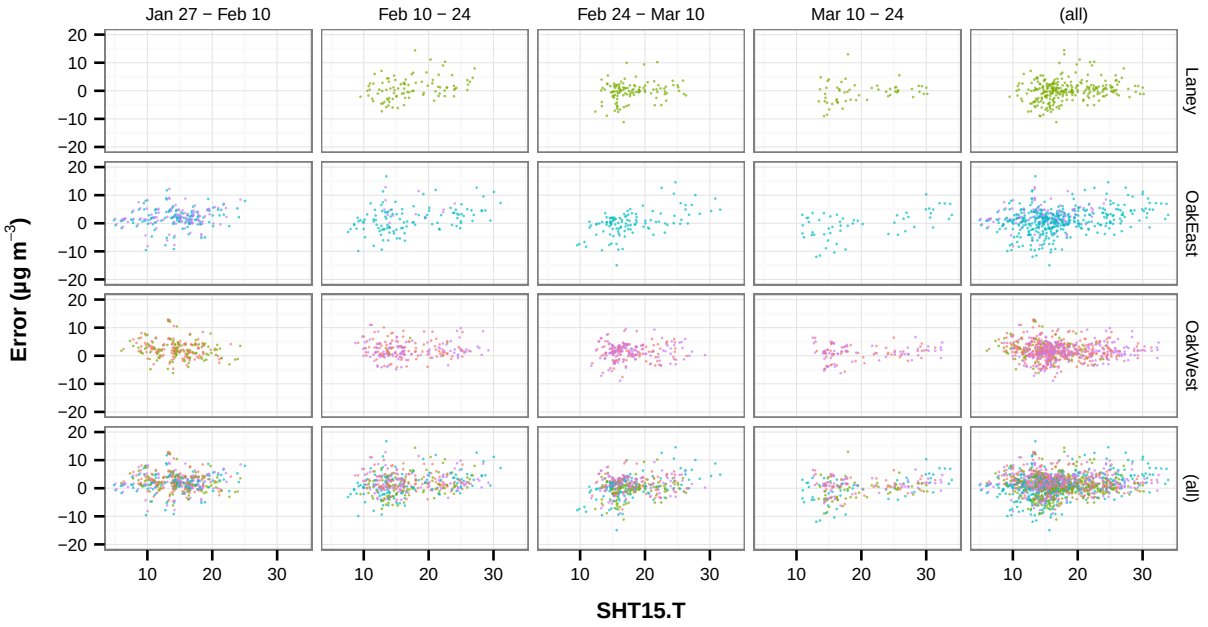

(a) Absolute scale ($\mu g\, m^{-3}$)

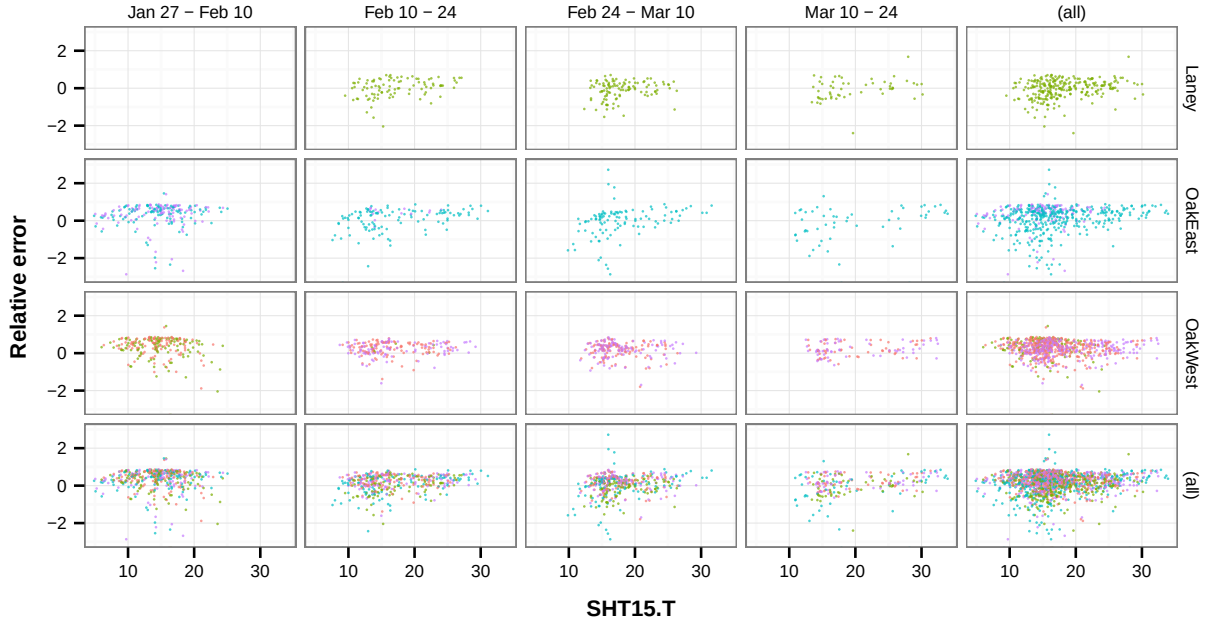

(b) Relative scale

Fig. D.11: Residuals vs chamber T. Panels are conditioned by site (top to bottom) and biweekly intervals (left to right).

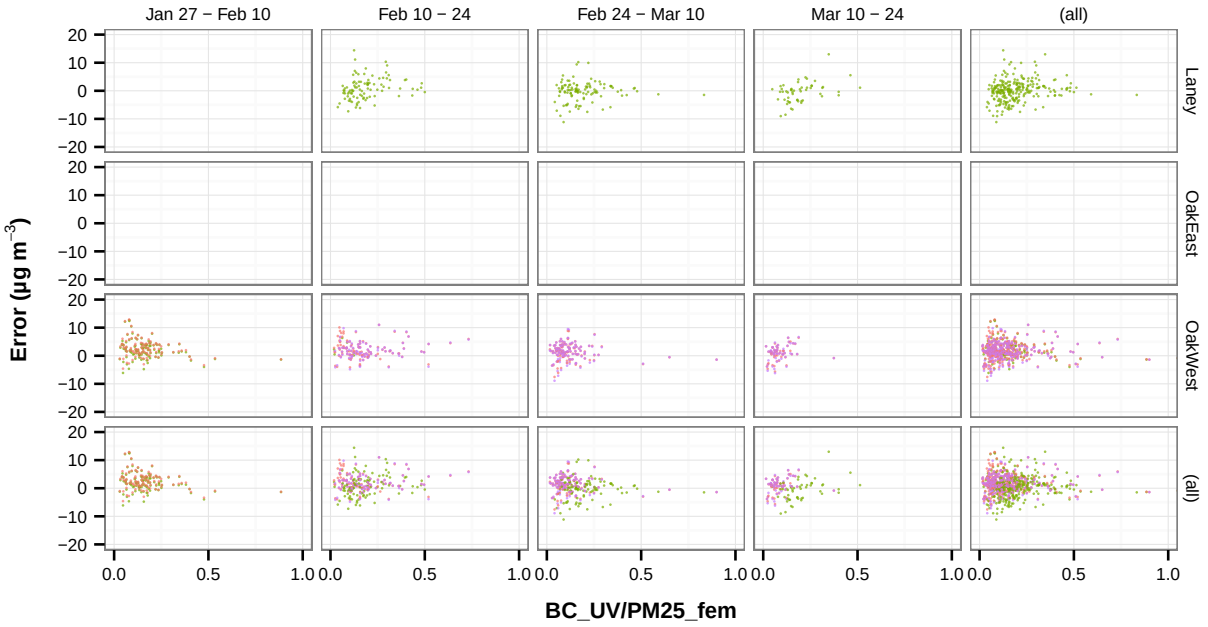

(a) Absolute scale ($\mu g\, m^{-3}$)

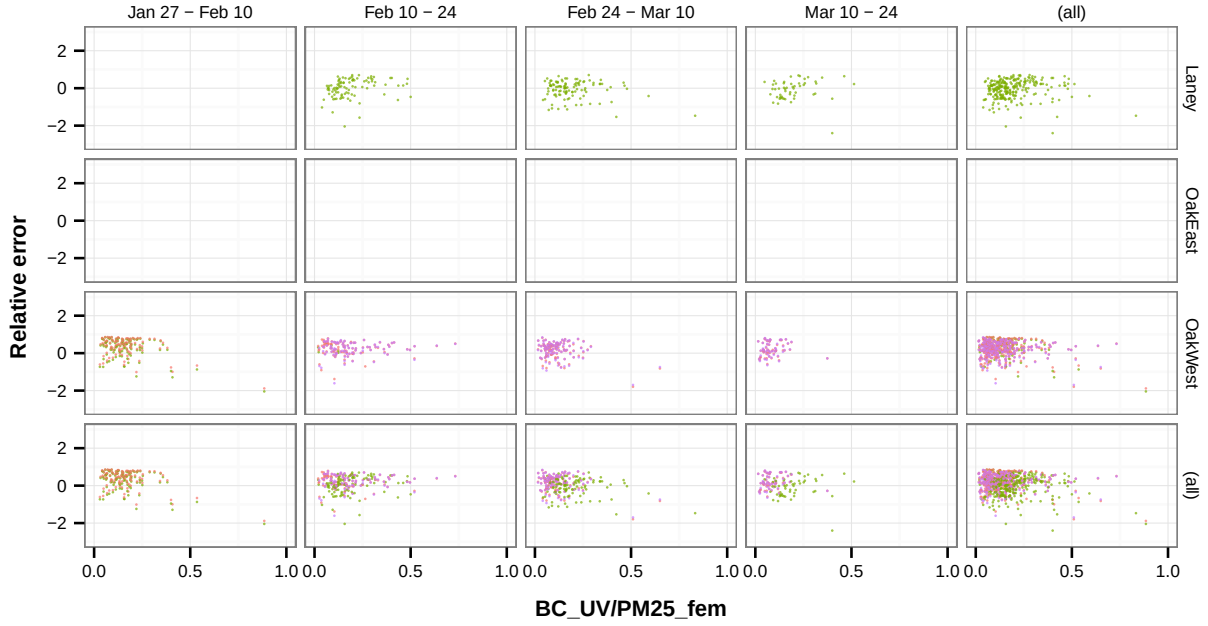

(b) Relative scale

Fig. D.12: Residuals vs BC_{UV} / $PM_{2.5}$ ratio. Panels are conditioned by site (top to bottom) and biweekly intervals (left to right).

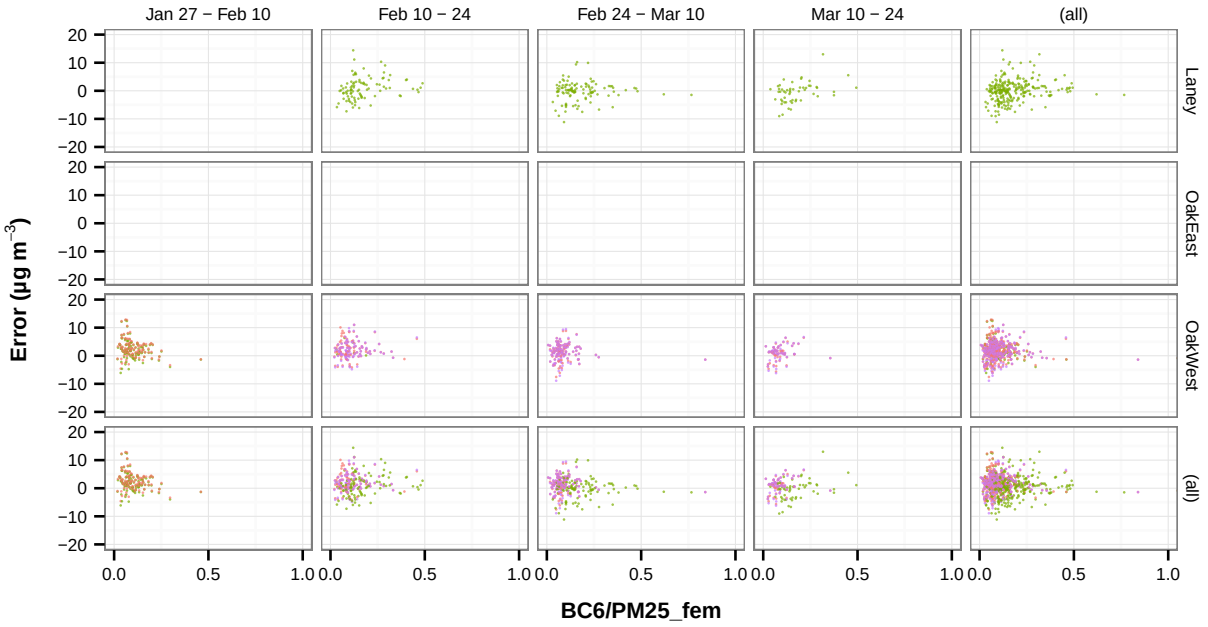

(a) Absolute scale ($\mu g\, m^{-3}$)

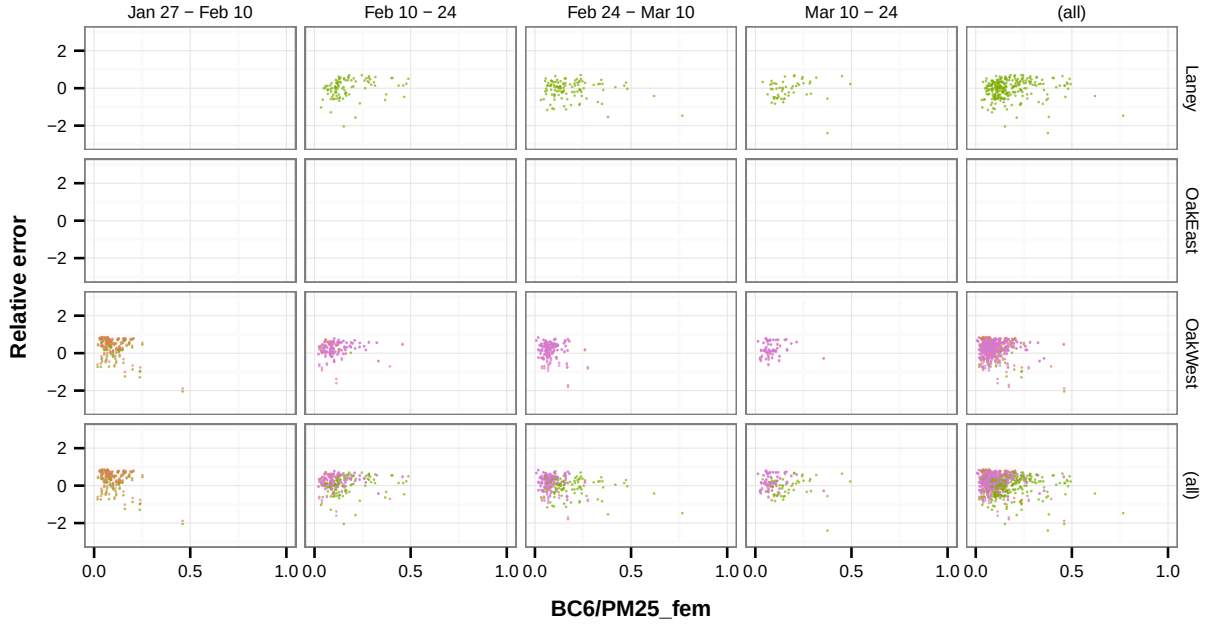

(b) Relative scale

Fig. D.13: Residuals vs BC_6 / $PM_{2.5}$ ratio. Panels are conditioned by site (top to bottom) and biweekly intervals (left to right).

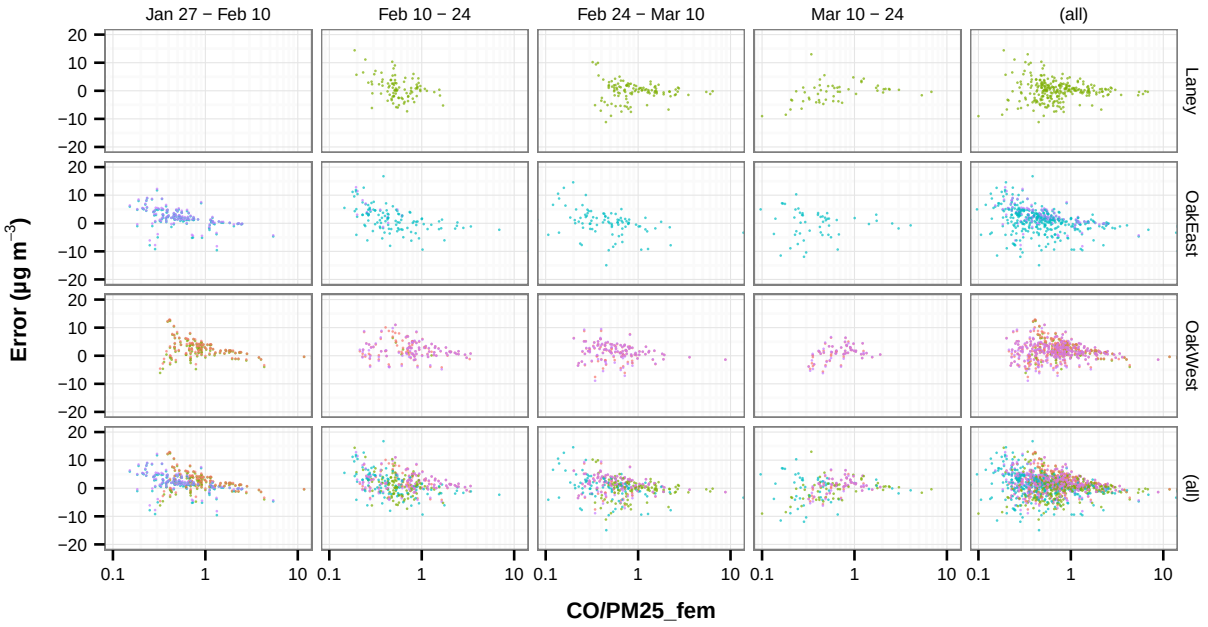

(a) Absolute scale ($\mu g\,m^{-3}$)

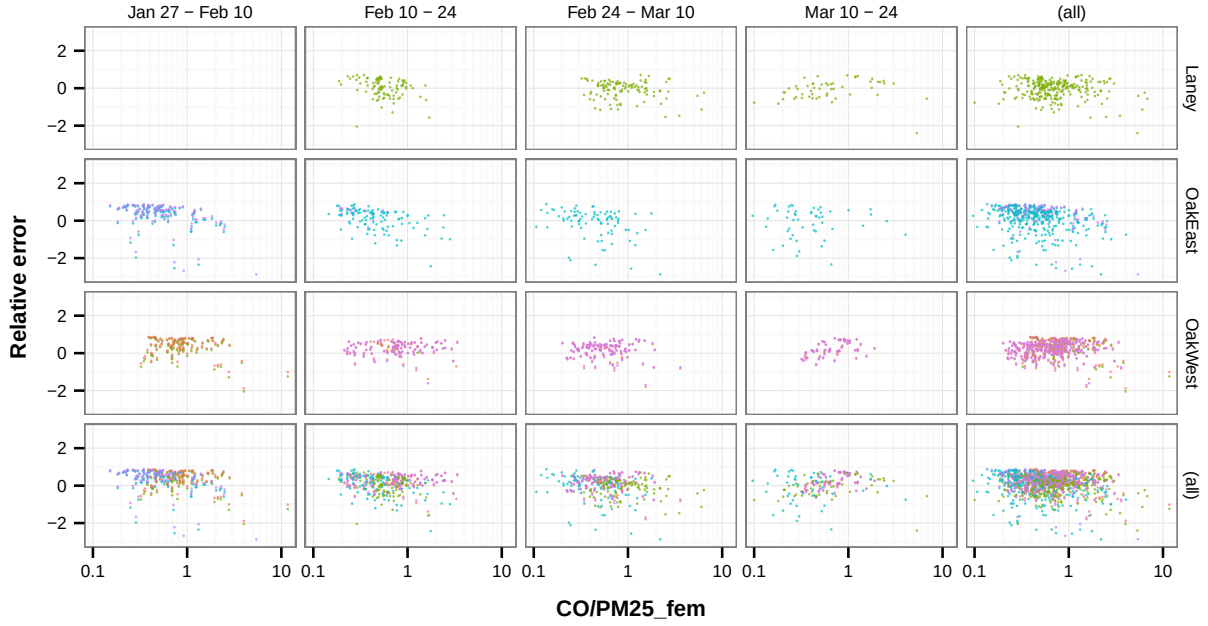

(b) Relative scale

Fig. D.14: Residuals vs CO / $PM_{2.5}$ ratio. Panels are conditioned by site (top to bottom) and biweekly intervals (left to right).

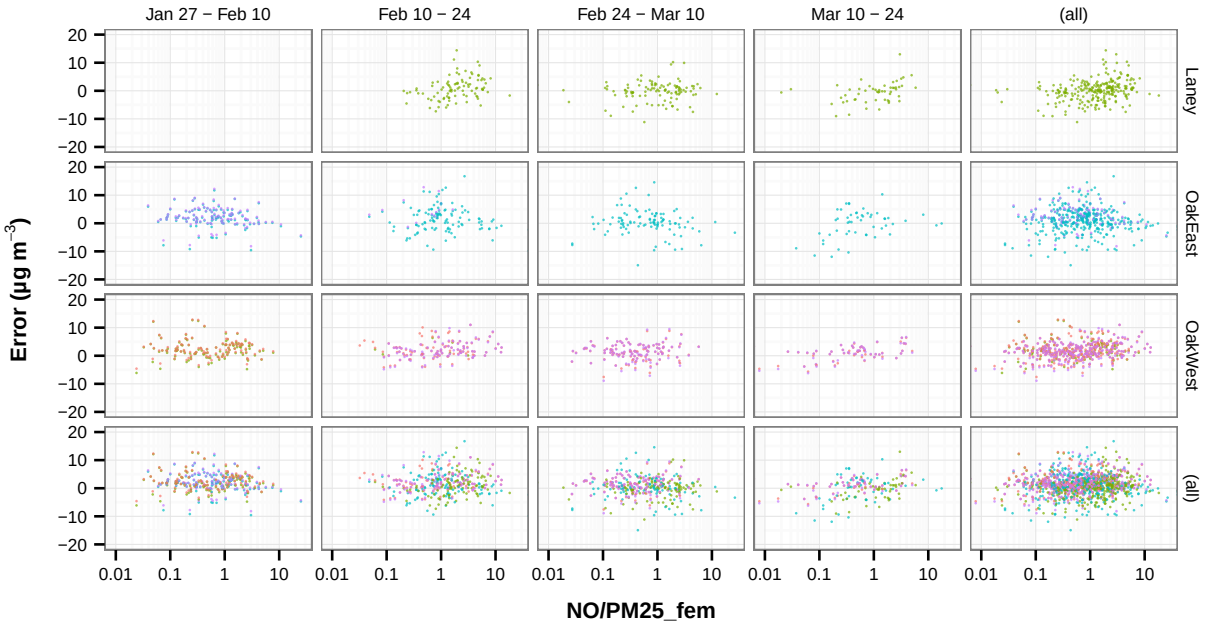

(a) Absolute scale ($\mu g\, m^{-3}$)

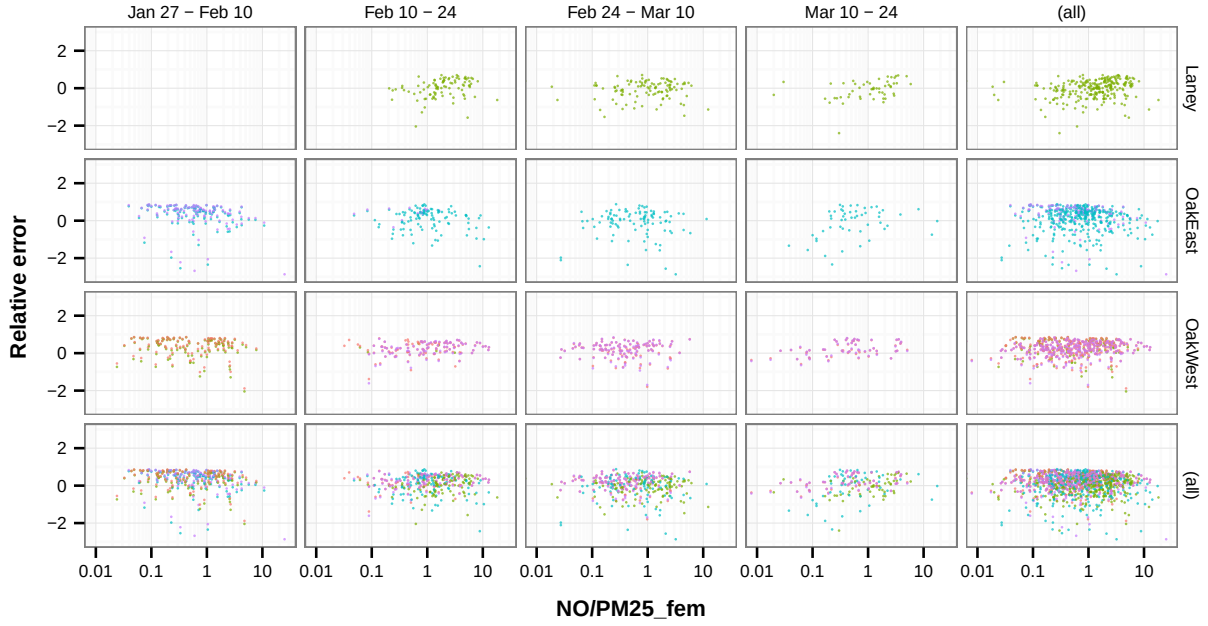

(b) Relative scale

Fig. D.15: Residuals vs NO / $PM_{2.5}$ ratio. Panels are conditioned by site (top to bottom) and biweekly intervals (left to right).

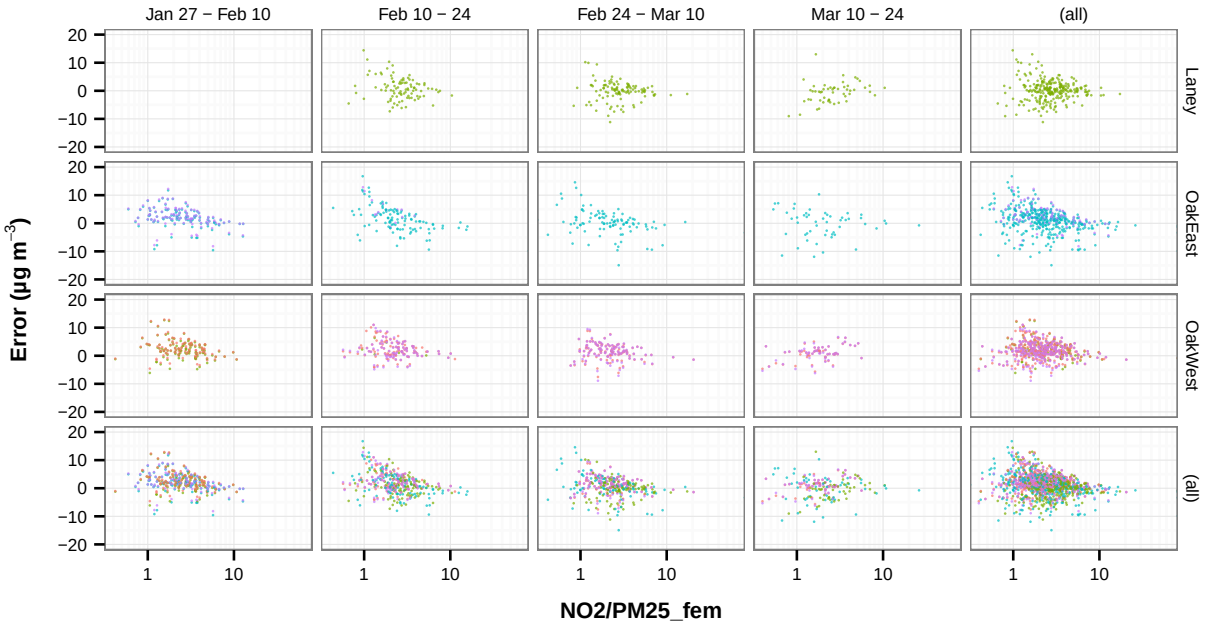

(a) Absolute scale ($\mu g\, m^{-3}$)

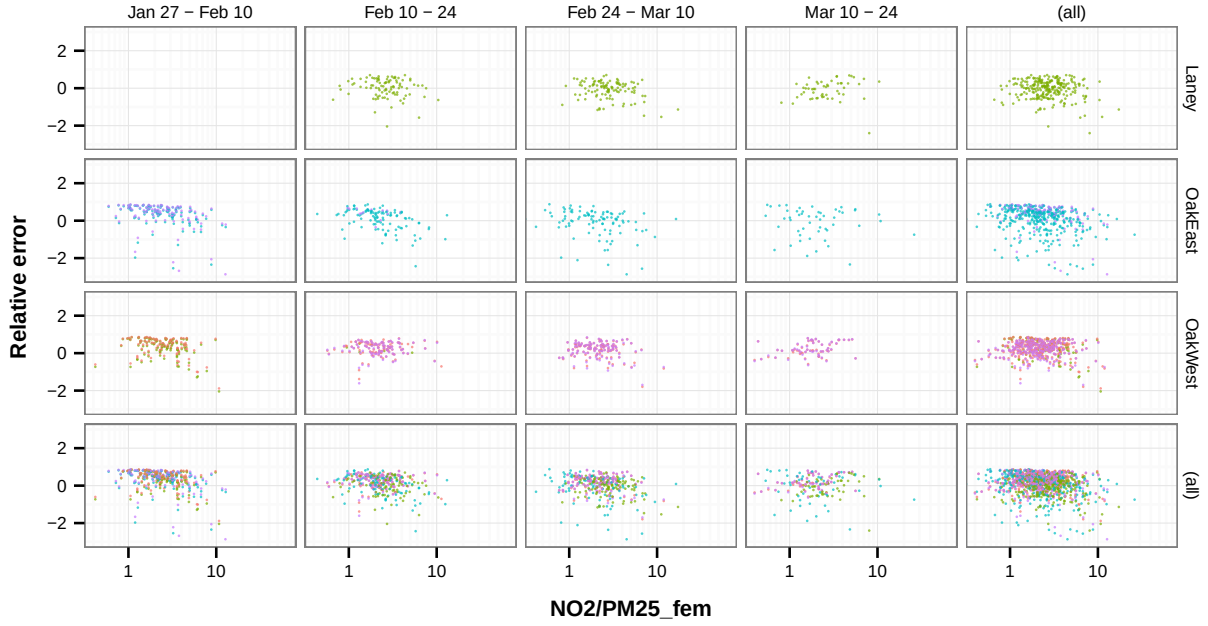

(b) Relative scale

Fig. D.16: Residuals vs NO2 / $PM_{2.5}$ ratio. Panels are conditioned by site (top to bottom) and biweekly intervals (left to right).

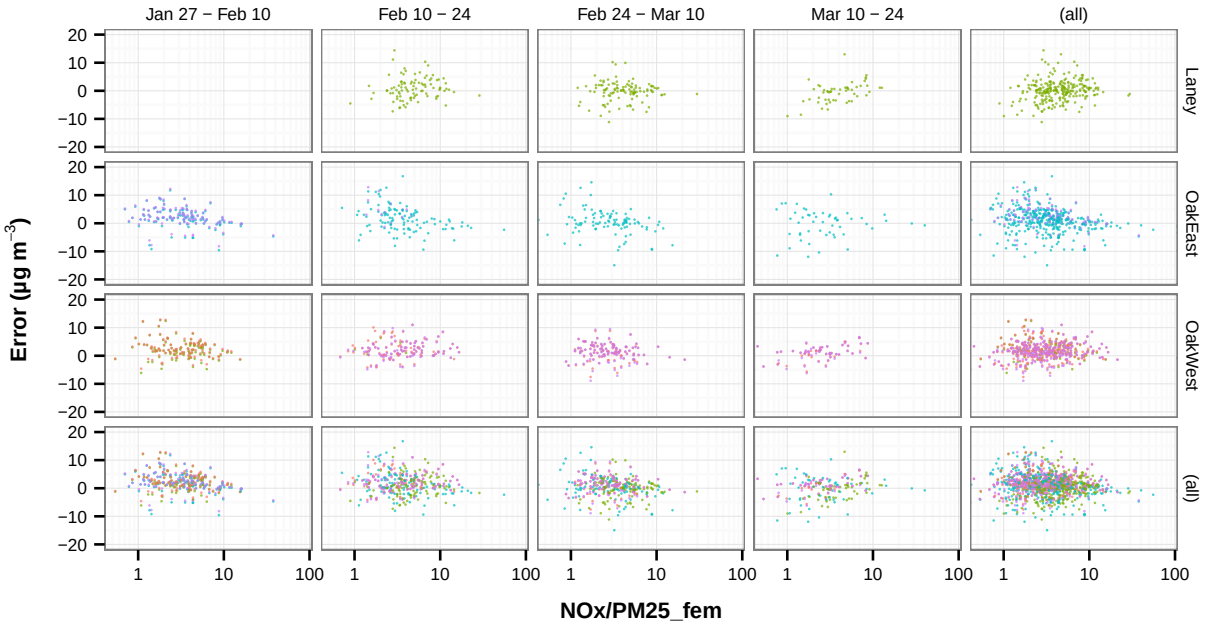

(a) Absolute scale ($\mu g\, m^{-3}$)

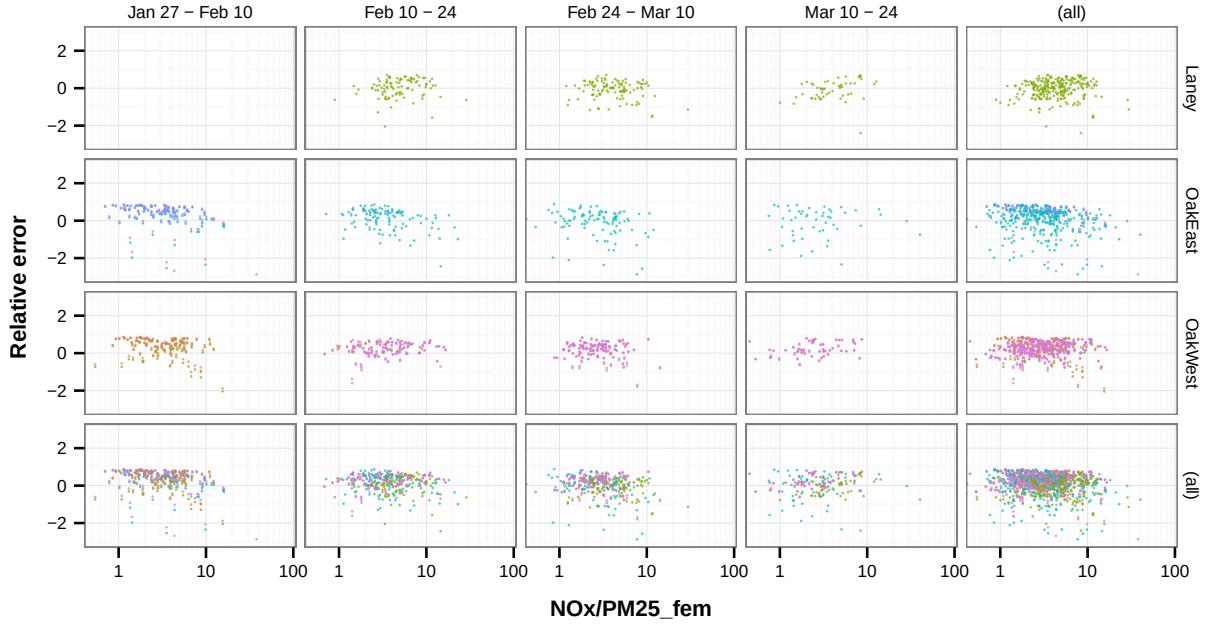

(b) Relative scale

Fig. D.17: Residuals vs NOx / $PM_{2.5}$ ratio. Panels are conditioned by site (top to bottom) and biweekly intervals (left to right).

D.3 Data

The following tables report 24 h averages and diurnal profiles of reference data from the Oakland West, Oakland East, and Laney College monitoring sites, as well as meteorology observed at the Oakland STP weather station, over the course of the study.

Table D.1: 24 h data from Oakland West.

Date	CO	NO	NO_2	NO_X	$O3$	$PM_{2.5}$	BC_{UV}	BC_6
01/14/2014	7.31	33.439	32.43	65.86	5.01	14.79	3.283	1.991
01/15/2014	6.95	25.357	30.64	56.00	12.51	15.09	2.498	1.501
01/16/2014	8.72	57.852	40.99	98.83	5.33	22.25	5.491	3.663
01/17/2014	12.85	87.561	42.80	130.36	5.57	33.83	5.487	3.560
01/18/2014	12.77	74.165	34.73	108.90	6.63	23.46	4.684	2.462
01/19/2014	14.09	83.396	33.13	116.52	8.62	27.21	6.673	3.835
01/20/2014	13.14	85.239	37.90	123.15	4.66	25.50	6.308	3.289
01/21/2014	13.64	102.809	37.21	140.03	4.22	18.96	2.337	2.606
01/22/2014	10.81	69.435	35.31	104.75	3.88	17.46	4.998	3.061
01/23/2014	4.94	10.109	19.00	29.11	22.10	14.25	4.088	1.152
01/24/2014	10.05	39.817	40.50	80.31	7.75	30.92	8.884	3.311
01/25/2014	12.02	49.052	37.20	86.24	9.37	25.46	3.604	2.166
01/26/2014	8.80	28.491	25.74	54.23	14.64	17.79	2.480	1.420
01/27/2014	5.21	4.139	19.61	23.75	17.74	12.61	1.022	0.687
01/28/2014	5.49	9.917	21.64	31.56	9.26	7.79	1.030	0.833
01/29/2014	3.82	3.895	16.51	20.39	11.74	6.08	0.807	0.661
01/30/2014	2.96	2.895	11.72	14.62	26.46	7.00	0.594	0.477
01/31/2014	3.70	6.217	14.70	20.94	20.06	5.92	0.920	0.445
02/01/2014	4.05	5.900	15.28	21.18	22.20	5.21	0.920	0.435
02/02/2014	4.20	1.000	8.83	9.85	27.77	5.67	0.755	0.367
02/03/2014	4.86	9.113	17.69	26.80	18.96	7.00	1.314	0.617
02/04/2014	5.21	10.957	18.13	29.08	16.48	7.29	1.194	0.728
02/05/2014	6.02	14.552	19.74	34.29	17.22	5.42	1.137	0.532
02/06/2014	5.66	7.130	18.52	25.67	15.70	8.38	1.002	0.725
02/07/2014	5.63	3.778	15.10	18.88	20.17	6.83	0.746	0.517
02/08/2014	4.59	0.557	4.71	5.27	28.05	2.12	0.252	0.172
02/09/2014	4.61	0.461	4.02	4.50	28.16	1.54	0.312	0.166
02/10/2014	5.58	8.096	19.43	27.53	13.20	5.33	0.670	0.667
02/11/2014	5.85	7.900	18.94	26.84	13.78	8.17	0.569	0.753
02/12/2014	6.03	5.374	18.95	24.33	14.51	9.46	0.530	0.668
02/13/2014	6.42	11.678	19.64	31.32	10.17	9.38	0.775	0.904
02/14/2014	5.67	6.722	15.60	22.31	10.98	2.79	0.474	0.577
02/15/2014	6.10	6.200	10.90	17.08	13.32	5.46	0.390	0.504
02/16/2014	5.93	3.578	11.20	14.77	24.95	6.21	0.386	0.342
02/17/2014	7.65	17.283	14.73	32.00	18.37	7.71	1.826	0.623
02/18/2014	9.11	34.587	22.77	57.35	12.78	8.83	3.534	1.209
02/19/2014	6.26	3.648	15.26	18.90	22.95	6.62	1.180	0.521
02/20/2014	5.27	19.219	19.97	39.24	17.51	7.29	1.119	0.749
02/21/2014	6.11	42.018	25.86	67.89	14.59	10.29	4.226	1.835
02/22/2014	4.90	23.330	19.92	43.25	16.72	11.21	2.409	0.993

Table D.1: *(continued)*

Date	CO	NO	NO_2	NO_X	$O3$	$PM_{2.5}$	BC_{UV}	BC_6
02/23/2014	2.96	4.617	11.91	16.53	21.98	8.58	1.236	0.486
02/24/2014	5.92	40.526	22.13	62.67	15.99	12.74	3.540	1.673
02/25/2014	3.14	3.217	17.35	20.58	30.32	11.62	1.662	0.743
02/26/2014	3.19	2.248	13.59	15.84	25.57	7.25	0.900	0.487
02/27/2014	2.55	1.578	12.64	14.23	34.23	5.62	0.892	0.323
02/28/2014	2.65	1.657	9.74	11.40	36.35	4.71	0.422	0.245
03/01/2014	3.55	3.116	12.58	15.70	29.80	4.71	0.705	0.265
03/02/2014	4.47	7.913	14.21	22.12	23.98	5.29	1.074	0.559
03/03/2014	4.21	5.304	17.98	23.29	18.43	6.00	0.602	0.536
03/04/2014	3.87	6.013	14.63	20.71	21.57	5.12	0.524	0.581
03/05/2014	4.42	10.600	16.30	26.89	14.63	8.33	0.878	0.929
03/06/2014	3.91	4.591	14.97	19.56	23.57	8.83	0.522	0.573
03/07/2014	4.34	5.152	17.70	22.86	18.80	9.25	0.588	0.583
03/08/2014	6.32	15.143	20.98	36.13	14.60	12.08	0.919	0.912
03/09/2014	4.71	5.548	17.81	23.37	18.29	10.29	0.918	0.936
03/10/2014	3.71	2.136	11.25	13.39	30.52	5.04	0.367	0.422
03/11/2014	3.44	2.932	8.32	11.23	36.51	3.26	0.352	0.346
03/12/2014	3.31	1.591	9.80	11.40	32.52	3.83	0.247	0.282
03/13/2014	5.34	15.109	22.12	37.23	17.39	8.50	1.087	1.120
03/14/2014	4.76	2.735	13.77	16.50	24.91	11.88	0.595	0.630
03/15/2014	6.98	14.957	17.38	32.34	17.14	10.38	0.893	0.872
03/16/2014	5.90	7.591	14.07	21.67	18.42	9.71	0.738	0.743
03/17/2014	4.71	4.217	12.19	16.30	28.90	7.57	0.502	0.520
03/18/2014	6.93	18.043	23.30	41.36	16.99	8.54	0.921	0.901
03/19/2014	7.74	29.352	24.80	54.04	16.81	10.96	1.228	1.280
03/20/2014	4.12	6.764	19.00	25.77	20.55	13.71	0.777	0.815
03/21/2014	2.57	1.974	10.89	12.85	30.68	15.25	0.423	0.490
03/22/2014	3.37	4.096	12.48	16.58	26.47	15.33	0.505	0.494
03/23/2014	3.22	1.043	9.89	10.93	32.67	12.42	0.510	0.499
03/24/2014	4.68	13.935	21.17	34.76	17.40	12.25	0.832	0.920
03/25/2014	3.52	5.474	15.26	20.76	26.74	7.96	0.530	0.573
03/26/2014	3.20	1.222	10.60	11.83	34.51	7.12	0.325	0.415
03/27/2014	3.15	0.932	8.68	9.62	36.60	6.87	0.398	0.410
03/28/2014	3.17	2.200	8.20	10.40	29.17	2.88	0.239	0.278
03/29/2014	3.52	0.609	6.49	7.10	31.08	1.67	0.253	0.241
03/30/2014	3.18	0.543	4.52	5.07	39.08	3.42	0.129	0.140

Table D.2: 24 h data from Oakland East.

Date	CO	NO	NO_2	NO_X	$O3$	$PM_{2.5}$
01/14/2014	6.02	23.718	26.57	50.30	12.26	9.29
01/15/2014	4.83	14.391	22.80	37.20	18.64	10.88
01/16/2014	5.22	20.750	23.49	44.23	19.54	10.75
01/17/2014	9.35	50.709	36.58	87.30	8.90	20.54
01/18/2014	8.15	33.932	34.84	68.76	7.70	18.00
01/19/2014	8.11	34.655	31.85	66.52	12.74	23.62
01/20/2014	8.71	44.441	38.41	82.85	5.71	21.67
01/21/2014	8.10	47.373	33.13	80.50	7.15	11.88
01/22/2014	6.51	35.105	33.19	68.29	7.30	12.38
01/23/2014	4.28	10.055	23.32	33.37	24.35	24.70
01/24/2014	7.12	23.787	36.65	60.43	8.36	37.62
01/25/2014	6.37	18.323	32.35	50.66	8.74	17.67
01/26/2014	4.66	11.277	24.27	35.55	14.99	14.21
01/27/2014	2.40	3.336	16.30	19.65	17.90	12.12
01/28/2014	2.72	5.909	17.55	23.45	9.50	9.08
01/29/2014	2.23	4.209	14.24	18.45	9.87	5.33
01/30/2014	2.14	3.982	10.14	14.12	23.51	4.54
01/31/2014	3.32	8.952	13.92	22.88	16.95	5.48
02/01/2014	3.16	6.627	15.27	21.91	15.27	5.46
02/02/2014	2.11	2.414	7.66	10.05	25.26	4.38
02/03/2014	3.55	11.405	15.08	26.50	17.48	7.58
02/04/2014	3.93	14.995	18.07	33.05	8.66	6.04
02/05/2014	2.66	7.441	12.32	19.77	18.31	4.79
02/06/2014	2.63	4.491	15.78	20.26	15.03	5.78
02/07/2014	3.24	7.026	17.17	24.20	15.49	6.25
02/08/2014	1.45	0.632	4.37	5.01	26.41	2.17
02/09/2014	1.39	0.541	4.21	4.77	25.18	2.00
02/10/2014	2.36	4.082	15.45	19.54	14.38	3.33
02/11/2014	2.85	5.491	15.97	21.46	13.87	7.00
02/12/2014	3.61	9.773	20.23	30.00	9.21	11.79
02/13/2014	4.40	18.823	20.88	39.71	4.33	10.67
02/14/2014	2.60	9.039	13.28	22.31	9.77	4.04
02/15/2014	2.50	9.677	8.80	18.48	10.21	4.29
02/16/2014	2.79	4.823	12.38	17.20	20.59	6.29
02/17/2014	3.22	10.577	14.89	25.47	13.66	6.29
02/18/2014	4.07	15.073	19.50	34.57	7.70	7.46
02/19/2014	2.67	5.650	16.27	21.91	16.81	5.54
02/20/2014	4.32	18.005	21.18	39.18	8.82	5.61
02/21/2014	3.73	13.857	19.10	32.97	10.33	7.17
02/22/2014	3.09	8.268	13.85	22.12	12.11	8.18

Table D.2: *(continued)*

Date	CO	NO	NO_2	NO_X	$O3$	$PM_{2.5}$
02/23/2014	3.19	6.364	13.02	19.39	13.11	9.79
02/24/2014	3.97	14.995	19.23	34.23	15.13	11.29
02/25/2014	2.89	3.300	15.38	18.69	23.38	11.27
02/26/2014	2.24	3.627	11.13	14.74	23.15	5.75
02/27/2014	1.60	1.396	7.45	8.86	35.10	3.33
02/28/2014	1.70	1.983	7.86	9.84	34.54	2.79
03/01/2014	1.07	6.074	6.24	12.29	26.35	3.52
03/02/2014		3.000	9.87	8.46	24.55	1.92
03/03/2014	3.35	8.861	20.21	19.85	12.11	5.61
03/04/2014	2.93	6.970	12.53	19.51	16.75	5.71
03/05/2014	2.90	7.757	11.62	19.39	12.98	8.00
03/06/2014	2.04	3.130	10.31	13.45	24.90	6.18
03/07/2014	3.26	9.422	14.93	24.35	13.66	6.38
03/08/2014	4.37	11.743	18.88	30.63	11.40	10.42
03/09/2014	3.30	5.009	17.31	22.30	18.22	9.33
03/10/2014	2.59	4.130	13.67	17.80	27.47	2.67
03/11/2014	2.53	7.565	9.77	17.34	32.06	2.96
03/12/2014	1.97	3.748	9.73	13.45	29.73	2.25
03/13/2014	3.02	12.887	17.83	30.71	19.32	5.71
03/14/2014	2.36	4.239	12.53	16.78	23.21	9.79
03/15/2014	3.13	5.643	15.58	21.22	16.66	8.33
03/16/2014	2.58	4.978	12.29	17.28	19.65	8.38
03/17/2014	1.95	2.817	11.71	14.52	25.34	6.21
03/18/2014	2.90	5.691	15.00	20.70	21.27	6.43
03/19/2014	2.93	4.882	18.01	21.34	23.01	5.57
03/20/2014	3.11	9.878	15.20	25.07	22.24	9.78
03/21/2014	1.85	2.009	10.07	12.08	28.30	12.58
03/22/2014	2.17	2.309	10.63	12.92	26.48	12.17
03/23/2014	2.10	1.657	9.62	11.28	32.23	12.25
03/24/2014	3.74	11.978	20.78	32.77	17.46	12.17
03/25/2014	2.33	5.765	11.50	17.27	25.88	5.08
03/26/2014	1.33	1.017	6.30	7.31	36.93	3.79
03/27/2014	1.82	3.448	9.73	13.16	32.17	7.62
03/28/2014	1.38	2.509	6.97	9.48	28.47	4.67
03/29/2014	1.60	1.370	7.67	9.04	27.38	3.17
03/30/2014	1.69	1.804	7.36	9.17	28.22	4.00

Table D.3: 24 h data from Laney College.

Date	CO	NO	NO_2	NO_X	$PM_{2.5}$	BC_{UV}	BC_6	UFP
01/26/2014	6.71	57.46	65.89	123.4				
01/27/2014	2.49	23.03	36.14	59.2		1.277	1.234	32.1
01/28/2014	2.97	23.23	22.69	45.9	7.45	1.245	1.235	34.5
01/29/2014	2.65	23.48	20.42	43.9	6.38	1.111	1.098	39.2
01/30/2014	2.02	10.56	15.71	26.2	6.71	1.284	1.248	28.7
01/31/2014	2.49	8.83	15.94	24.8	9.57	0.833	0.750	20.9
02/01/2014	3.74	16.48	20.15	36.6	5.17	1.065	0.915	22.2
02/02/2014	2.24	1.31	10.07	11.4	4.62	0.697	0.509	12.0
02/03/2014	3.71	16.44	21.54	38.0	7.00	1.251	1.093	23.4
02/04/2014	4.36	18.76	24.52	43.3	7.33	1.410	1.229	27.8
02/05/2014	4.53	19.02	24.51	43.5	6.04	1.339	1.180	31.0
02/06/2014	4.57	15.96	23.93	39.9	7.75	1.496	1.440	26.2
02/07/2014	4.51	16.36	20.89	37.3	8.12	1.639	1.438	30.8
02/08/2014	3.86	4.50	7.51	12.0	1.83	0.377	0.369	16.2
02/09/2014	4.23	4.08	7.11	11.2	3.50	0.472	0.448	12.6
02/10/2014	5.70	22.35	23.81	46.1	6.62	1.854	1.859	31.0
02/11/2014	5.88	26.36	24.59	50.9	9.29	1.601	1.574	29.3
02/12/2014	6.07	15.90	25.92	41.8	12.00	1.392	1.312	27.3
02/13/2014	4.88	26.98	27.04	54.0	9.32	1.966	1.913	28.9
02/14/2014	2.43	23.96	21.51	45.5	5.62	1.843	1.797	29.7
02/15/2014	2.67	18.61	14.19	32.8	6.38	1.174	1.045	16.8
02/16/2014	2.79	6.51	15.06	21.6	5.04	0.566	0.505	18.4
02/17/2014	2.85	11.45	17.25	28.7	5.50	0.867	0.723	16.2
02/18/2014	5.18	29.36	27.71	57.1	15.00	2.150	1.993	26.2
02/19/2014	4.35	13.45	22.61	36.1	6.54	1.328	1.295	24.7
02/20/2014	5.77	28.61	26.75	55.4	10.12	1.873	1.705	25.0
02/21/2014	6.88	41.05	28.46	69.5	10.21	2.445	2.269	36.4
02/22/2014	6.03	18.26	19.53	37.8	10.17	1.235	1.132	16.5
02/23/2014	5.39	7.10	12.17	19.3	8.54	0.728	0.647	10.6
02/24/2014	7.49	33.71	24.07	57.8	11.17	2.220	1.951	
02/25/2014	5.41	8.77	19.37	28.1	11.71	1.210	1.175	
02/26/2014	5.12	8.87	17.10	26.0	6.52	1.165	1.103	
02/27/2014	5.22	9.32	15.99	25.3	5.71	0.997	1.002	31.7
02/28/2014	5.31	6.99	17.30	24.3	3.29	1.061	1.047	23.4
03/01/2014	5.54	2.02	11.24	13.2	2.96	0.431	0.345	11.0
03/02/2014	6.53	4.96	13.08	18.0	5.04	1.008	0.864	16.0
03/03/2014	5.98	19.38	26.38	45.8	6.12	1.917	1.834	34.5
03/04/2014	4.13	6.80	15.46	22.2	3.71	0.823	0.758	16.2
03/05/2014	5.13	25.31	17.57	42.9	9.71	2.158	2.058	32.1
03/06/2014	4.60	12.51	19.64	32.1	9.42	1.397	1.409	28.6

Table D.3: *(continued)*

Date	CO	NO	NO_2	NO_X	$PM_{2.5}$	BC_{UV}	BC_6	UFP
03/07/2014	4.53	11.41	19.18	30.6	7.92	1.163	1.102	27.2
03/08/2014	6.25	13.70	22.56	36.3	10.21	1.358	1.165	24.0
03/09/2014	6.65	9.94	20.90	30.8	9.12	1.336	1.202	22.2
03/10/2014	5.03	5.87	14.99	20.9	3.83	0.755	0.721	23.1
03/11/2014	4.31	2.77	10.60	13.4	1.58	0.413	0.357	18.0
03/12/2014	4.97	4.28	11.35	15.6	2.17	0.480	0.435	10.9
03/13/2014	4.40	25.92	27.21	53.1	9.74	2.399	2.240	34.9
03/14/2014	3.09	15.10	21.33	36.4	12.38	2.070	1.925	33.5
03/15/2014	4.20	12.37	19.03	31.4	7.38	1.341	1.133	20.1
03/16/2014	4.76	9.29	14.89	24.2	9.46	1.257	0.953	20.2
03/17/2014	3.29	9.90	19.55	29.5	6.79	1.377	1.222	31.1
03/18/2014	4.55	19.39	26.91	46.3	7.92	1.825	1.634	33.5
03/19/2014	5.53	24.92	29.70	54.6	10.58	2.285	1.970	32.1
03/20/2014	4.70	13.69	21.56	35.2	11.48	1.670	1.520	24.8
03/21/2014	4.10	10.43	14.88	25.3	13.92	1.284	1.212	27.8
03/22/2014	4.46	5.62	13.81	19.4	12.79	0.872	0.761	13.9
03/23/2014	4.78	3.19	11.21	14.4	11.12	0.821	0.684	
03/24/2014	5.94	10.17	21.79	32.0	10.79	1.352	1.190	25.5
03/25/2014	5.07	13.11	19.35	32.5	6.29	1.603	1.430	28.7
03/26/2014	4.84	11.76	15.20	27.0	6.04	1.362	1.286	28.0
03/27/2014	4.94	10.36	16.11	26.5	8.30	1.437	1.375	31.1
03/28/2014	5.18	14.86	16.13	31.0	8.83	1.977	1.775	34.0
03/29/2014	4.88	5.10	12.33	17.4	4.42	0.843	0.786	16.1
03/30/2014	4.93	3.86	10.83	14.7	3.71	0.547	0.503	20.3

Table D.4: Diurnal profile, Oakland STP.

Hour (LST)	**WSpeed** (m/s)	**WDir** (0=N)	**Temp** (Celsius)	**Press** (mbar)
0000h	2.33	232	11.3	1018
0100h	2.32	209	11.1	1018
0200h	2.40	195	10.8	1018
0300h	2.41	182	10.6	1018
0400h	2.51	167	10.5	1018
0500h	2.51	135	10.4	1018
0600h	2.42	144	10.3	1018
0700h	2.47	156	10.4	1018
0800h	2.69	170	11.4	1018
0900h	2.82	186	12.3	1019
1000h	2.99	225	13.0	1019
1100h	3.14	252	13.7	1019
1200h	3.48	268	14.4	1018
1300h	3.95	277	15.1	1017
1400h	4.25	274	15.4	1017
1500h	4.32	269	15.4	1017
1600h	4.06	267	15.1	1017
1700h	3.79	266	14.4	1017
1800h	3.39	272	13.7	1017
1900h	3.26	277	13.1	1017
2000h	3.02	279	12.6	1017
2100h	2.72	267	12.3	1017
2200h	2.43	254	11.9	1018
2300h	2.37	228	11.6	1018

Bibliography

Aoki, Paul M. et al. (2009). "A Vehicle for Research: Using Street Sweepers to Explore the Landscape of Environmental Community Action". In: *Proceedings of the SIGCHI Conference on Human Factors in Computing Systems*. CHI '09. Boston, MA, USA: ACM, pp. 375–384. DOI: 10.1145/1518701.1518762.

Balzano, Laura (2007). "Addressing fault and calibration in wireless sensor networks". Master's Thesis. University of California, Los Angeles.

Barnett, Adrian G and Annette J Dobson (2010). *Analysing Seasonal Health Data*. Berlin, Heidelberg: Springer.

Barregard, Lars et al. (2006). "Experimental exposure to wood-smoke particles in healthy humans: effects on markers of inflammation, coagulation, and lipid peroxidation". In: *Inhalation Toxicology* 18.11, pp. 845–853. DOI: 10.1080/08958370600685798.

Barregard, Lars et al. (2008). "Experimental exposure to wood smoke: effects on airway inflammation and oxidative stress". In: *Occupational and Environmental Medicine* 65.5, pp. 319–324.

Basu, R et al. (2003). "Does maternal smoking confound the relation between $PM_{2.5}$ and birth weight? [abstract]". In: *Proceedings of the 131st Annual Meeting of APHA*. San Francisco, CA.

Baxter, Lisa K et al. (2013). "Exposure prediction approaches used in air pollution epidemiology studies: Key findings and future recommendations". In: *Journal of Exposure Science and Environmental Epidemiology* 23.6, pp. 654–659.

Blackwell, Jack A and Andrea Tuttle (2003). *California Fire Siege 2003*. Tech. rep.

Bosetti, Cristina et al. (2010). "Ambient particulate matter and preterm birth or birth weight: a review of the literature". In: *Archives of Toxicology* 84.6, pp. 447–460. DOI: 10.1007/s00204-010-0514-z.

Brauer, Michael et al. (2012). "Exposure assessment for estimation of the global burden of disease attributable to outdoor air pollution". In: *Environmental Science and Technology* 46.2, pp. 652–660. DOI: 10.1021/es2025752.

Breton, Carrie, Caron Park, and Jun Wu (2011). "Effect of prenatal exposure to wildfire-generated $PM_{2.5}$ on birth weight [abstract]". In: *Epidemiology* 22, S66. DOI: 10.1097/01.ede.0000391864.79309.9c.

Brugge, Douglas et al. (2010). "Community-based participatory research in Boston's neighborhoods: A review of asthma case examples". In: *Archives of Environmental and Occupational Health* 65.1, pp. 38–44. DOI: 10.1080/19338240903390214.

Budde, M, M Busse, and Michael Beigl (2012). "Investigating the use of commodity dust sensors for the embedded measurement of particulate matter". In: *Ninth International Conference on Networked Sensing Systems (INSS)*, pp. 1–4.

Burkart, J et al. (2010). "Characterizing the performance of two optical particle counters (Grimm OPC1.108 and OPC1.109) under urban aerosol conditions". In: *Journal of Aerosol Science* 41.10, pp. 953–962. DOI: 10.1016/j.jaerosci.2010.07.007.

Burnett, Richard T et al. (2014). "An integrated risk function for estimating the global burden of disease attributable to ambient fine particulate matter exposure". In: *Environ Health Perspect* 122.4, pp. 397–403. DOI: 10.1289/ehp.1307049.

Cameron, Peter A et al. (2009). "Black Saturday: the immediate impact of the February 2009 bushfires in Victoria, Australia". In: *The Medical Journal of Australia* 191.1, pp. 11–16.

Catalano, R and T Hartig (2001). "Communal bereavement and the incidence of very low birthweight in Sweden." In: *Journal of Health and Social Behavior* 42.4, pp. 333–341.

Catalano, Ray et al. (2005). "Sex ratios in California following the terrorist attacks of September 11, 2001". In: *Human Reproduction* 20.5, pp. 1221–1227. DOI: 10.1093/humrep/deh763.

Chen, L, K Verrall, and S Tong (2006). "Air particulate pollution due to bushfires and respiratory hospital admissions in Brisbane, Australia". In: *International Journal of Environmental Health Research* 16.3, pp. 181–191.

Chow, Judith C et al. (2002). "Designing monitoring networks to represent outdoor human exposure." In: *Chemosphere* 49.9, pp. 961–78. ISSN: 0045-6535.

Chowdhury, Zohir et al. (2007). "An inexpensive light-scattering particle monitor: field validation". In: *Journal of Environmental Monitoring* 9.10, pp. 1099–1106. DOI: 10.1039/b709329m.

CITI-SENSE (2012). *CITI-SENSE: Development of sensor-based Citizens' Observatory Community for improving quality of life in cities (7th EC RTD Framework Program, contract No. 308524)*.

Darrow, Lyndsey A, Tracey J Woodruff, and Jennifer D Parker (2006). "Maternal smoking as a confounder in studies of air pollution and infant mortality." In: *Epidemiology* 17.5, pp. 592–593. DOI: 10.1097/01.ede.0000229951.26189.27.

Delfino, R J et al. (2009). "The relationship of respiratory and cardiovascular hospital admissions to the southern California wildfires of 2003". In: *Occupational and Environmental Medicine* 66.3, pp. 189–197. DOI: 10.1136/oem.2008.041376.

Demuth, Dustin et al. (2013). "The AirQuality SenseBox". In: *EGU General Assembly Conference Abstracts*. Vol. 15, p. 5146.

Dennekamp, Martine and Michael J Abramson (2011). "The effects of bushfire smoke on respiratory health". In: *Respirology* 16.2, pp. 198–209. DOI: 10.1111/j.1440-1843.2010.01868.x.

DiSalvo, Carl et al. (2012). "Toward a Public Rhetoric Through Participatory Design: Critical Engagements and Creative Expression in the Neighborhood Networks Project". In: *Design Issues* 28.3, pp. 48–61. DOI: 10.1162/DESI_a_00161.

Dutta, Prabal et al. (2009). “Common Sense: Participatory Urban Sensing Using a Network of Handheld Air Quality Monitors”. In: *Proceedings of the 7th ACM Conference on Embedded Networked Sensor Systems*. SenSys ’09. Berkeley, California: ACM, pp. 349–350. DOI: 10.1145/1644038.1644095.

Edwards, Rufus D et al. (2006). “An inexpensive dual-chamber particle monitor: laboratory characterization.” In: *Journal of the Air and Waste Management Association* 56.6, pp. 789–799.

Emmanuel, S C (2000). “Impact to lung health of haze from forest fires: the Singapore experience”. In: *Respirology* 5.2, pp. 175–182.

European Union (2008). *Directive 2008/50/EC of the European Parliament and of the Council of 21 May 2008 on ambient air quality and cleaner air for Europe*.

Fowler, C T (2003). “Human health impacts of forest fires in the southern United States: a literature review”. In: *Journal of Ecological Anthropology* 7, pp. 39–63.

Frickel, Scott et al. (2010). “Undone science: charting social movement and civil society challenges to research agenda setting”. In: *Science, Technology & Human Values* 35.4, pp. 444–473.

Fujita, Eric M and David Campbell (2010). *West Oakland Monitoring Study*. Tech. rep. Desert Research Institute, pp. 1–115.

Fujita, Eric M. et al. (Dec. 2013). “Spatial variations of particulate matter and air toxics in communities adjacent to the Port of Oakland”. In: *Journal of the Air and Waste Management Association* 63.12, pp. 1399–1411. ISSN: 1096-2247. DOI: 10.1080/10962247.2013.824393.

Ghio, A J et al. (2011). “Exposure to wood smoke particles produces inflammation in healthy volunteers”. In: *Occupational and Environmental Medicine*. DOI: 10.1136/oem.2011.065276.

Gilliland, Frank et al. (2005). “Air pollution exposure assessment for epidemiologic studies of pregnant women and children: lessons learned from the Centers for ChildrenâĂŹs Environmental Health and Disease Prevention Research”. In: *Environmental health perspectives* 113.10, p. 1447.

Glinianaia, Svetlana V et al. (2004). “Particulate air pollution and fetal health”. In: *Epidemiology* 15.1, pp. 36–45. DOI: 10.1097/01.ede.0000101023.41844.ac.

Gonzalez, Priscilla et al. (2011). “Community-based participatory research and policy advocacy to reduce diesel exposure in West Oakland, California”. In: *American Journal of Public Health*. DOI: 10.2105/AJPH.2010.196204.

Hänninen, Otto et al. (2009). “Population exposure to fine particles and estimated excess mortality in Finland from an East European wildfire episode”. In: *Journal of Exposure Science and Environmental Epidemiology* 19.4, pp. 414–422. DOI: 10.1038/jes.2008.31.

Harrison, Jill Lindsey (2011). “Parsing “Participation” in Action Research: Navigating the Challenges of Lay Involvement in Technically Complex Participatory Science Projects”. In: *Society and Natural Resources* 24.7, pp. 702–716. ISSN: 0894-1920. DOI: 10.1080/08941920903403115.

Hasenfratz, D, O Saukh, and L Thiele (2012). "On-the-fly calibration of low-cost gas sensors". In: *Ninth European Conference on Wireless Sensor Networks (EWSN)*. Springer, pp. 228–244.

Health Effects Institute (2010). *Traffic-related air pollution: a critical review of the literature on emissions, exposure, and health effects*. Special Report 17. HEI Panel on the Health Effects of Traffic-Related Air Pollution.

Hedges, Scott (2002). *Planning and implementing a real-time air pollution monitoring and outreach program for your community (Report No. EPA/625/R-02/2012)*. Tech. rep. U.S. EPA.

Henderson, Sarah B et al. (2011). "Three measures of forest fire smoke exposure and their associations with respiratory and cardiovascular health outcomes in a population-based cohort". In: *Environmental Health Perspectives* 119.9, pp. 1266–1271. DOI: 10.1289/ehp.1002288.

Holstius, D et al. (2013). "A near-roadway risk screening tool for urban planners". In: *Proceedings of the 106th Annual Conference of the Air and Waste Management Association (AWMA), Sep 25–28, Chicago*.

Holstius, David M and Edmund Seto (2011). "Birth weight following pregnancy during the 2003 Southern California wildfires". In: *Proceedings of the 23rd Annual Conference of the International Society of Environmental Epidemiology (ISEE)*.

Holstius, David M et al. (2012). "Birth weight following pregnancy during the 2003 Southern California wildfires". In: *Environmental Health Perspectives* 120.9, pp. 1340–1345.

Holstius, David M et al. (2014). "Field calibrations of a low-cost aerosol sensor at a regulatory monitoring site in California". In: *Atmospheric Measurement Techniques* 7, pp. 1121–1131.

Honicky, Richard et al. (2008). "N-smarts: Networked Suite of Mobile Atmospheric Real-time Sensors". In: *Proceedings of the Second ACM SIGCOMM Workshop on Networked Systems for Developing Regions*. NSDR '08. Seattle, WA, USA: ACM, pp. 25–30. DOI: 10.1145/1397705.1397713.

Jaffe, Dan et al. (2008). "Interannual variations in $PM_{2.5}$ due to wildfires in the Western United States". In: *Environmental Science and Technology* 42.8, pp. 2812–2818.

Jerrett, Michael et al. (2005). "A review and evaluation of intraurban air pollution exposure models". In: *Journal of Exposure Analysis and Environmental Epidemiology* 15.2, pp. 185–204.

Jiang, Yifei et al. (2011). "MAQS: A Personalized Mobile Sensing System for Indoor Air Quality Monitoring". In: *UbiComp '11, September 17-21, 2011*. Beijing: ACM, pp. 271–280.

John, Walter (2011). "Size distribution characteristics of aerosols". In: *Aerosol Measurement: Principles, Techniques, and Applications*. Ed. by P Kulkarni, P A Baron, and K Willeke. 3rd. 4. John Wiley and Sons, pp. 41–54.

Johnston, Fay H et al. (2002). "Exposure to bushfire smoke and asthma: an ecological study". In: *The Medical Journal of Australia* 176.11, pp. 535–538.

Kinney, P L et al. (2000). "Airborne concentrations of $PM_{2.5}$ and diesel exhaust particles on Harlem sidewalks: a community-based pilot study". In: *Environmental Health Perspectives* 108.3, pp. 213–218.

Kochi, Ikuho et al. (2010). "The economic cost of adverse health effects from wildfire-smoke exposure: a review". In: *International Journal of Wildland Fire* 19.7, pp. 803–817. DOI: 10.1071/WF09077.

Kumagai, Y, M S Carroll, and P Cohn (2004). "Coping with interface wildfire as a human event: Lessons from the disaster/hazards literature". In: *Journal of Forestry* 102.6, pp. 28–32.

Künzli, Nino et al. (2006). "Health effects of the 2003 Southern California wildfires on children". In: *Am J Resp Crit Care Med* 174.11, pp. 1221–1228. DOI: 10.1164/rccm.200604-519OC.

Kuznetsov, Stacey and Eric Paulos (2010). "Rise of the Expert Amateur: DIY Projects, Communities, and Cultures". In: *Proceedings of the 6th Nordic Conference on Human-Computer Interaction: Extending Boundaries*. NordiCHI '10. Reykjavik, Iceland: ACM, pp. 295–304. ISBN: 978-1-60558-934-3. DOI: 10.1145/1868914.1868950. URL: http://doi.acm.org/10.1145/1868914.1868950.

LeBesco, Kathleen (2011). "Neoliberalism, public health, and the moral perils of fatness". In: *Critical public health* 21.2, pp. 153–164.

Lighty, J S, J M Veranth, and A F Sarofim (2000). "Combustion aerosols: factors governing their size and composition and implications to human health". In: *Journal of the Air and Waste Management Association* 50.9, pp. 1522–1565.

Lim, Stephen S et al. (Dec. 2012). "A comparative risk assessment of burden of disease and injury attributable to 67 risk factors and risk factor clusters in 21 regions, 1990-2010: a systematic analysis for the Global Burden of Disease Study 2010." In: *Lancet* 380.9859, pp. 2224–60. ISSN: 1474-547X.

Litton, Charles D et al. (2004). "Combined optical and ionization measurement techniques for inexpensive characterization of micrometer and submicrometer aerosols". In: *Aerosol Science and Technology* 38.11, pp. 1054–1062.

Loh, Penn et al. (2002). "From asthma to AirBeat: community-driven monitoring of fine particles and black carbon in Roxbury, Massachusetts." In: *Environmental Health Perspectives* 110.Suppl 2, p. 297.

Mallard, Alexandre (1998). "Compare, standardize and settle agreement: On some usual metrological problems". In: *Social Studies of Science* 28.4, pp. 571–601.

— (2001). "From the Laboratory to the Market: The Metrological Arenas of Research-Technology". In: *Instrumentation Between Science, State and Industry*. Springer, pp. 219–238.

Martien, Phil (2014). *The Community Air Risk Evaluation (CARE) program*. Tech. rep. URL: http://www.baaqmd.gov/Divisions/Planning-and-Research/CARE-Program.aspx.

McCracken, John P et al. (2009). "Combining individual-and group-level exposure information: child carbon monoxide in the Guatemala woodstove randomized control trial". In: *Epidemiology* 20.1, pp. 127–136.

McKone, Thomas E, P Barry Ryan, and Halûk Özkaynak (2009). "Exposure information in environmental health research: Current opportunities and future directions for particulate matter, ozone, and toxic air pollutants". In: *Journal of Exposure Science and Environmental Epidemiology* 19.1, pp. 30–44.

Mead, M I et al. (2013). "The use of electrochemical sensors for monitoring urban air quality in low-cost, high-density networks". In: *Atmospheric Environment* 70.C, pp. 186–203. DOI: 10.1016/j.atmosenv.2012.11.060.

Molenar, John V (2003). "Theoretical analysis of $PM_{2.5}$ mass measurements by nephelometry". URL: http://vista.cira.colostate.edu/improve/publications/graylit/014_AerosolByNeph/AerosolbyNeph.pdf.

Moore, David et al. (2006). "Population health effects of air quality changes due to forest fires in British Columbia in 2003." In: *Canadian Journal of Public Health* 97.2.

Morgan, Geoffrey et al. (2010). "Effects of bushfire smoke on daily mortality and hospital admissions in Sydney, Australia". In: *Epidemiology* 21.1, pp. 47–55. DOI: 10.1097/EDE.0b013e3181c15d5a.

Mott, Joshua A et al. (2005). "Cardiorespiratory hospitalizations associated with smoke exposure during the 1997 Southeast Asian forest fires". In: *International Journal of Hygiene and Environmental Health* 208.1-2, pp. 75–85.

Mun, Min et al. (2009). "PEIR, the Personal Environmental Impact Report, As a Platform for Participatory Sensing Systems Research". In: *Proceedings of the 7th International Conference on Mobile Systems, Applications, and Services*. MobiSys '09. Krakow, Poland: ACM, pp. 55–68. DOI: 10.1145/1555816.1555823.

Naeher, Luke P et al. (2007). "Woodsmoke health effects: a review". In: *Inhalation Toxicology* 19.1, pp. 67–106. DOI: 10.1080/08958370600985875.

Nafis, Chris (2012). *Automatically measuring and graphing air quality with an inexpensive device*. URL: http://www.howmuchsnow.com/arduino/airquality/grovedust/ (visited on 03/01/2013).

National Research Council (2012). *Exposure Science in the 21st Century: A Vision and a Strategy*. Tech. rep. National Research Council.

Nethery, Elizabeth et al. (2008). "From measures to models: an evaluation of air pollution exposure assessment for epidemiological studies of pregnant women". In: *Occupational and environmental medicine* 65.9, pp. 579–586.

Nikzad, Nima et al. (2012). "CitiSense: improving geospatial environmental assessment of air quality using a wireless personal exposure monitoring system". In: *Proceedings of the conference on Wireless Health*. ACM, p. 11.

Northcross, Amanda L et al. (2013). "A low-cost particle counter as a realtime fine-particle mass monitor". In: *Environmental Science: Processes and Impacts* 15.2, p. 433. DOI: 10.1039/c2em30568b.

Olivares, G, I Longley, and G Coulson (2012). "Development of a low-cost device for observing indoor particle levels associated with source activities in the home". In: *22nd Annual Meeting of the International Society of Exposure Science*. Seattle, WA.

O'Rourke, Dara and Gregg P Macey (2003). "Community environmental policing: Assessing new strategies of public participation in environmental regulation". In: *Journal of Policy Analysis and Management* 22.3, pp. 383–414.

Ottinger, Gwen (2009). "Epistemic Fencelines: Air Monitoring Instruments and Expert-Resident Boundaries". In: *Spontaneous Generations: A Journal for the History and Philosophy of Science* 3.1, pp. 55–67. DOI: 10.4245/sponge.v3i1.6115.

Özkaynak, Halûk et al. (2013). "Air pollution exposure prediction approaches used in air pollution epidemiology studies". In: *Journal of Exposure Science and Environmental Epidemiology*.

Parker, Jennifer D, Pauline Mendola, and Tracey J Woodruff (2008). "Preterm birth after the Utah Valley Steel Mill closure: a natural experiment". In: *Epidemiology* 19.6, pp. 820–823. DOI: 10.1097/EDE.0b013e3181883d5d.

Pastor Jr., Manuel, Rachel Morello-Frosch, and James L Sadd (2010). *Air pollution and environmental justice: Integrating indicators of cumulative impact and socio-economic vulnerability into regulatory decision-making (CARB Report No. 04-308)*. Tech. rep. 213. California Air Resources Board.

Paulos, Eric, RJ Honicky, and Elizabeth Goodman (2007). "Sensing atmosphere". In: *ACM Conference on Embedded Networked Sensor Systems (SenSys 2007)*.

Phuleria, H C, P M Fine, and Y Zhu (2005). "Air quality impacts of the October 2003 Southern California wildfires". In: *Journal of Geophysical Research*.

Pingkuan, Di (2008). *Diesel Particulate Matter Health Risk Assessment for the West Oakland Community*. Tech. rep. URL: http://www.arb.ca.gov/ch/communities/ra/westoakland/westoakland.htm.

Pope, Daniel P et al. (2010). "Risk of low birth weight and stillbirth associated with indoor air pollution from solid fuel use in developing countries". In: *Epidemiologic Reviews* 32.1, pp. 70–81.

Reid, Stephen B (2007). *Documentation of emission estimation techniques for sources of diesel particulate matter (DPM) associated with truck-based businesses and construction projects in West Oakland, California (Contract No. 2006-144) (STI-907006-3174-TM)*. Tech. rep. Sonoma Technology.

Rioux, Christine L et al. (2010). "Characterizing urban traffic exposures using transportation planning tools: an illustrated methodology for health researchers". In: *Journal of urban health* 87.2, pp. 167–188.

Ritz, Beate and Michelle Wilhelm (2008). "Ambient air pollution and adverse birth outcomes: methodologic issues in an emerging field." In: *Basic and Clinical Pharmacology and Toxicology* 102.2, pp. 182–190. DOI: 10.1111/j.1742-7843.2007.00161.x.

Rous, Trevor and Alan Hunt (2004). "Governing peanuts: the regulation of the social bodies of children and the risks of food allergies". In: *Social science & medicine* 58.4, pp. 825–836.

Sällsten, Gerd et al. (2006). "Experimental wood smoke exposure in humans". In: *Inhalation Toxicology* 18.11, pp. 855–864. DOI: 10.1080/08958370600822391.

Samaranayake, Samitha et al. (2014). "Real-Time Estimation of Pollution Emissions and Dispersion from Highway Traffic". In: *Computer-Aided Civil and Infrastructure Engineering*, pp. 1–13. DOI: 10.1111/mice.12078.

Sastry, Narayan (2002). "Forest fires, air pollution, and mortality in southeast Asia". In: *Demography* 39.1, pp. 1–23.

Shilton, Katie (2011). "Building values into the design of pervasive mobile technologies". Dissertation. University of California, Los Angeles.

Siddiqui, Amna R et al. (2008). "Prenatal exposure to wood fuel smoke and low birth weight". In: *Environmental Health Perspectives* 116.4, pp. 543–549. DOI: 10.1289/ehp.10782.

Slama, Rémy et al. (2008). "Meeting report: atmospheric pollution and human reproduction." In: *Environmental Health Perspectives* 116.6, pp. 791–798. DOI: 10.1289/ehp.11074.

Smith, Kirk R (2011). *Development of the UCB-L particle monitor for future California applications in environmental justice*. Tech. rep., pp. 1–26.

Smith, Peter Andrey and Mayeta Clark (June 2013). *Microsampling Air Pollution*. New York. URL: http://well.blogs.nytimes.com/2013/06/03/microsampling-air-pollution/.

Snyder, Emily G et al. (Oct. 2013). "The changing paradigm of air pollution monitoring." In: *Environmental Science and Technology* 47.20, pp. 11369–77. ISSN: 1520-5851.

Spracklen, D V et al. (2009). "Impacts of climate change from 2000 to 2050 on wildfire activity and carbonaceous aerosol concentrations in the western United States". In: *Journal of Geophysical Research* 114, p. D20301. DOI: 10.1029/2008JD010966.

Swiston, J R et al. (2008). "Wood smoke exposure induces a pulmonary and systemic inflammatory response in firefighters". In: *European Respiratory Journal* 32.1, pp. 129–138. DOI: 10.1183/09031936.00097707.

Teige, V E et al. (2011). "BErkeley Atmospheric CO2 Network (BEACON) - Bringing Measurements of CO2 Emissions to a School Near You. Abstract #ED53C-0814." In: *American Geophysical Union, Fall Meeting 2011*.

Tham, Rachel et al. (2009). "The impact of smoke on respiratory hospital outcomes during the 2002-2003 bushfire season, Victoria, Australia". In: *Respirology* 14.1, pp. 69–75. DOI: 10.1111/j.1440-1843.2008.01416.x.

US EPA (2012). *National Ambient Air Quality Standards for Particulate Matter; Final Rule*.

— (2013). "Next Generation Air Monitoring Workshop Series". In: *Air Sensors 2013: Data Quality and Applications*. Research Triangle Park, NC. URL: https://sites.google.com/site/airsensors2013/.

Viswanathan, Shekar et al. (2006). "An analysis of effects of San Diego wildfire on ambient air quality". In: *Journal of the Air and Waste Management Association* 56, pp. 56–67.

Watson, John G (2002). "Visibility: Science and regulation". In: *Journal of the Air and Waste Management Association* 52, pp. 628–713. ISSN: 1096-2247.

Watson, John G et al. (1998). *Guidance for using continuous monitors in $PM_{2.5}$ monitoring networks*. Tech. rep. May. Office of Air Quality Planning and Standards, U.S. EPA.

Wegesser, Teresa C, Kent E Pinkerton, and Jerold A Last (2009). "California wildfires of 2008: coarse and fine particulate matter toxicity." In: *Environmental Health Perspectives* 117.6, pp. 893–897. DOI: 10.1289/ehp.0800166.

Wegesser, Teresa C et al. (2010). "Lung antioxidant and cytokine responses to coarse and fine particulate matter from the great California wildfires of 2008." In: *Inhalation Toxicology* 22.7, pp. 561–570. DOI: 10.3109/08958370903571849.

Weissman, A et al. (1989). “The influence of increased seismic activity on pregnancy outcome”. In: *European Journal of Obstetrics and Gynecology and Reproductive Biology* 31.3, pp. 233–236.

Westerling, A L and B P Bryant (2008). “Climate change and wildfire in California”. In: *Climatic Change* 87.S1, pp. 231–249. DOI: 10.1007/s10584-007-9363-z.

Westerling, A L et al. (2006). “Warming and earlier spring increase western U.S. forest wildfire activity”. In: *Science* 313.5789, pp. 940–943. DOI: 10.1126/science.1128834.

Whitby, Kenneth T (1978). “The physical characteristics of sulfur aerosols”. In: *Atmospheric Environment (1967)* 12, pp. 135–159.

Wilcox, A J (2001). “On the importance—and the unimportance—of birthweight”. In: *International Journal of Epidemiology* 30.6, pp. 1233–1241.

Willett, Wesley et al. (2010). “Common Sense Community: Scaffolding mobile sensing and analysis for novice users”. In: *Proceedings of the Conference on Pervasive Computing*, pp. 301–318.

Wilson, J. Gaines et al. (2005). “A review of intraurban variations in particulate air pollution: Implications for epidemiological research”. In: *Atmospheric Environment* 39.34, pp. 6444–6462. ISSN: 13522310. DOI: 10.1016/j.atmosenv.2005.07.030.

Wilson, WE et al. (2002). “Monitoring of particulate matter outdoors”. In: *Chemosphere* 49.9, pp. 1009–1043.

Wilson, William E and Helen H Suh (1997). “Fine particles and coarse particles: Concentration relationships relevant to epidemiologic studies”. In: *Journal of the Air and Waste Management Association* 47.December, pp. 1238–1249.

Woodruff, Tracey J et al. (2009). “Methodological issues in studies of air pollution and reproductive health”. In: *Environmental Research* 109.3, pp. 311–320.

World Health Organization (2005). *WHO Air Quality Guidelines Global Update 2005: Report on a Working Group Meeting, Bonn, Germany, 18-20 October 2005*. Tech. rep. Bonn, Germany: WHO Regional Office for Europe.

Wu, Jun, Arthur M Winer, and Ralph J Delfino (2006). “Exposure assessment of particulate matter air pollution before, during, and after the 2003 Southern California wildfires”. In: *Atmospheric Environment* 40.18, pp. 3333–3348.

Xiang, Yun et al. (2012). “Collaborative Calibration and Sensor Placement for Mobile Sensor Networks”. In: *The 11th ACM/IEEE Conference on Information Processing in Sensor Networks, April 16-19, 2012*. Beijing, pp. 73–83. ISBN: 9781450312271.

Zou, Bin et al. (2009). “Air pollution exposure assessment methods utilized in epidemiological studies”. In: *Journal of Environmental Monitoring* 11.3, pp. 475–490.